Decoding Passive Optical Network Surveillance Based Upon Constraint Management Techniques

Gerson Flávio Mendes de Lima

Uberlândia

2014

Gerson Flávio Mendes de Lima

Decoding Passive Optical Network Surveillance Based Upon Constraint Management Techniques

Texto da tese apresentada ao Programa de Pós-Graduação em Engenharia Elétrica da Universidade Federal de Uberlândia, perante a banca de examinadores, como parte dos requisitos para a obtenção do título de Doutor em Ciências.

Área de concentração: Processamento da Informação, Computação Gráfica

Orientador: Prof. Edgard Lamounier,PhD
Co-Orientador: Alexandre Cardoso,Dr

Uberlândia

2014

Gerson Flávio Mendes de Lima

Decoding Passive Optical Network Surveillance Based Upon Constraint Management Techniques

Texto da tese apresentada ao Programa de Pós-Graduação em Engenharia Elétrica da Universidade Federal de Uberlândia, perante a banca de examinadores, como parte dos requisitos para a obtenção do título de Doutor em Ciências.

Área de concentração: Processamento da Informação, Computação Gráfica

Uberlândia, 10 de Setembro de 2014
Banca Examinadora:

_____
Prof. Edgard Lamounier,PhD – FEELT/UFU

_____
Alexandre Cardoso, Dr – FEELT/UFU

_____
Gilberto Arantes Carrijo, PhD – FEELT/UFU

_____
Keiji Yamanaka, PhD – FEELT/UFU

_____
Sergio Barcelos,PhD – FIBERWORK

_____
Frederico Gadelha Guimaraes, Dr – UFMG

This work is dedicated to my wife and son,
The greatest legacy that parents leave their children is the example.

Acknowledgements

*"Great discoveries and advances invariably
involve the cooperation of many minds."*
(Alexander Graham Bell)

Abstract

Lima, G. F. M. **Passive Optical Networks Surveillance Decoding using Constraint-Based Techniques**. 126 p. Ph.D. Thesis Qualify – Faculty of Electrical Engineering, Federal University of Uberlândia, 2014 .

Constraints techniques have been applied to a large amount of applications for Engineering Design. In fact, the challenges imposed by graphics and equation constraints result in valuable features when considering - Computer Aided Design (CAD) / - Computer Aided Engineering (CAE) software, this include supporting faster decision process by engineers. On the other hand, Passive Optical Networks (PON) are progressively becoming reality, while commercial deployments are reported worldwide. Operating these networks, however, requires adequate means for a cost effective monitoring. This includes troubleshooting faults with the possibility to remotely differentiate between an equipment failure and a fibre break and, subsequently, to localize it in the network. This is of great importance for Telecommunication Carriers. The use of Optical Time Domain Reflectometry (OTDR) techniques is widely used in point-to-point optical network topologies. However, it has major limitations in tree-structured PONs, where all backscattered traces merge at the Optical Line Terminal (OLT) location. Therefore, it is difficult to differentiate between the branches. As after splitters where the OTDR signals are superimposed. This work proposes a Constraints-based Differential Evolutionary algorithm that allows for the separation of the superimposed signal of a - Passive Optical Networks (PON) network and couple it with a - Fiber to The Home (FTTH) CAD design. This process intends on bringing compound an in-service PON management, considering the status of fiber links and its geographical distribution branches of different lengths, with the capability of localizing and quantifying several faults successively in the same or in different branches of a PON Network.

Keywords: Constraints-based techniques, FTTH , PON , Differential Evolution.

Resumo

Lima, G. F. M. **Decoding Passive Optical Network Surveillance Based Upon Constraint Management Techniques**. 126 p. Qualificação de doutorado – Faculdade de Engenharia Elétrica, Universidade Federal de Uberlândia, 2014 .

O uso de técnicas de restrições são empregadas em uma grande escala de aplicações de engenharia. De fato os desafios impostos para as restrições gráficas e matemáticas resultam em características extremamente eficientes para os softwares de CAD / CAE, permitindo a criação de ferramentas de apoio a tomada de decisão muito eficazes. As redes FTTx (PON) estão se tornando progressivamente uma realidade comercial, e as suas implementações são relatadas em todo o mundo. Todavia, o funcionamento destas redes exige meios adequados para o monitoramento de baixo custo, especialmente, a possibilidade para detectar as falhas remotamente, assim como diferenciar entre uma falha de equipamento e uma ruptura de fibra, e subsequentemente, localizá-la geograficamente é de grande importância para as empresas de telecomunicações. O uso de técnicas de reflectometria óptica no domínio do tempo (OTDR) é amplamente utilizado nas redes de ópticas ponto-a-ponto. Entretanto esta técnica tem limitações quando utilizada em redes de topologias distribuidas, pois o sinal é dividido nos ramos da rede e são somados no Terminal de Linha Óptica (OLT), difícultando a diferenciação do sinal de cada ramo da rede separadamente onde os sinais (OTDR) são sobrepostos entre si. Este trabalho propoe um algoritmo de Evolução Diferêncial que permite a simulação matemática de divisores ópticos e a separação do sinal sobreposto de redes com divisores, integrando estes com o projeto CAD de uma rede FTTH, empregando técnicas de restrições. O resultado é apresentado em uma solução de acoplamento do mundo "optico" de sinais de reflectometria (OTDR)em redes PON com o mundo "fisico" do projeto em CAD, considerando as ligações de fibra e os seus ramos (divididos ou splitados).

Palavras-chave: Tecnicas de Restrições , FTTH , PON , Evolução Diferêncial .

List of Figures

List of Tables

List of Acronyms

CAD - Computer Aided Design

CAE - Computer Aided Engineering

PON - Passive Optical Networks

FTTH - Fiber to The Home

OLT - Optical Line Terminal

CSV - Comma Separated Values

MDU - Multiple Dwelling Units

MTU - Multi Tenanted Units

STU - Single Tenanted Units

SFWU - Single Family Dwelling Units

NAP - Network Access Point

ONT - Optical Network Terminal

Contents

Appendix 104

Research Publications

Publications

1. LIMA,G.F.M.;LAMOUNIER,E.&CARDOSO,A. A Constraint Techiniques to Support Electronic TV Network Design. In: *Published book - LAP - Lambert Academic Publishing AG & Co. KG*, 2010.

2. PERETTA, I. S.; LIMA, G. F. M.; TAVARES, J. A. & YAMANAKA, K. A Spoken Word Boundaries Detection Strategy for Voice Command Recognition. *Learning & Nonlinear Models*, 2010.

3. LIMA,G.F.M.;PERETTA, I. S.;TAVARES, J. A.; LAMOUNIER,E.; CARDOSO,A.& YAMANAKA, K. Optimization of Lighting Design Usign Genetic Algorithms. In: *9 th IEEE/IAS International Conference on Industry Applications* , 2010.

4. TAVARES, J. A.;PERETTA, I. S.;LIMA,G.F.M.;PAIS, M. S.;YAMANAKA, K. Algoritmo Baseado no Operador de Energia de Teager (TEO) para Segmentação de Linhas e Palavras em Textos Manuscritos e Impressos In: *VII Workshop Computational Vision, 2011, Curitiba p. 219-224.*

5. LIMA, G. F. M. ; LAMOUNIER JUNIOR, EDGARD AFONSO ; IGOR SANTOS PERETTA ; CARDOSO, A. ; BARCELOS, SERGIO ; MURAMOTO, W. S. ; RIGON, ELSO. A TEO-Based Algorithm to detect events over OTDR Measurements in FTTH PON Networks. In: *4TH IEEE LATIN-AMERICAN CONFERENCE ON COMMUNICATIONS 2012, 2012, CUENCA - ECUADOR.. LATINCOM 2012 - PROCEEDINGS, 2012.*

6. LIMA, G. F. M. ; LAMOUNIER, E. , CARDOSO, A. , PERETTA, I. S. , PERETTA, I. S. , BARCELOS, S. , MURAMOTO, W. , RIGON, E. . A TEO-Based Algorithm to Detect Events Over OTDR Measurements in FTTH PON Networks *Revista IEEE América Latina, v. 11, p. 886-891, 2013.*

CHAPTER **1**

Introduction

Innovations in Telecommunications have produced a tremendous increase in communication traffic and, consequently, a constant bandwidth demand and growth. This quickly led service providers to respond by bringing the optical fiber closer and closer to the premises, and finally directly into the home (GIRARD, 2005).
In this chapter, we present the motivation, statements and objectives for the present work presently under development.

1.1 Motivation

Fiber networks currently carry today data traffic over a thousand times higher than that of 10 years ago. It is believed that this traffic will grow much higher in the coming years due to the introduction of 100Gb/s transmission technologies. Besides, this scenario is related to the fast-paced market introduction of FTTH (Fiber-To-The-Home) broadband access services (LIMA; LAMOUNIER; BARCELOS, 2012), (LIMA, 2013). Thus, carrier's customers are demanding ever-growing service downtime fines in their Service Level Agreements - SLA. Nowadays, fiber cuts have thus become very expensive to carriers due to both lost revenue and tarnished business images. To reduce fiber network downtime, improve network service availability and increase profitability, telecom carriers and utility companies must rely on automatic optical fiber monitoring systems and efficient maintenance services (ALCATEL, 2009).

Moreover, the network maintenance manager must consume the minimum operational cost in such activities to assure that the optical fiber plant renders the maximum profit. However, as mentioned, the extraordinary fiber plant growth and increased number of network node sites has recently turned monitoring and maintenance tasks into arduous challenges (URBAN et al., 2013). To succeed in this new market, network managers must look for more advanced tools that can quickly, automatically and precisely assist them in monitoring and maintaining the intricacies of such modern high capacity fiber networks (SANKAWA et al., 1990).

The application of optical technology in telecommunication systems such as local area networks, cable TV systems and fiber-to-the home systems has been the subject of increased interest (GIRARD, 2005). Among the several kinds of optical network architectures, the passive branched type have been able to meet the needs for narrowing band customers as well as satisfy future upgrade requirements (URBAN et al., 2013). After the installation of such networks, it is important to be able to locate any fiber link faults. As the capacity of passive optical networks (PONs) increases, allowing hundreds of clients to share the same infrastructure, the importance of performance monitoring increases. When a fault occurs, technicians must be dispatched to identify, locate and fix the failure. The time, efforts involved, and truck-roll for fault identification, dramatically, increase the operational expenditure and erode the profit margins for the Telecommunication Companies (RAD; FATHALLAH; RUSCH, 2010).

In addition, it is well known that optical-time-domain reflectometry (OTDR) is efficient for testing optical devices and point-to-point monitoring (YEH, 2005). However, it is not effective for point-to-multipoint (PMP) networks like PONs. The existing solutions for PON monitoring impose significant technical challenges, with most techniques presenting a limited capacity (IIDA et al., 2007), (HANN; YOO; PARK, 2006), (PARK et al., 2006). Service providers report that more than 80% of installed PON failures occur within the first/last mile, i.e., within the distribution/drop segments of the network. Fiber-to-the home (FTTH) installations lack an efficient technology appropriate for the link quality monitoring of a PON (even the 1:32 BPON standard, ITU G.983) (RAD; FATHALLAH; RUSCH, 2010). Even with all PON deployments that are expected to take place in the next years, operators will repeatedly face the challenge that testing PONs poses (SIMARD, 2009).

Based on experience, the best PON-testing method that has emerged is derived from optical time-domain reflectometry (OTDR) (GIRARD, 2005). The OTDR method has shown reliable results, while reducing the overall cost of testing. Since the OTDR method is a single ended method; it significantly reduces staff time, which is a key advantage (CHABOT, 2009). FTTH networks using PON technology can be characterized and maintained every step of the way using a fiber-optic test and measurement equipment. OTDRs can also be used not only from the ONTs towards the coupler and - Optical Line Terminal (OLT) at the central office, but also, from the OLT towards the point to multipoint network. Mathematical splice loss predictions can be used to be more accurate and, consequently, to help to properly characterize the networks.

The PON deployment depends highly on the geography of clients on the network. PON provides services to both residential and business users. Residential users occupy - Multiple Dwelling Units (MDU) and - Single Family Dwelling Units (SFWU). Business users occupy multi tenanted units (- Multi Tenanted Units (MTU)), such as office blocks or towers and single tenanted units (- Single Tenanted Units (STU)), such as stand-alones

office building or warehouses (VAUGHN et al., 2004). Geographical distribution can vary from installation to installation and depends on a variety of parameters.

The standard for out-of-band optical time-domain reflectometry (OTDR), based on Rayleigh backscattering and power reflections used to monitor point-to-point links, is ineffective in point-to-multipoint TDM-PONs (ITU, 2005). The OTDR trace at the central office (CO) is a linear sum of the backscattered and reflected power from all the network branches. Therefore, it is difficult and even impossible for the CO manager to distinguish the events in one branch from others (URBAN et al., 2013).

Many FTTH management problems result from the very little information available to the CO manager concerning the network. This directly affects the quality of service and dramatically increases the administration, the maintenance, and the provisioning costs. For example, when two branches experience an equidistant failure event it becomes indistinguishable. Even when a fiber fault results in an unambiguous event, the faulty branch is not identified, requiring a truck-roll tour and outside intervention by technicians. Every branch must be checked separately from its end by means of an upstream power meter and/or OTDR transmission in order to identify that which is faulty. Moreover, when an optical network terminal (- Optical Network Terminal (ONT)) is not communicating with the CO, the manager cannot make a remote diagnosis and determine the cause, whether this is due to a fiber cut or simply because the ONT is disconnected or turned off (RAD; FATHALLAH; RUSCH, 2010).

In Point to Multipoint Networks (PMP), the OTDR trace at the central office (CO) is a linear sum of the backscattered and reflected powers from all the network branches. It is difficult for the CO network manager to distinguish the events in one branch from those in others. The most important one is the difficulty in identifying a specific broken branch in the PON tree architecture.(HANN; YOO; PARK, 2006). To guarantee quality of service through the PON, monitoring techniques should be provided under the in-service state through both fault diagnosis and maintenance (RAD; FATHALLAH; RUSCH, 2010).

Passive optical splitter (power splitting element/branching device) or optical coupler is a device used to broadcast an optical signal from one fiber to many fibers. In the most general case, an optical splitter is configured as 1xN, which is 1 input port to N output ports. Optical signals on the input port are branched to all the output ports. Optical splitters may also be used to multiplex the optical signals from several fiber lines onto a single line. However, the use of an optical coupler poses several problems in the OTDR testing (ANDERSON; BELL, 2004). If the OTDR is connected to the N side of a 1xN optical splitter, then the waveform shows a large loss, limiting the OTDR's ability to test far beyond the optical splitter. This is due to the fact that the loss is represented as an effective loss in the OTDR's dynamic range. Furthermore, when connected to the input side of a 1xN optical splitter, the waveform shows a smaller drop than when the OTDR was connected to one of the N output ports. In this cases the higher signal level results
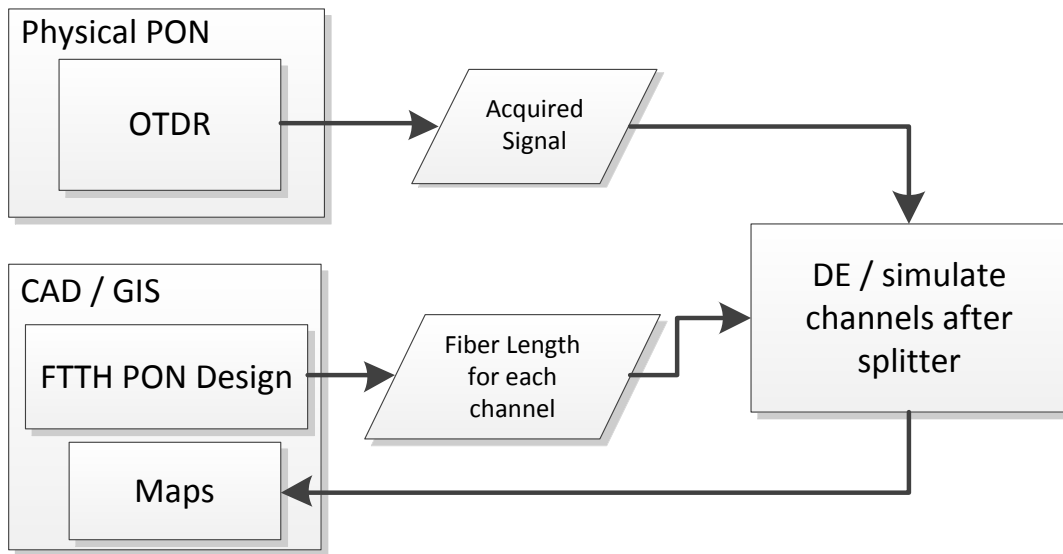
Figure 1 – Proposed Methodology

because the combined signatures of all N fibers on the branching side of the optical coupler are superimposed and this makes it very difficult (sometimes impossible) to associate events on the waveform with the specific lines on which the events occur. This is probably the most common problem faced by technicians when dealing with optical splitter. Some solutions arise, through fiber faults monitoring techniques, as proposed by C.H. Yeh (YEH F.Y. SHIH; CHI, 2008) and the fiber-break monitoring system as proposed by A.A.A. Bakar (BAKAR M.Z. JAMALUDIN; ABDULLAH, 2007).

However, in this work, we developed a set of constraint-based algorithms to build a system that controls optical network surveillance, integrating the graphical network design (CAD/GIS) with the OTDR measures from CO. In the same solution set, a Differential Evolutionary Algorithm (CHAKRABORTY, 2008) was implemented resulting in a signal separation of each branch of the network, associating events on the waveform with the specific lines on which the events occur in a map. This work used an arrangement created specifically to investigate a concept proof to determine an OTDR splitter relationship between separated branches (superimpose mathematics equation) for In-service application using a FTTH optimized OTDR, placing onto the map of the separated OTDR signal after the PON splitter. The motivation of this work is to separate the OTDR signal in order to plot over a map (CAD), the separated signal and use it to provide location based on information to improve maintenance procedures. Therefore, the signal separation is very important for providing an innovative tool that joins the OTDR fiber signal separated after the splitter coupled with GIS information. This methodology is shown in Figure 1.

Design constraints allow for the implementation of a conjunction of resources using Visualization Information techniques to compound a relationship between the geographical position of the different types of optical network elements and use routines to detect events on the network (LIMA; JUNIOR, 2010) (SILVA, 2006) (LAMOUNIER, 1996).

The algorithm will use the OTDR reflectometry technology to analyse the optical power signal, estimating the fiber's length and overall attenuation, including splice and mated-connector losses, and coupling with a CAD network design relating each optical signal event with its relative geographic coordinates.

1.2   Thesis Statement

The purpose of this work is to investigate constraint-based techniques to support the the OTDR signal separation after a Splitter over a FTTH PON Network. In so doing, a solver based on Differential Evolutionary algorithms is proposed and evaluated through equations tested in laboratory. This methodology is applied as constraints into a CAD platform that couple the optical signal and network design creating an in-service PON management tool.

1.3   Objective and Research Goals

This work aims at evaluating a system based on the use of constraint techniques and computational intelligence algorithms to implement a solution to manage and monitor FTTH passive optical networks (Fiber-To-The-Home). This is achieved by using a set of techniques to evaluate networks in operation (in-service) and also by using a wavelength that does not interfere in the normal functioning of a telecommunication network, allowing the system to be monitored in real time. The system will be able to geographically analyse, locate and quantify (throughout the optical network and its coverage) several types of optical event. The main goal is to be able to separate the signal after a Splitter and locate it geographically on different branches of the network with complete accuracy. This will hopefully, eliminate the need for "Mirrors", or to be used as a "Bragg Grating" (HILL; MELTZ, 1997) accessory for field technicians.

This research also proposes a mathematical equation that allows one to computationally "Simulate" occurring events in the mixing reflectometry (OTDR) signals after the passive optical network splitters (PON) and thus provide the signal separation at each different branch of the splitter, using for this feature a specifically developed evolutionary Algorithm (GOLDBERG, 1989).

The investigated technique is inspired on a common method known in literature as "Blind Source Separation", where the separation of a set of signals from a random mixed set of signals is used, without the aid of information (Or with very little information) about the original signals or the mixing process. This methodology is widely used in voice recognition systems and for the separation of sound signal (ACHARYYA, 2008).

After the signal separation, each signal will be stored in a separate specific data structure that performs the coupling of signals reflectometry OTDR on the network, associated to

their subscribers served by telecommunication services. Therefore, this will provide an intelligent surveillance system for PON able to relate the physical components of the infrastructure in the existing network events associated with the optical signal measured by reflectometry (OTDR) "Optical world", using an interface based on uses of Information Visualization techniques (LIMA; LAMOUNIER; CARDOSO, 2010) (LIMA et al., 2011) to provide efficacy and usability.

1.4   Thesis Contribution

After developing the research work, inspired on the goals and objectives outlined above, it is understood that this thesis makes the following contributions:

❏ An algorithm that allows for the analysis of the Reflectometry (OTDR) signal, and detect events from within the loud signal;

❏ An Artificial Intelligence methodology to separate the mixed OTDR Signal after the Optical Network Splitters;

❏ A Proposed Mathematical equation to simulate the Passive Optical Splitter.

❏ A Constraint-Based Database with Geographic Capabilities of FTTH PON network in a GIS/CAD system allowing the user to view at the same time the physical network infrastructure and the Optical world "Signal" in real time in the same environment, using Information visualization techniques;

❏ Development of an experimental prototype that validates the items above;

1.5   Thesis Organization

❏ Fundamentals - Brief history about FTTH PON Technology, exploring the key concepts of Optical Network components and Optical Time Domain Reflectometer (OTDR) signal characteristics adopted in this thesis.

❏ Related Work - An Explanation for other similar and related works that inspired this investigation.

❏ Experimental Methodology - A Detailed experimental arrangement created for simulation proposes, for performing a sequence of tests, a Splitter Equation and OTDR simulation.

❏ System Architecture - Detailed Genetic Algorithm implementation, Differential Evolutionary Algorithm implementation and Results Comparison.

❏ Results and Implementation Detail - Implementation detail of Signal Coupling with CAD tool, explanation about the Graphics User Interface.

❏ Conclusion and Future Work - Results comparative, conclusion and advice on Future Work.

❏ Bibliography

❏ Appendix A - A TEO-Based Algorithm to detect events over OTDR Measurements in FTTH PON Networks.

❏ Appendix B - Routines to Genetic Algorithm - Matlab

❏ Appendix C - Routines to Differential Evolutionary Algorithm - Matlab

Chapter **2**

Fundamentals

2.1 Introduction

Wider deployment of fiber over the last years has been driven by the increase in customer needs for higher communication capacity joint with a cost-efficient, fully reliable and accurate monitoring solution. Thus, supporting fault detection, identification, and localization in different fiber access topologies will be a key part of such solutions (URBAN et al., 2013).

In this chapter, we present a technology overview of the key concepts of this research. The main idea is to allow for a deeper understanding of the experimental premises adopted in the development process. This chapter also presents a detailed review of FTTx technology giving an explanation as to its brief historical development to the current bandwidth usage worldwide, including network technologies and testing methods. The description of constraint management methodologies adopted in this research, is also explained.

2.2 FTTH PON Technology

Since the development of the optical fiber, the personal computer and the Internet, bandwidth consumption has shown incessant growth worldwide. Eventual distinctions depend on many factors, such as culture, climate, local infrastructure new technologies of services as well as physical space or distance. The development of the single mode optical fiber (with its almost unlimited bandwidth) has opened up opportunities to massive deployment of long-haul and metropolitan point-to-point (P2P) fiber-optic networks (HARAN GLEN KRAMER; RUO DING, 2007). The use of fiber-optic cable, rather than copper cable, resulted in three important changes (GIRARD, 2005).

❑ Massive increase of capacity ;

❑ Significant cost reductions (equipment, operation and maintenance);

❏ Great improvement on quality of service (QoS).

Figure 2 illustrates a typical network structure, while Figure 3 presents example of fiber-optic P2P networks and shows some of the techniques that have been used to increase their capacity. Originally, a single channel was carried over each optical link. In turn, it was limited to approximately 100km with sufficient optical power. The advent of wavelength-division multiplexing (WDM) made it possible to carry many channels (using different wavelengths) over a single fiber, without cross-interference. Next, dense wavelength-division multiplexing (DWDM) further increased this capacity, allowing for even more wavelength channels.
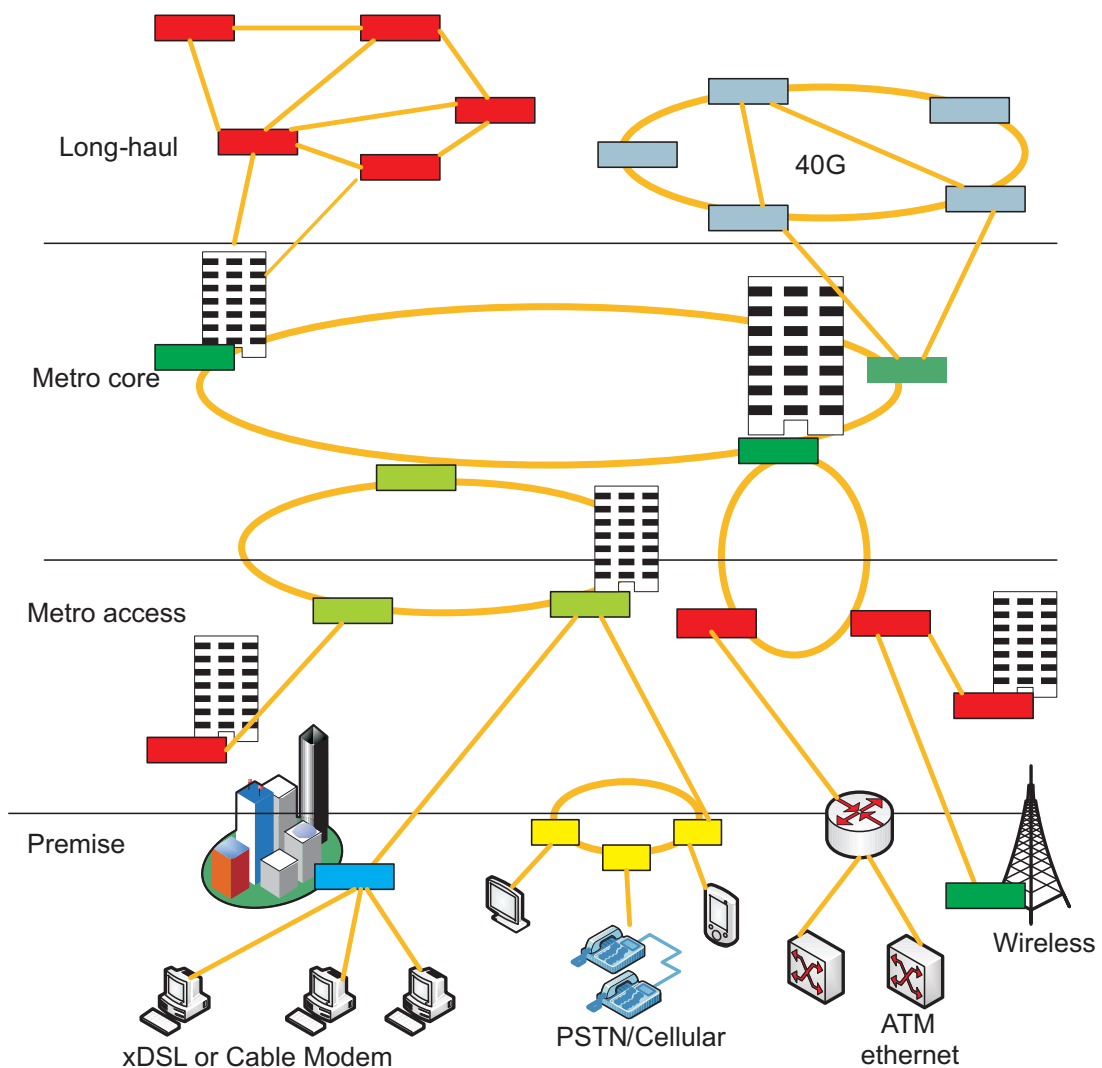
Figure 2 – Terrestrial fiber-optic networks

In addition, the use of erbium-doped fiber amplifiers (EDFAs), which amplify optical signals directly, (without optical-electrical-optical conversion) has allowed for the construction of long-haul (P2P) networks with few or no electronic components. A point-to-point (P2P) network is a dedicated communication link operating over a fiber pair;

one for downstream transmission and the other for upstream transmission. Metropolitan-area networks (MANs) are also fiber-based and make use of lower-cost coarse wavelength-division multiplexing (CWDM) to transmit multiple channels (typically 18 over low-water-peak fiber) per fiber over relatively short P2P links. Although most access networks, serving small businesses and residential customers, are still copper-based, subscribers in some countries around the world have a P2P fiber-optic connection to a central office (CO) (GIRARD, 2005).

As shown in Figure 3, this requires a dedicated optical line terminal (OLT) at the (CO). As well as a pair of optical fibers for each subscriber, where an optical network unit (ONU) is connected to the fiber pair.
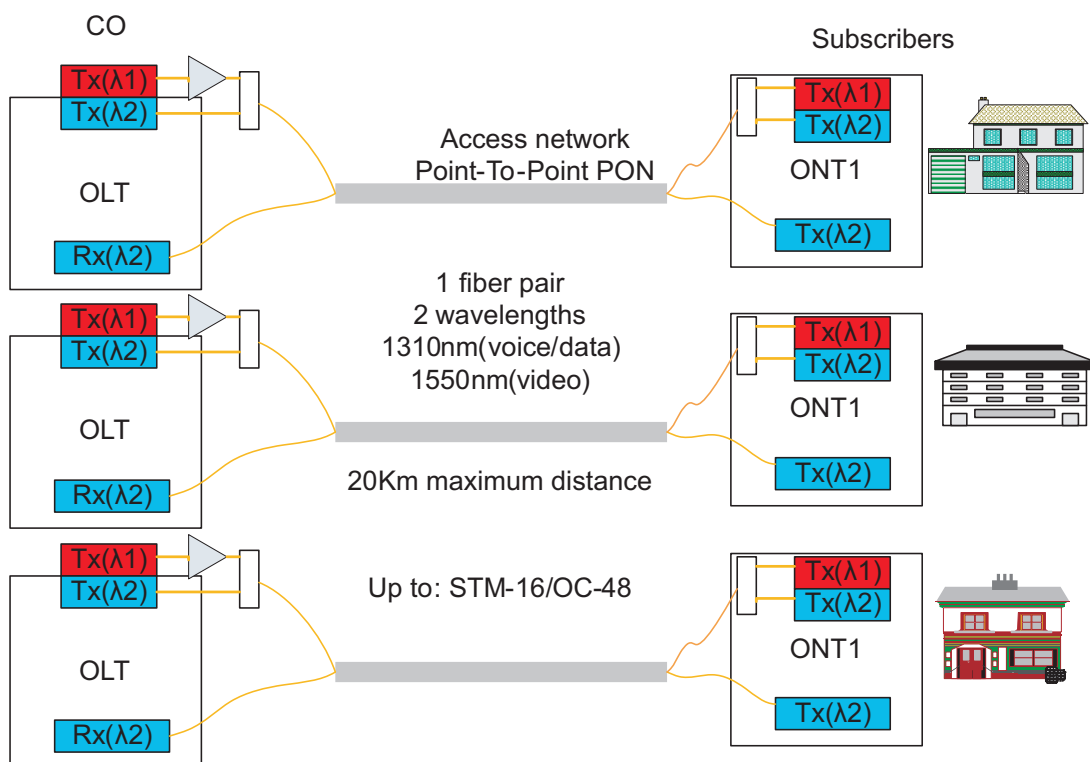
Figure 3 – Point-to-Point (P2P) optical networks

Optical fibers have not been widely used for the "last mile" because of the high cost and limited availability of optical access services (GIRARD, 2005). This segment is typically cooper-based and the high-speed service available to residential clients and small business is limited to generic digital subscriber lines (xDSL) and hybrid fiber coax (HFC). The main alternative to fiber optics (wireless transmission with direct broadcast service DBS) requires an antenna and a receiver. The fiber optics networks overcomes most of these limitations. It is important to note that one of the obstacles when providing fiber-optic services directly to residences and small businesses, including small offices and home offices (SOHOs), has to do with the high cost of connecting each subscriber to the CO (i.e., the cost of deploying the fiber cable) (GIRARD, 2005). A high number of point-to-point (P2P) connections would require many active components and a high-fiber-count. This

lean to prohibitive installation and maintenance costs, when compared to a traditional copper distribution network, which is getting very old and requires maintenance. Figure 4 shows different optical fiber connections used on the access network.
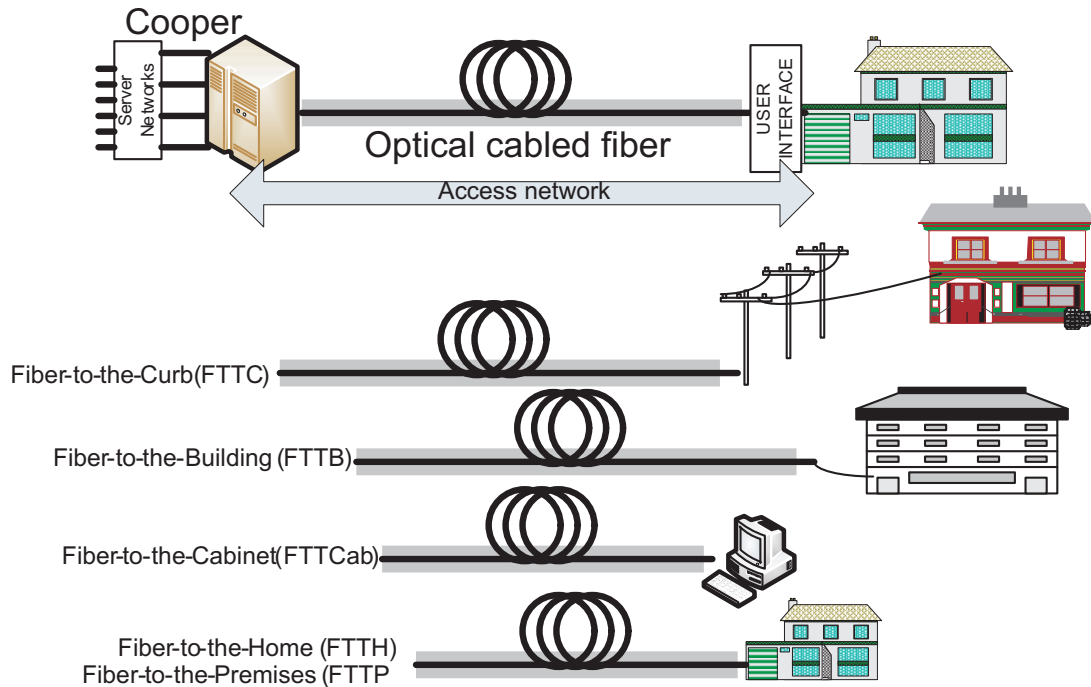
Figure 4 – Variations of the access network architecture

While also supporting P2P architecture, fiber-to-the-home (FTTH) also known as Fiber To The Premises (FTTP) provides a point-to-multipoint (P2MP) connection that offers an attractive solution to these problems. Moreover, with FTTH P2MP PONs, there are no active components between the CO and each subscriber. This fact allows several subscribers to share the same connection. This is accomplished by using one or more passive splitters to connect, in some cases, up to 32 subscribers to the same feeder fiber. This P2MP architecture dramatically reduces the network installation, management, and maintenance costs.

Figure 5 and Figure 6 show a P2MP PON. Each OLT at the CO is connected through a single feeder fiber to a splitter, which in turn, is connected to all subscribers, sharing the available bandwidth. Each subscriber has a connection to a single fiber and different wavelengths are used on this fiber for upstream and downstream transmission of voice and data as well as downstream video transmission.

The parameters involved in the optical network design, in practice, are directly dependent on the spatial disposition of each optical component representation, inside the circuit, the network architecture or the topology. Different architectures exist for connecting a subscriber to a PON. However, each PON requires at least the following (Figure 7) (GIRARD, 2005):

❏ An optical line terminal (OLT) at the CO in P2MP and P2P PONs;
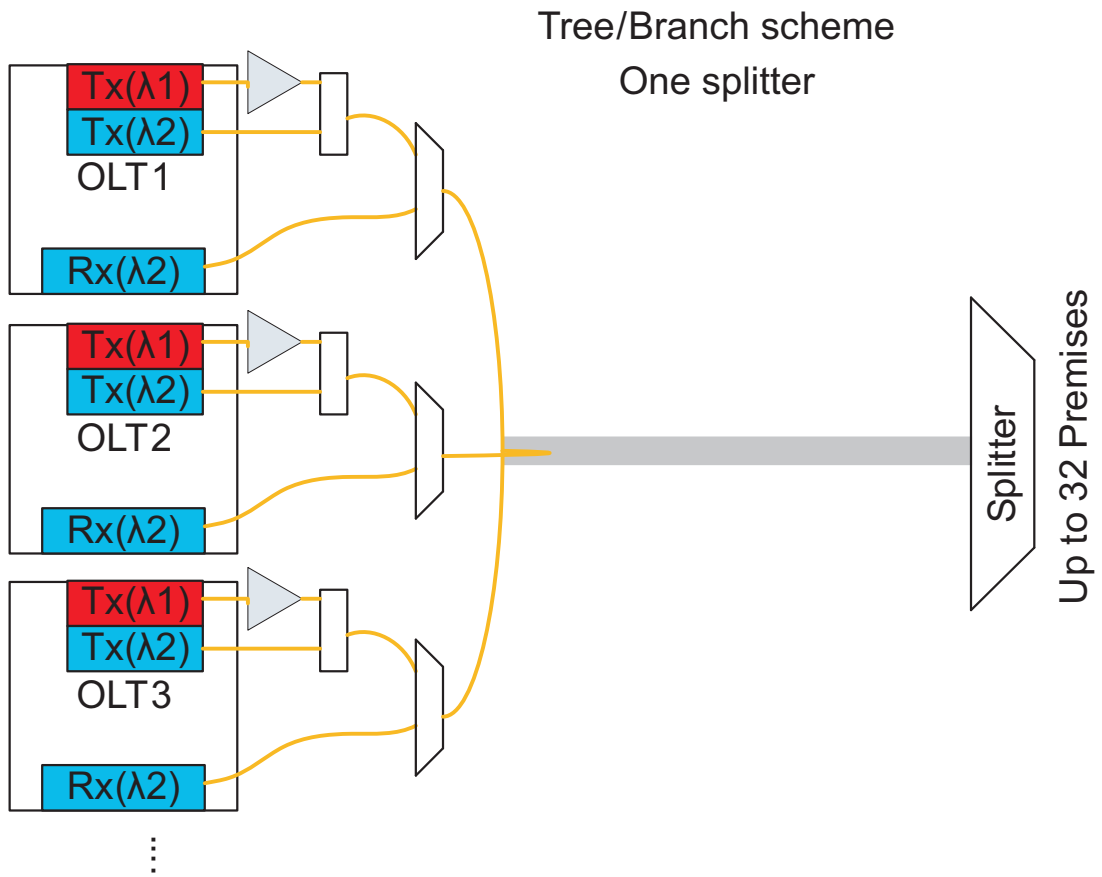
Figure 5 – P2MP single-splitter (tree-branched) PON
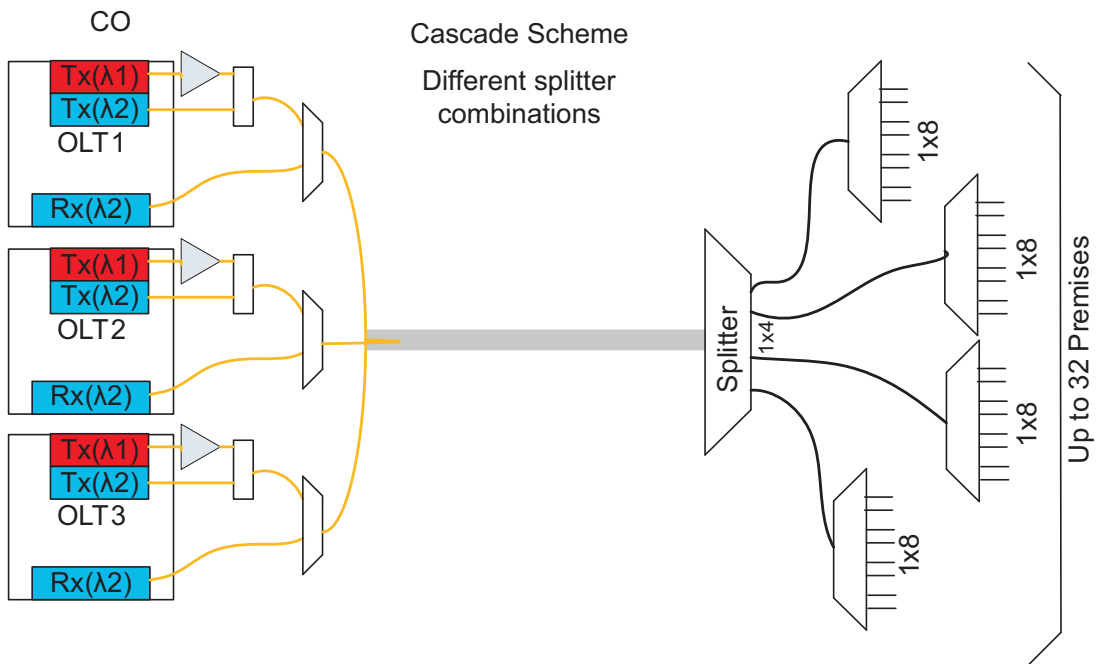
Figure 6 – P2MP cascade-design PON

❑ Video distribution equipment also at CO;

❑ A feeder from the CO to a splitter in the P2MP PONs (The fiber is part of a multifiber cable);

❑ One splitter per feeder fiber (PONs can use multiple splitters in a cascade or tree design topology);

❑ Distribution fibers and drop cables between the splitter branches and the optical network terminals (ONTs);

❑ An ONT (ONU connected to the UNI) located at each subscriber's premises in P2MP AND P2P PONs.

The feeder, splitter(s), distribution and drop cables form the optical distribution network (ODN) of the P2MP PON. Since PON, typically, provides service for up to 32 subscribers (BPON), many networks (each originating from the same CO) are usually required to serve a community. The OLT at the CO is interfaced with the public switched telephone network (PSTN) and the internet (see Figure 7). Video signals enter the system from the cable television (CATV) head-end or from DBS satellite feed. The video sources can be converted to optical format by an optical video transmitter. Next, the signal is amplified and coupled through a wide wavelength-division multiplexing (WWDM) coupler (not shown in Figure 7) to the optical signal form the OLT. Alternatively, the video signals can be interfaced with the OLT in digital form for IPTV or in analogue form for overlay. These signals are transmitted in upstream form to the ONTs.
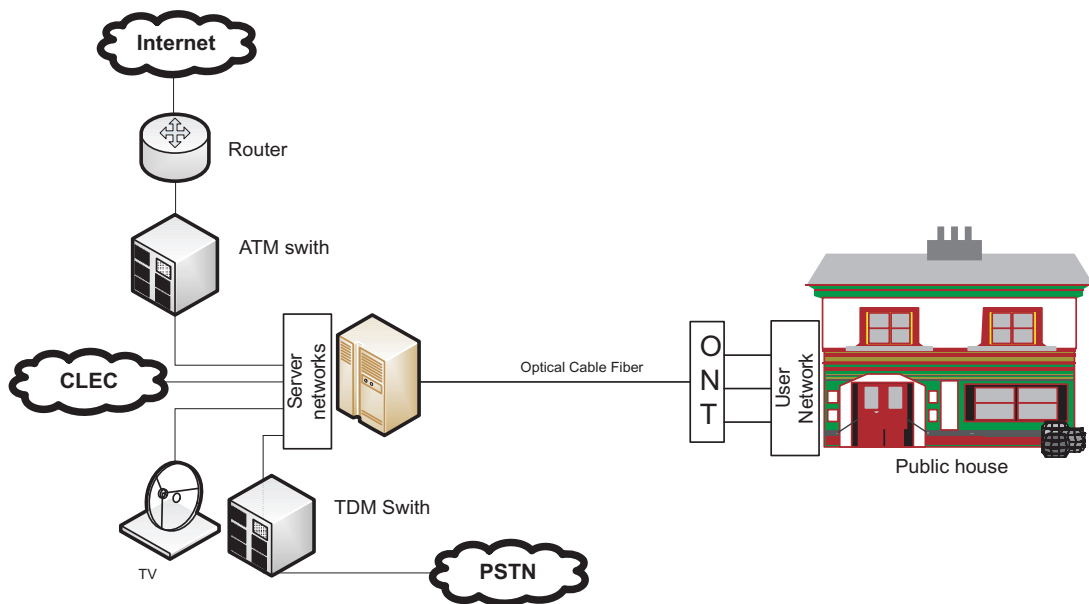
Figure 7 – FTTH PON basic system architecture

The feeder fiber from the CO is brought to a fiber distribution hub (FDH), where one or more splitters are located, typically, near a group of customers (a Km or so). From

that point, one or more passive splitters (depending on the splitter topology) are used to connect customers. Each customer premises is provided with an ONT connected to one splitter branch. The ONT provides connections for the different services (voice, Ethernet, and video).

2.3   Passive Optical Components

The main passive components in a PON are:

❏ 1 x 2 WWDM coupler(s) (two couplers if analogue video is used in P2MP);

❏ 1 x N splitter (IN P2MP);

❏ Fiber-optic cables (feeder, distribution and drop);

❏ Connectors and cable assemblies

❏ Fiber management systems/enclosures

Details of each important component are explained in the following.

2.3.1   Optical Fiber Cable

The optical fiber cable is another key component of a PON (P2P and P2MP). Fiber has an increased advantage over copper resulting from the physical transmission of photons instead of electrons (SALEH; TEICH, 2013). In glass, optical attenuation is much less than the attenuation of electrical signals in copper and much less dependent on signal frequency (SALEH; TEICH, 2013).

The light is "guided" down the center of the fiber, called the "core". The core is surrounded by an optical material called the "cladding" which traps the light in the core, using an optical technique called "total internal reflection" (SALEH; TEICH, 2013). The fiber itself is coated with a "buffer" aimed to protect the fiber from moisture and physical damage (Figure 8).

The buffer is what one strips off the fiber for termination or splicing. The core and cladding are usually made from ultra-pure glass. Although some fibers are all plastic or a glass core and plastic cladding. The core is designed in a manner that it attains a higher index of refraction (an optical parameter that is a measure of the speed of light in the material) than the cladding. This causes "total internal reflection" to trap light in the core up to a certain angle, which defines the "numerical aperture" of the fiber. Glass fiber is coated with a protective plastic covering, called the "primary buffer coating", which protects it from moisture and other damage. More protection is provided by the "cable" which has the fibers and strength members inside an outer protective covering called the "jacket ".
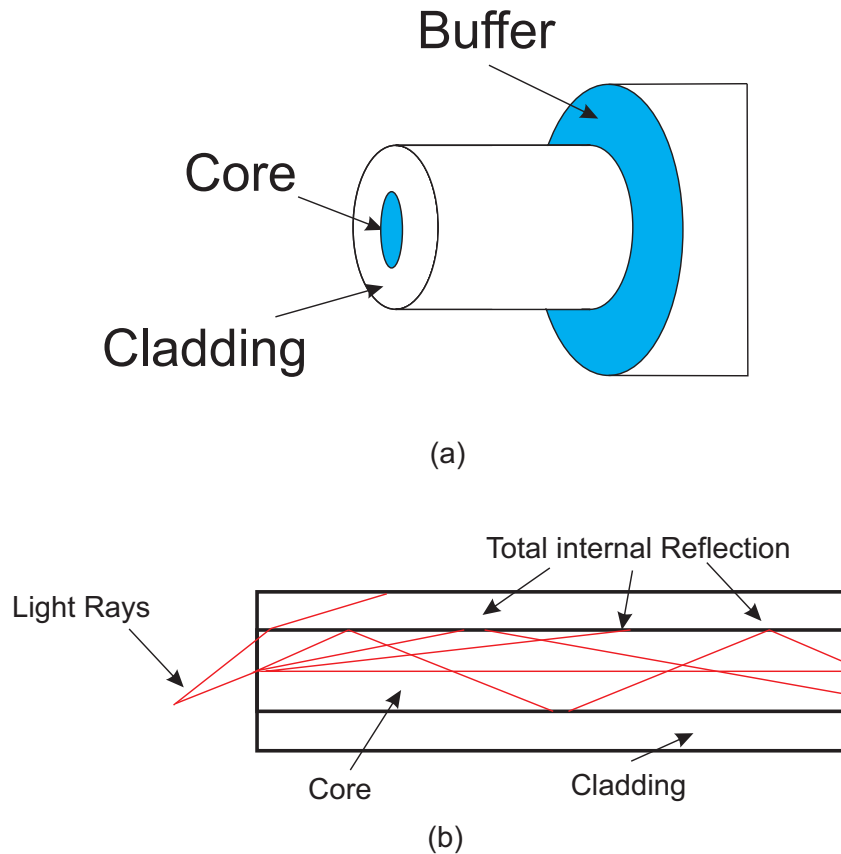
Figure 8 – a) Optical Cable perspective b) Optical Cable lateral view

2.3.1.1   Fiber Types: Multi-mode & Single-mode, Core/Cladding Size

Optic fiber is found in two forms, multi-mode and single-mode. Within these categories, fibers are identified by their core and cladding diameters expressed in microns (one millionth of a meter), e.g. 50/125 micron multi-mode fiber. Most fibers are 125 microns external diameter (a micron is one one-millionth of a meter and 125 microns is 0.005 inches- a slightly larger than the typical human hair).

Multi-mode fiber has light travelling along the core in many rays, called modes. It has a larger core (usually 50 or 62.5 microns) which supports the transmission of multiple modes (rays) of light. Multi-mode is generally used with LED sources at wavelengths of 850 and 1300 nm for slower local area networks (LANs) and lasers at 850 (VCSELs) and 1310 nm (Fabry-Perot lasers) for networks running at gigabits per second or more.

Single-mode fiber has a much smaller core, only about 9 microns, so that the light travels in only one ray (mode). It is used for telephony and CATV with laser sources at 1300 and 1550 nm because it has lower loss and virtually infinite bandwidth. Plastic Optical Fiber (POF) has a large core (about 1mm) fiber, usually step index, which is used for short, low speed networks. PCS/HCS (plastic or hard clad silica, plastic cladding covering a glass core) has a smaller glass core (around 200 microns) and a thin plastic cladding.

Step index multi-mode was the first fiber design (SALEH; TEICH, 2013). It has a higher attenuation and is too slow for many uses, due to the dispersion caused by the different path lengths of the various modes travelling in the core. Step index fiber is not widely used. Actually, only POF and PCS/HCS (plastic or hard clad silica, plastic cladding covering a glass core) use a step index design today.

Graded index multi-mode fiber uses variations in the composition of the glass in the core to compensate for the different path lengths of the modes. It offers hundreds of times more bandwidth than step index fiber - up to about 2 gigahertz. Two types are in use, 50/125 and 62.5/125, where the numbers represent the core/cladding diameter in microns (GIRARD, 2005).

Single-mode fiber shrinks the core down (so small) that the light can only travel in a single ray. This increases the bandwidth to almost infinity. However, is practically limited to about 100,000 gigahertz (which is still a considerable sum!). Single mode fiber has a core diameter of 8-10 microns, specified as "mode field diameter", the effective size of the core, and a cladding diameter of 125 microns.

Specialty Fibers have been developed for applications that require unique fiber performance specifications. Erbium-doped single-mode fibers are used in fiber amplifiers. These are devices used in extremely long distance networks for regenerating signals. Fibers are optimized for bandwidth at wavelengths appropriate for DWDM systems or to reverse chromatic dispersion. This is an active area of fiber development.

Fiber Sizes and Types Fiber comes in two types, single-mode and multi-mode. Except for fibers used in special applications, single-mode fiber can be considered as one size and type. If you deal with long haul telecom or submarine cables, it is necessary to work with special single-mode fibers. Multi-mode fibers, originally, came in several sizes, optimized for various networks and sources. However, the data industry standardized on 62.5 core fiber in the mid-80s (62.5/125 fiber has a 62.5 micron core and a 125 micron cladding. This is now called OM1 standard fiber).

Recently, as gigabit and 10 gigabit networks have become widely used (SALEH; TEICH, 2013), an older fiber design has been revived (GIRARD, 2005). 50/125 fiber was used from the late 70s with lasers for Telecom applications before single mode fiber became available. 50/125 fiber (OM2 standard) offers higher bandwidth with the laser sources used in the gigabit LANs and can allow gigabit links to go longer distances. Newer OM3 or laser-optimized 50/125 fiber today is considered by most to be the best choice for multi-mode laser optimized applications. To identify the types of fiber in a cable, there are standardized color codes for the cable jacket covered under TIA-598. Figure 9 shows the spectral attenuation and chromatic dispersion (CD) of G.652 fiber. These two types of fibers are avaliable for PON. It is important to note that there are no CD and PMD impairment for PONs. For FTTH applications, low attenuation in this operating region would provide a better position on the network for future upgrade. The true value of this
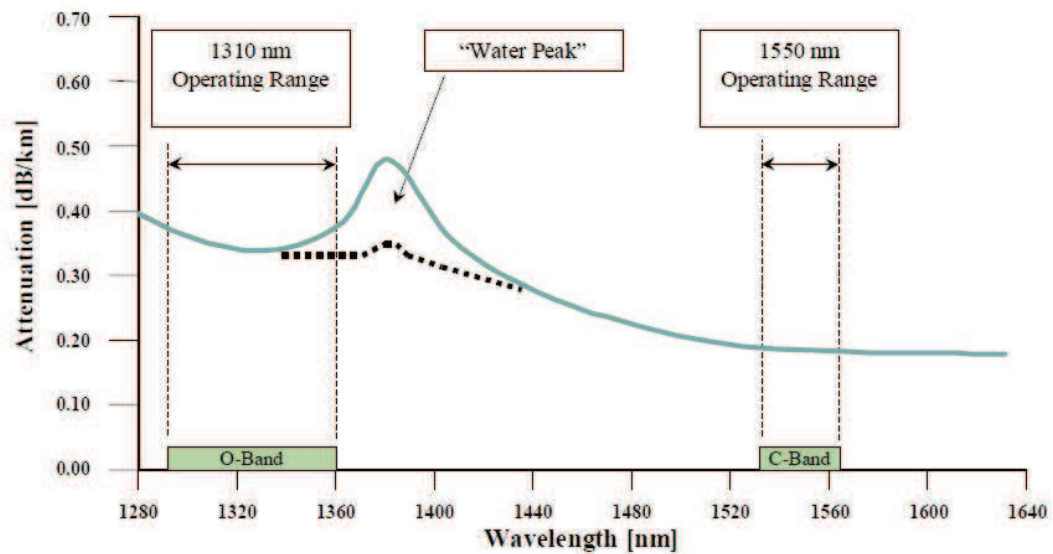
Figure 9 – Typical chromatic dispersion and spectral attenuation on FTTH PON fiber (GIRARD, 2005)

level of performance depends upon the design/operation priorities of the transmission network under consideration (YAMASAKI, 2011).

The limitations imposed by attenuation and chromatic dispersion have directly influenced the development of a variety of different single-mode optical fibers. Enhancements have been developed and have optimized performance in certain target applications. However, improving the performance of one attribute, typically, places limitations on others (ALCATEL, 2009).

2.3.1.2 Fiber Specifications

The usual fiber specifications are size (core/cladding diameter in microns), attenuation coefficient (dB/km at appropriate wavelengths) and bandwidth (MHz-km), for multi-mode fiber and chromatic polarization-mode or dispersion for single-mode fiber. While manufacturers have other specs for designing and manufacturing the fiber to industry standards, like numerical aperture (the acceptance angle of light into the fiber), ovality (how round the fiber is), concentricity of the core and cladding, etc., these specs do not generally affect users who specify fibers for purchase or installation.

2.3.1.3 Attenuation

The primary specification of optical fiber is its attenuation. Attenuation defines a loss of optical power. The attenuation of an optical fiber is expressed by the attenuation coefficient, which is defined as the loss of the fiber per unit length, in dB/km (Figure 10).

The attenuation of the optical fiber is a result of two factors: absorption and scattering. Absorption is caused by the conversion of light into heat through molecules in the glass.
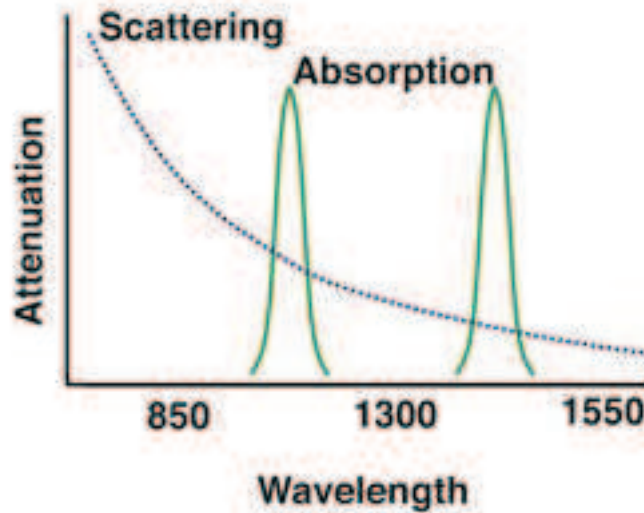
Figure 10 – Fiber attenuation

Primary absorbers are residual OH+(hydroxyl ions) and dopants used to modify the refractive index of the glass. This absorption occurs at discrete wavelengths, determined by the elements absorbing the light. The OH+ absorption is predominant and occurs most strongly around 1000 nm, 1400 nm and above 1600 nm (FATHALLAH; RUSCH, 2007).

The largest cause of attenuation is scattering. Scattering occurs when light collides with individual atoms in the glass and is anisotropic [1]. Light which is scattered at angles outside the numerical aperture of the fiber will be absorbed into the cladding or transmitted back toward the source. Scattering is also a function of wavelength, proportional to the inverse fourth power of the wavelength of the light. Thus, if one doubles the wavelength of the light (SALEH; TEICH, 2013); The scattering losses are reduced by 2 to the 4th power or 16 times.

For example, the loss of multi-mode fiber is much higher at 850 nm (called short wavelength) at 3 dB/km, while at 1300 nm (called long wavelength) it is only 1 dB/km. That means at 850 nm, half the light is lost in 1 km, while only 20% is lost at 1300 nm.

Therefore, for long distance transmission, it is advantageous to use the longest practical wavelength for minimal attenuation and maximum distance between repeaters. Together, absorption and scattering produce the attenuation curve for a typical glass optical fiber. Fiber optic systems transmit through the "windows" created between the absorption bands at 850 nm, 1300 nm and 1550 nm, where physics also allows one to basically fabricate lasers and detectors. Plastic fiber has a more limited wavelength band. This limits

---

[1] Anisotropic is the property of being directionally dependent, as opposed to isotropy, which implies identical properties in all directions. It can be defined as a difference, when measured along different axes, in a material's physical or mechanical properties (absorbance, refractive index, conductivity, tensile strength, etc.)

practical use to 660 nm LED sources.

The general critical issues related to a fiber can be divided into two categories as follows:

Optical:

❏ Absorption/attenuation;

❏ Chromatic dispersion and polarization mode dispersion (CD and PMD);

❏ Non-linear effects and

Mechanical:

❏ Bending;

❏ connection/joint;

The fiber used for PONs is the single-mode dispersion unshifted fiber, based on ITU-T Recommendation G.652 or IEC 60793-2 Ed 2 (ITU G.652, 2009). Non-linear effects (NLEs) can be a problem in fiber optical cables in PONs using high-power video signals at 1550nm. These are due to changes in the fiber's dielectric properties (index of refraction) or simulated scattering when using a very high electric field. In other words: the higher the optical power levels (at constant surface area), the higher the electric field. However, when a certain input intensity is reached, the output intensity will follow a non-linear curve, thus it no longer increases linearly. This particular input intensity is called the non-linear threshold. The field intensity for a given power level is greater with a smaller fiber core. Longer fiber lengths decrease the threshold for NLE. Table 1 presents how the Non-Linear Effects (NLEs) affect PONs. The most detrimental effect comes from the Brillouin stimulated scattering, which is due to the very high power used in overlaid analogue video transmission. Digital IP video should dramatically decrease this effect.

Table 1 – General non-linear effects and how they affect PONs.

Phenomenon	Name	Nature	Applicability	Remarks
Index of Refraction	SPM	1λ	Maybe	1550nm
	XPM	$N\lambda$	–	WWDM
	4WM	$N\lambda$	–	WWDM
Stimulated scattering	Brillouin	1λ i-1λ j	Expected	1550nm
	Raman	1λ-BB	–	1550-1600

XPM=Self-phase modulation XPM=Cross-phase modulation 4WM=Four-wave mixing BB=Broadband

2.3.1.4 Mechanical Issues

As for mechanical aspects, they too can potentially affect the performance of a PON. The main issues are:

❏ Bending (micro-bending, macro-bending);

❏ Discontinuities/gaps/voids;

❏ Misalignments/mismatches;

❏ Cracks/angular or straight breaks;

❏ Dirt in connections;

❏ Fiber melt/fusion splicing;

When the fiber bends too much, the angle of total internal reflection between the fiber core and the cladding is no longer met. Thus, since the angle of total internal reflection is what ensures the effective propagation of light inside the core, macro-bending can be a major issue as it will reduce the optical energy of the signal. Longer wavelengths around (1625 nm and 1650 nm) are more sensitive to macro-bending than shorter wavelengths. Micro-bending, is a microscopic bend in the fiber core and is a possible cause of polarization mode dispersion (PMD) in the optical fiber. The discontinuities, gaps, voids, misalignments, mismatches, angular faults, cracks and dirt typically occur during the connection of two fibers. All of the above cases affect the signal travelling through an optical fiber and they mostly occur where human intervention is required (e.g., when joining a fiber). In addition, if extremely high optical power is used, localized laser heating may occur and potentially, generate a thermal shock-wave back to source (SALEH; TEICH, 2013). At 1 m/s, the wave produces effects balanced between thermal diffusion and light absorption: thermal lensing caused by the periodic bubbling effect.

2.3.1.5 Cable Construction

The optical fiber has a primary acrylate coating that can be easily removed for splicing the fibers. Secondary protections, loose or tight, avoid direct pressure on the optical fiber. The reinforcement elements, both central and peripheral, prevent cable damage due to stresses during installation and operation. The cables have one or two plastic and metallic or dielectric armed covers to protect them from environmental and mechanical factors associated with storage, installation and operation. The sheaths and its thickness is chosen according to the final application, considering constraints such as maximum diameter or maximum weight permissible. Some of the parameters of the fiber can be affected by the manufacturing process or installation of cable: cut wavelength and PMD. A correct design and manufacturing process allows these values to always be under the limits set

by the relevant ITU-T recommendation (GIRARD, 2005). The optical and geometrical characteristics are little affected by the process of wiring, which gathers prominently featured recommendations for long-span transmission installations. Optical cables are designed to protect the optical fibers from damage, which can occurs due to the rigours of installation and from the demands of the surrounding environment. However, no single optical cable design is universally superior in all applications. To meet application-specific requirements, outside plant (outdoor), indoor/outdoor cables and inside plant (indoor) cables must be designed for their intended installation environment. The consequences of optimizing a cable design for outdoor use can prove counter productive to meeting the requirements for indoor placement and vice versa. For example, the most popular cable jacket material for outdoor use will not pass flame-resistance tests required for placement indoors (GIRARD, 2005). In general, optical cables installed in an outdoor environment are exposed to more severe mechanical and environmental conditions than cables installed in the protected, climate-controlled, indoor environment. Outdoor installations (usually lashed aerially, pulled through ducts or directly buried in the ground) are subjected to combinations of ultraviolet (UV) radiation, standing water, cable-gnawing rodents, extreme temperatures, and other hazards specific to outdoor deployment. Indoor installations (horizontal, riser, or plenum applications) must conform to building codes and be flame retardant. Cables designed for indoor/outdoor applications strike a performance compromise between dedicated indoor and outdoor cables. Indoor-outdoor cable designs provide flexibility for utilizing one cable design but are more expensive and should only be utilized in transition applications to link dedicated outdoor cables with dedicated indoor cables. At a minimum, there are at least three different cable products necessary to construct the physical plant of the network design depicted. First, a higher-fiber-count cable will be required for the "Feeder" and "Distribution" portions of the network to establish the optical fiber routing from the central office/head-end to the network access point (NAP). Second, a cable containing one or two optical fibers will be required to link the NAP to the network interface device at the individual subcriber's premises. Third, an interconnect cable assembly of some type will most likely to be required to link patch panels in the CO/HE.

The optical cable serves two functional roles which are vital to the deployment and durability of the optical fiber in the field. Some of the most significant basic cable design elements include the following:

❏ Identification and organization;

❏ Tensile strength;

❏ Resistance to mechanical stress (bend, impact, compression, twist);

❏ Temperature sensitivity;

❏ Water blocking protection (outside applications);

❏ Resistance to outdoor environmental hazards – ultraviolet (UV) radiation, rodents,chemicals and lightning (outside applications);

❏ Flame retardants (inside applications).

2.3.2 Optical Fiber Connectors

According to Telcordia GR-326, Generic Requirements for Single-Mode Optical Connectors and Jumper Assemblies, optical fiber connectors are used to join optical fibers where a connect/disconnect capability is required. The basic connector unit is a connector assembly. A connector assembly consists of an adapter and two connector plugs. Due to the sophisticated polishing and tuning procedures that may be incorporated into optical connector manufacturing, connectors are generally assembled onto optical fibers at a supplier's manufacturing facility. However, the assembly and polishing operations involved can be performed in the field, for example, to make cross-connect jumpers to size (HAYES, 2009). An optical fiber connector joins two ends of an optical fiber, and enables quicker connection and disconnection than splicing. The fiber endfaces of the two connectors are pressed together, resulting in a direct glass to glass or plastic to plastic contact, avoiding any glass to air or plastic to air interfaces, which would result in higher connector losses (KEISER, 2003). Fiber optic connectors can be divided into three groups: simplex, duplex and multiple fiber connectors. Simplex connector means only one fiber is terminated in the connector. Simplex connectors include FC, ST, SC, LC, MU and SMA. Duplex connector means two fibers are terminated in the connector. Duplex connectors include SC, LC, MU and MT-RJ. SC, LC and MU connectors have both simplex and duplex version. Multiple fiber connector means more than two fibers (for up to 24 fiber) are terminated in the connector. These are usually ribbon fibers with fiber counts of 4, 6, 8, 12 and 24. The most popular ribbon fiber connector is the MT connector. In PON applications, high-power analogue video signal is carried, therefore the APC connector is required. The APC connector is an angled (8 degrees) connector and as such provides very low reflection (ORL) 65 dB or better.

2.3.2.1 Enclosures

There are a number of enclosures used in PONs:

❏ The splitter enclosure;

❏ The splice enclosure;

❏ The drop enclosure
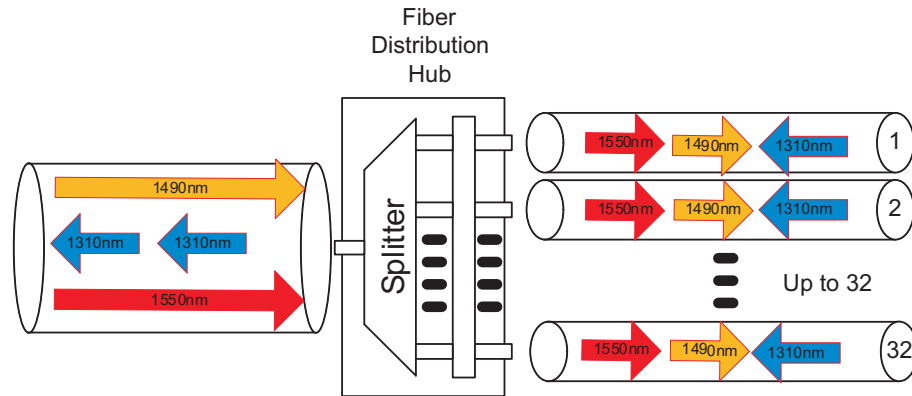
Figure 11 – Bidirectional 1 x N PON splitter

There are two IEC standards that are particularly important for enclosures: IEC 61758-1 Ed.1.0, interface standard for closures, General & Guidance, and IEC62134-1, Fibre-optic enclosures, Generic Specification (IEC 61758-1,).

2.3.3   Splitter

The Splitter (as Shown in Figure 11) is a bidirectional broadband branching device that has one input port and multiple output ports. The input (downstream) optical signal is divided among the output ports, allowing multiple users to share a single optical fiber and consequently share the available bandwidth of that fiber. In the upstream direction, optical signals form a number of ONTs, which are combined into the single fiber. Splitters are passive devices due to the fact they require no external energy source other than the incident light beam. These are classified as broadband and only add losses principally due to the fact that they divide the input (downstream) power. Splitter loss is usually expressed in dB and depends mainly on the number of output ports (about 3 dB for each 1 x 2 split).

It should be noted that, contrary to what one might expect, the splitter adds approximately the same loss for light travelling in the upstream direction as it does for downstream direction.

There may be one splitter of several cascaded splitters in an FTTH PON, depending on the network topology (See Figure 5 and Figure 6). ITU-T Recommendation G.983 currently allows split ratios up to 32 (ITU G.983.1, 2005), whereas Recommendation G.984 extends this up to 64 splits (ITU G.984.1, 2008). Splitters can be packaged in different shapes and sizes depending on the basic technology used. The most common types are the plans wave guide (typical used for high split counts) and the fused tapered (FBT) fiber couples (typically used for relatively low split counts). Figure 12 illustrates the FBT fiber technology. The amount of light coupled varies with the core-to-core proximity (1), the interaction length (2) and phase B (3).

Power splitters are used to divide the optical power into different channels. The

Fused Biconic Taper (FBT) Fiber
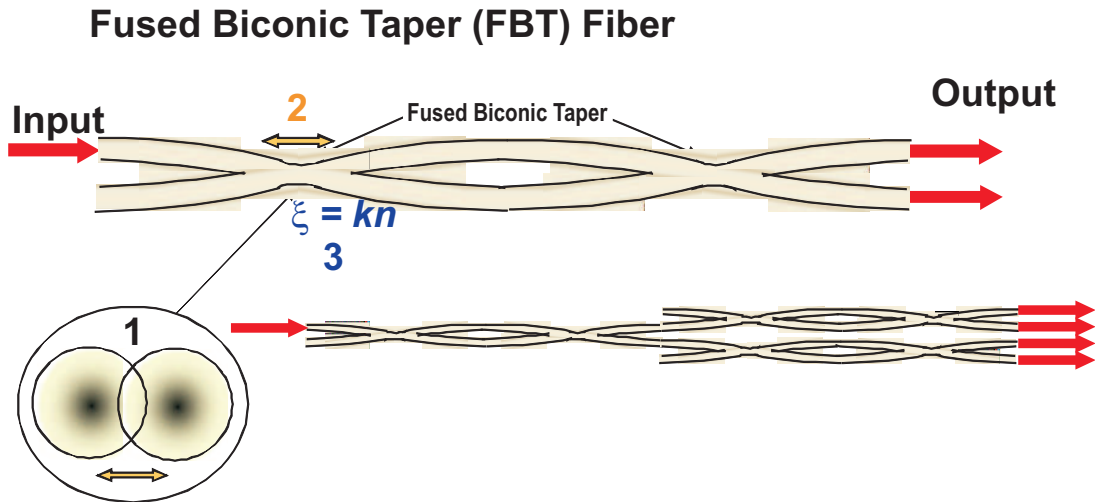
Figure 12 – Splitter design based on fused bi-conic tapered fiber (FBT)

splitter supports one port at one end and up to N ports at the other end. Typically, the maximum number of ports is 64. Therefore, a signal sent from one end, can be distributed to 64 possible customers, simultaneously. This application is ideal for video distribution (GIRARD, 2005). For data and voice, the use of time division multiple access (TDMA) enables customers to receive and send exactly what they choose, without knowing, what other customers are receiving and sending. Additional technologies, such as WDM PON, are under investigation for point-to-multipoint networks (GROBE; ELBERS, 2008). The most attractive alternative is wavelength division multiple access (WDMA), which dedicates a particular wavelength to each customer. A splitter's (Figure 3) primary benefit is its nature as a passive component, requiring no maintenance and no power activation. However, its primary drawback is high rate of insertion loss. Insertion loss is defined as $10*\log (1/n)$; where n is the number of ports (2 to 64). Table 2 shows the expected insertion loss that corresponds to a specific number of ports.

Table 2 – Number of ports/Insertion loss relation

Number of Ports	Insertion Loss (dB)
2	3
4	6
8	9
16	12
32	15
64	18

This superimposition makes it very difficult, and sometimes impossible to associate events on the waveform with the specific lines on which the events occur (RAD, 2010).This is probably the most common problem faced by OTDR operators when dealing with splitters. Along the waveform on the OTDR trace, the scattered light of all output fibers is superimposed into a single waveform. This superimposing of the scattered light from the
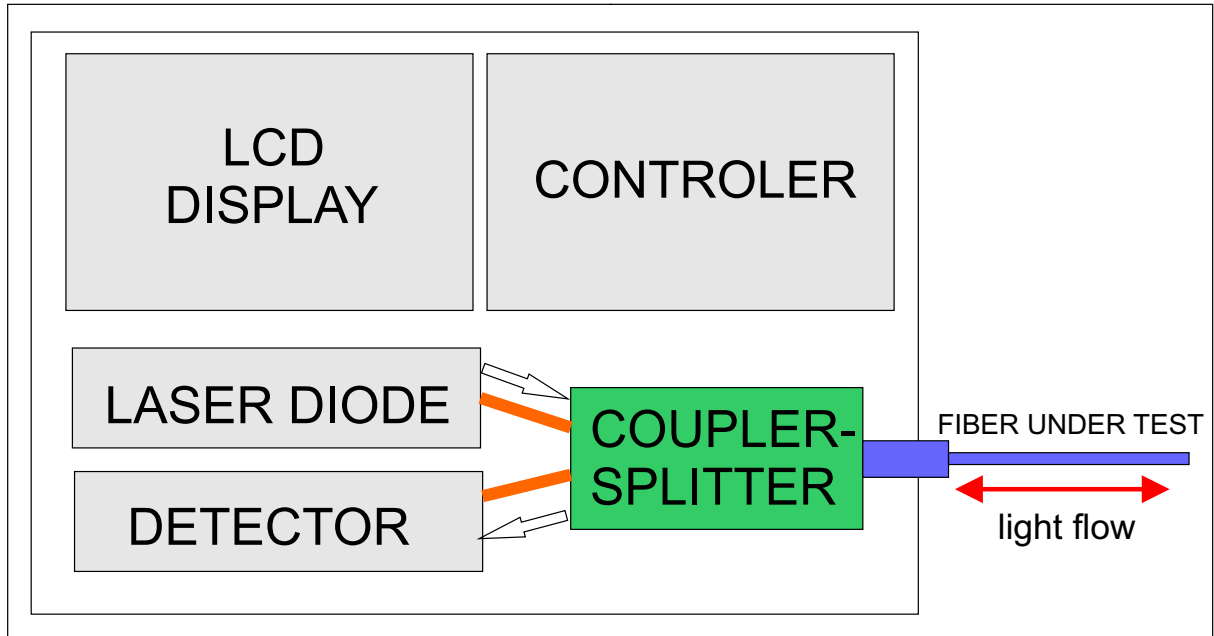
Figure 13 – OTDR Block Diagram

output makes the OTDR signature ambiguous. Due to the combination of the scattered light into a single composite waveform, it is very difficult to associate events on the output side of the splitter to its respective branch.

2.4 OTDR Concepts

An OTDR is composed of a laser source, an optical sensor, a coupler/splitter, a display section, and a controller section as presented in Figure 13. A laser diode sends out pulses of light on command from one controller, adjusting the duration of the pulse (Pulse Width) for different measuring conditions. The light goes through the coupler-splitter and into the fiber under test (FUT). The coupler-splitter has three ports, one for the source, the fiber under test, and the sensor. This device allows the light to travel only in specific directions: from the laser source to the fiber under test. Also from the fiber under test to the sensor. Thus, pulses from the source go out into the fiber under test and the returning Backscatter and Fresnel reflections are routed to the sensor (SIMARD, 2009).

The objective of the OTDR measurement is to determine the backscattering impulse response of the fiber under test. The OTDR's pulse approximates an ideal delta-function impulse rather than being a perfect copy of it. The result of a convolution with a finite pulse leads to a smoothed version of the impulse response (ANDERSON; BELL, 2004).

The typical OTDR measurement curve (Figure 14) uses the vertical scale to represent the reflected level on a logarithmic scale (in dB), whereas the horizontal axis corresponds to the distance between the instrument and a location in the fiber under test. The mea-
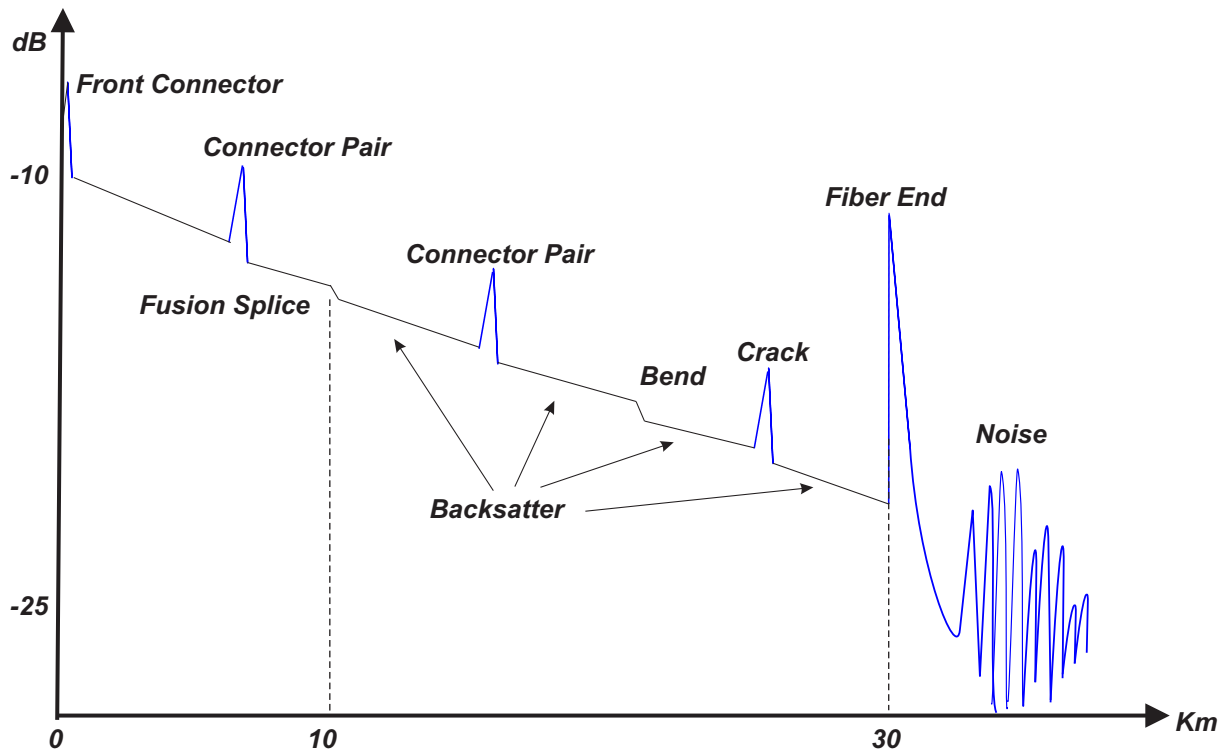
Figure 14 – Typical OTDR trace

sured response exhibits three types of features: (1) straight lines caused by distributed Rayleigh backscattering, (2) positive spikes caused by discrete reflections and, finally (3) steps that can be positive or negative depending on physical fiber properties (AK-WANIZAM, 2009).

The first event from left to right is the reflection of the front connector that matches the OTDR to the fiber under test. As this reflection covers the near-end measurement zone, it is an undesirable event that hides information concerning the fiber to be tested. A clean high-quality connector with low reflectance is mandatory to achieve best results. A bad connector not only decreases launch power by insertion loss, but also causes the returning light to be re-reflected back into the fiber under test again, generating multiple echoes of ghost patterns. The trace is plotted as power vs. distance and the slope of the straight lines gives the fiber attenuation in dB/Km. Fusion splices and bends show only insertion loss without a reflection. These are called non-reflective events.

A mismatch in the refractive index causes a Fresnel reflection leading to spikes super-imposed on the backscatter signal. Mechanical splices, connectors and cracks, in general, show a tiny air gap, which reflects light rather than scattering it. They belong to reflective events. A non-terminated open fiber end can cause a strong reflection depending on the condition of the fiber end surface. At a glass-to-air transition, up to 4% of the optical power can be reflected back to the OTDR. Behind the fiber end, no optical signal can be detected and the curve drops to the receiver noise, which ultimately, limits the detectable
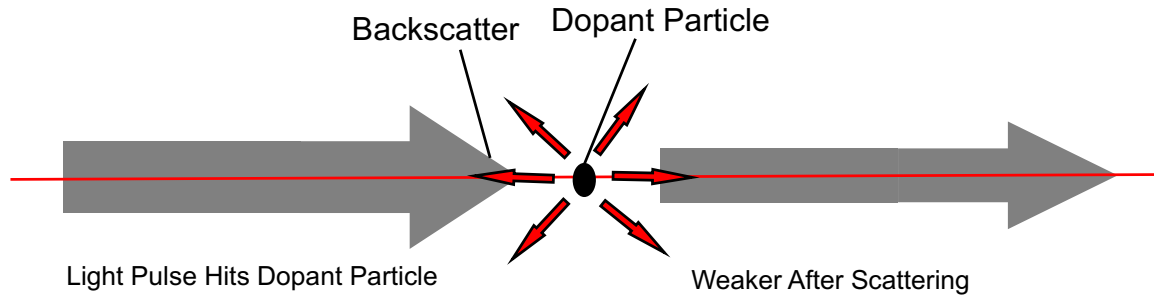
Figure 15 – Rayleigh Scattering

power level.

2.4.1 Rayleigh Scattering

Rayleigh scattering refers to the scattering of light off the air molecules and can be extended to scattering from particles up to about a tenth of the wavelength of the light. The blue color of the sky is caused by the scattering of sunlight by the molecules of the atmosphere (CLAYS; PERSOONS, 1991). The scattering is more effective at short wavelengths (the blue end of the visible spectrum). Thus the light scattered down to the earth at a large angle with respect to the direction of the sun's light is predominantly at the blue end of the spectrum (TSUJIKAWA et al., 2007). This effect can be considered to be elastic scattering, since the photon energies of the scattered photons is not changed. Clouds, in contrast to the blue sky, appear white to achromatic gray.

When a pulse of light is sent down to a fiber, a part of the pulse runs into microscopic particles (dopants) in the glass and becomes scattered in all directions. About 0.0001% is scattered back in the opposite direction of the pulse and it is called backscatter Figure (15). Since the dopants in optical fiber are uniformly distributed throughout the fiber, due to the manufacturing process, this scattering effect occur along its entire length. Longer wavelengths of light exhibits less scattering than shorter wavelengths.

2.4.2 Fresnel Reflection

Whenever light is travelling in a material (such as an optical fiber), it encounters a different density material (such as air). Some of the light up to 4% is reflected back towards the light source while the rest continues out of the material (BESPROZVAN-NICH; NABOKA, 2000) 16. These sudden changes in density occur at the ends of fibers, or at fiber breaks and sometimes at splice points. The amount of reflection depends on the magnitude of change in material density described by the Index of Refraction IOR (JUDD, 1979). Larger IOR means higher densities and the angle that the light spikes the interface between the two materials is also higher.

This is used by the OTDR to, precisely, determine the location of fiber breaks. Although
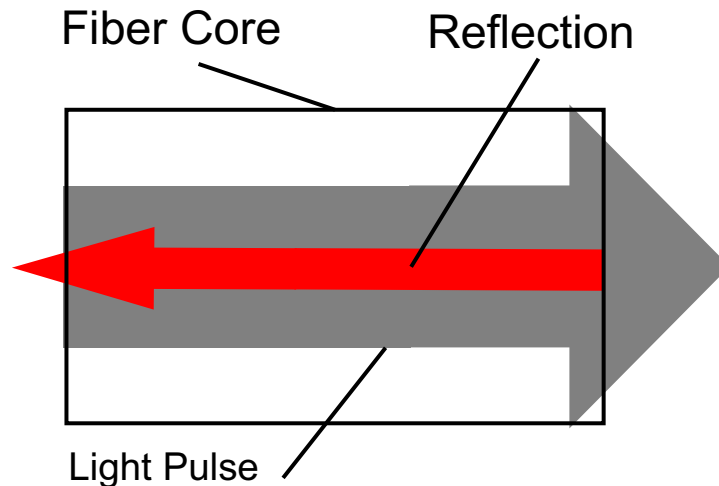
Figure 16 – Fresnel Reflection

the OTDR measures only the backscatter level and not the level of transmitted light, there is a very close correlation between the backscatter level and the transmitted pulse level. The backscatter light is a fixed percentage of transmitted light. The ratio of the backscattered light is also known as backscatter coefficient. If the amount of the transmitted light drops suddenly from a Point A to a Point B in the fiber (caused by a tight bend, a splice between two fibers or by a defect), then the corresponding backscatter from Point A to Point B will drop by the same amount. The same loss factors that reduce the levels of a transmitted pulse will show up as a reduced backscatter level from the pulse.

2.4.3   Dead Zones

Dead zones are related to the presence of reflections when the reflected signal saturates the OTDR receiver (DERICKSON, 1998). The receiver's electronic circuit is slow to recover its sensibility, after the saturation results in information loss. If the receiver saturates due to strong signals, it will take some time to recover from this overload condition. Consequently, the measured fiber response is superimposed by the receiver's overload behaviour, yielding a distinct fiber segment covered by an exponentially diminishing tail.

A Dead zone is classified in two ways. Firstly, an "Event Dead Zone" is related to a reflective discrete optical event. In this situation, the measured dead zone will depend on a combination of the pulse length and the size of the reflection resulting in a distance between the beginning of a reflection and the -1.5 dB point on the falling edge of the reflection as indicated in Figure 17. After the event dead zone, an adjacent reflective event can clearly be recognized.

Secondly, an "Attenuation Dead Zone" is related to a non-reflective event. In this situation, the measured dead zone will depend on a combination of the pulse length. It is defined as the distance from the start of a reflection to the point where the receiver has recovered to within a 0.5 dB margin around the settled backscatter trace.
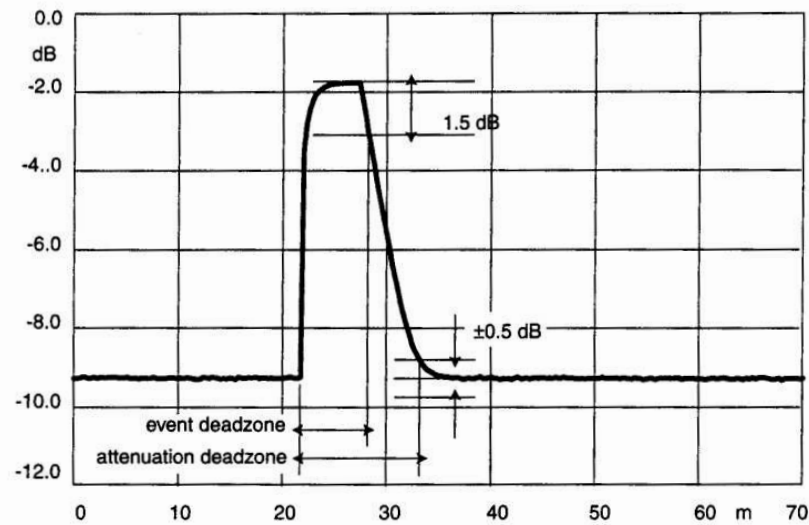
Figure 17 – Attenuation and event dead zone

Commonly, a 35dB reflection is used for dead zone specifications, in other words, about 0,03% of optical power at this point is reflected and superimposed with backscattered light – the power level which is a function of the chosen pulse width. Therefore, the actual height, seen on the OTDR display, depends upon both reflectance and pulse width, for a given fiber. Note that very short width pulses do not necessarily lead to shorter dead zone attenuations. This is related to the fact that as the pulse gets narrower, the difference between the backscatter level and the top of the reflection increases. With a finite receiver bandwidth, the exponential tail of the falling edge adds, significantly, to the dead zone.

2.5   Constraint Management

The word constraint has several connotations. It has been taken to mean a relation over a Cartesian product, a Boolean predicate, a fuzzy relation, a continuous figure of merit analogous to energy and various other arbitrarily complex symbolic relationships. A concise definition is given by (STEPHANOPOULOS, 1987): "A constraint is a relation stating what should be true about one or more objects".

Engineering Design is constraint-oriented (LAMOUNIER, 1996). Much of the design process involves the recognition, formulation and satisfaction of constraints. Serrano (SERRANO, 1987) defines a constraint as a requirement that restricts a component or component relationships, where component and object are taken to mean the same.

In particular, engineering design is specified in terms of their geometric and engineering constraints (SILVA, 2006). Using a constraint satisfaction paradigm the designer is allowed to concentrate on "what", not on "how". The constraint implicit in the knowledge and data sources may be analysed and represented naturally. These constraints may be

uniformly introduced and used in various directions on the knowledge available in the system.

Geometric constraints are relationships between two different geometric entities (e.g. the relationship between a tangent line and a circle). On the other hand engineering constraints are equations used to represent basic principles of engineering, as the power loss in the optical fiber. FTTH PON optical networks architecture have its specific constraints specially defined in this thesis. The following section shows how this constraint architecture has been defined by means of the proposed solution. More details about design constraint management can be found at (LAMOUNIER, 1996) , (SILVA, 2006) and (LIMA, 2008).

2.5.1 FTTH PON Design Constraints

For FTTH Network Design, the Geometric Constraints are the existing relationships between two different geometric entities. Engineering Constraints are equations that represent the physical concepts of electronic components (e.g., Optical Power, Optical Cable loses, Optical Connectors, Splitters, interferences, noise frequencies filters, etc). Both constraints can be seen as a unique set of equations (LIMA; JUNIOR, 2010). The possibility, of modifying some parameters and to propagate them upstream and downstream over an electronic cable network must be considered. This automation is related to algebraic manipulations (Solution of constraint sets) required by the user. The hybrid constraints concept is the ideal solution as a method for solving the system of equations and geometric constraints. These systems rely on numeric and interactive solving techniques (LAMOUNIER, 1996). Graph-based models can decompose the equations into smaller sets in order to achieve a more efficient equation solution set. The concept of coupled constraints, allow direct manipulations of under-constrained FTTH PON network parameters. The next section, shows the characterization of constraint-based approaches for the OTDR signal and the physical coupling constraint network distribution both into a single platform.

2.5.2 The Constraint Data Model for FTTH PON Network

Figure 18 shows a constraint representation of the Optical Cable and one Splitter. In the FTTH Schema on the left, the physical representation for the connection between one Optical Feeder to a splitter by optical cables to the optical cable C1, is presented.

On the right, the Geometric Graph represents the existing relationship of each of the geometric constraints, the feeder optical cable C1 and the splitter S1. Finally, the Equation Graph (c) on the right is illustrated through the use of a specifically developed equation graph.
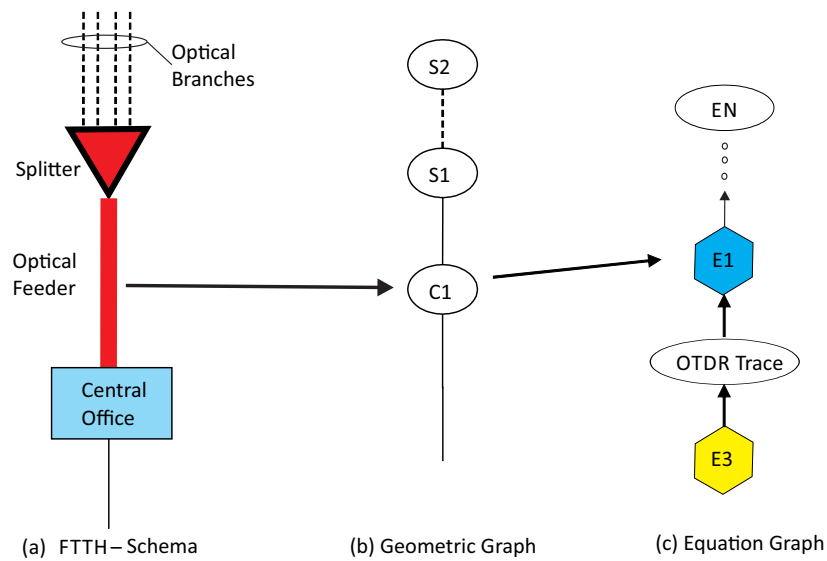
Figure 18 – Graph representation of an Optical Cable and a Splitter.

The Geometric Graph is manipulated by the user inside a CAD environment, using a graphical interface (GUI) and for example, when some graphical parameter is modified, it provokes a modification on the equation graph in a synchronous form. So that the User will watch, at the same time, two different worlds, one being the physical world represented by computer graphics environment and the other is the "optical world", represented by the OTDR data measurements, controlled by the Equation Graph.

2.6 Concluding Remarks

The purpose of this chapter was to provide an overview of the fundamentals of FTTH PON technology, explaining the technical characteristics and network architectures, describing the basic concepts employed herein and the prerequisites for understanding the assumptions used in the proposed experiments and in software development.

We should note that a very important concept for the work under development called "dead zone" was presented , and used to define parameters for the OTDR signal simulation section.

CHAPTER **3**

Related Work

3.1 Introduction

To support this work and identify the features of interest in the field of research, we conducted a literature review with recently published works related to FTTH PON monitoring and strategies used to detect degradations and faults in the fiber network. This should not be considered an exhausted list, however, we focus on research results that mainly propose tools for computational simulation.

3.2 Events Detection in Optical Fiber Networks

The FTTH business needs new network maintenance technologies that can, economically and effectively, cope with the massive FTTH fiber plants that are yet to come. Liu, Fenglei and Zarowski, Christopher J. (LIU; ZAROWSKI, 2001) propose a method for detecting and locating connection splice faults (events) in fiber optics by digital signal processing (DSP) of noise on optical time-domain reflectometry (OTDR) data. This is motivated by the fact that as fiber becomes more widely adopted as a communications medium, methods of automated fault detection/location will become more important.
The approach taken uses Gabor series expansion coefficients to coarsely localize the faults (FEICHTINGER; STROHMER, 2002). Due to the presence of measured noise, these coefficients are random variables, and it is the Gabor coefficients with a non-zero mean that determine fault presence and location. Coefficients with non-zero mean are found with the aid of the Rissanen minimum description length (MDL)criterion for model order estimation (RISSANEN, 1983). The results show that the method is able to distinguish connection splice events from noise and the Rayleigh component in the OTDR data (Figure 19).

Therefore, in this paper (FENGLEI; ZAROWSKI; J., 2004) develops the rank-1 matched subspace detection and estimation algorithm that employs more computation
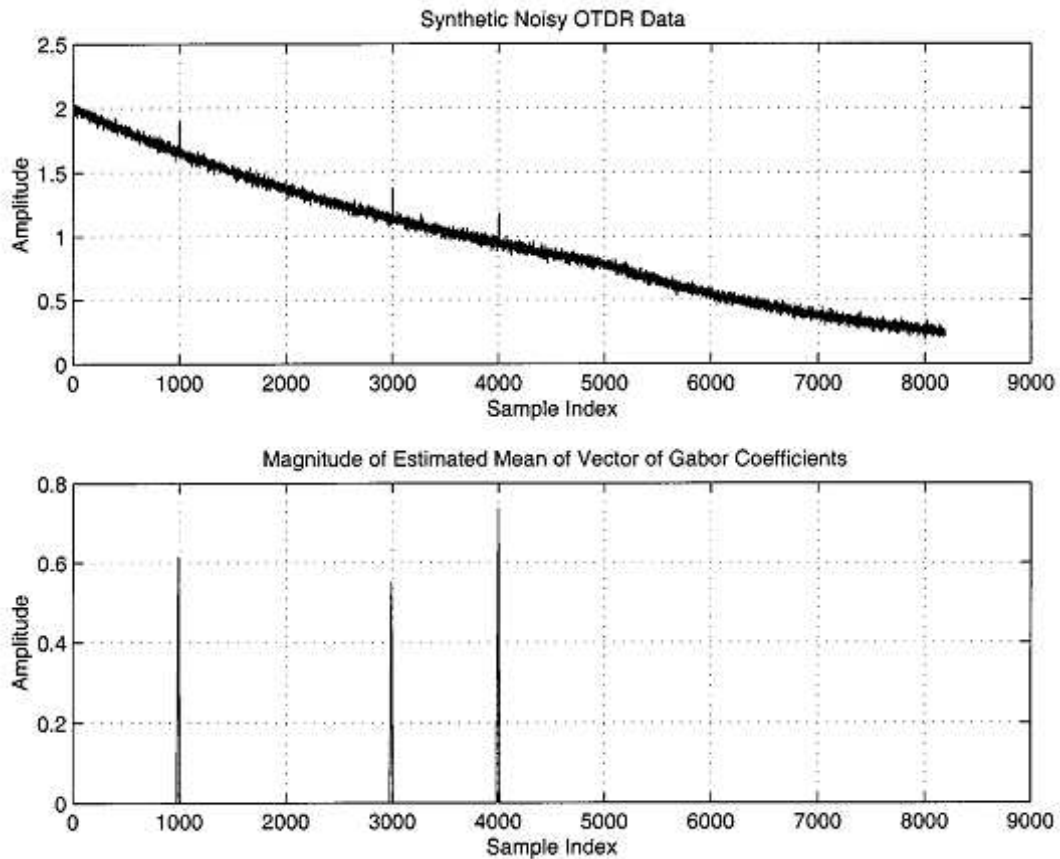
Figure 19 – Algorithm results over a loud OTDR Signal (LIU; ZAROWSKI, 2001)

to achieve a greater accuracy in event position estimation. It is based on the matched subspace detection theory of Scharf and Friedlander (SCHARF; FRIEDLANDER, 1994).

Kim (KIM et al., 2008) presents a method for calculating the attenuation factor and detecting the reflective and non-reflective events using the Kalman filter (WELCH; BISHOP, 1995). For data whose signal-to-noise ratio is sufficiently high, they propose a second order linear model by approximating the measurement data, after the logarithm is applied. In this work, we design the optimal and suboptimal linear Kalman filters based on this model. Through a representative experiment, the proposed method is verified to precisely calculate the attenuation factor and detect the events with minimal computational resources.

Inspired on sound signal processing, Lima (LIMA; LAMOUNIER; BARCELOS, 2013) also proposes an algorithm based on the Teager Energy Operator (TEO), method developed for testing and evaluating FTTH networks from the Central Office. This method allows for the identification of event failures in the optical branches after the PON splitter, as presented in Appendix 1.

3.3 Monitoring Techniques for PON

In 2009, MS Ab-Rahman (AB-RAHMAN B NG, 2009) proposed the Survivability of a PON monitoring and restoration with microcontroller, using a combination of the hardware and software, designed for PON appliances. The system uses access control system (ACS) for fiber-to-the-home passive optical network (FTTH-PON). It has a specially designed hardware, interfaced with a Ethernet integrated microcontroller to monitor the status of optical signal flows and to provide the restoration against fiber failures/faults in FTTH-PON. It also introduces the centralized troubleshooting system by means of Smart Access Network Testing, Analyzing, and Database (SANTAD) as shown in Figure 20. This access control system (ACS) is a subsystem that controls the troubleshooting mechanism carried out by SANTAD (AB-RAHMAN B NG, 2009). This design is implemented together with optical line terminal (OLT) at central office (CO) to centralized monitoring and for controlling each optical fiber line's status as well as detecting any failure that occurs in the network system, downwardly from CO towards multiple optical network units at different customer residential locations.
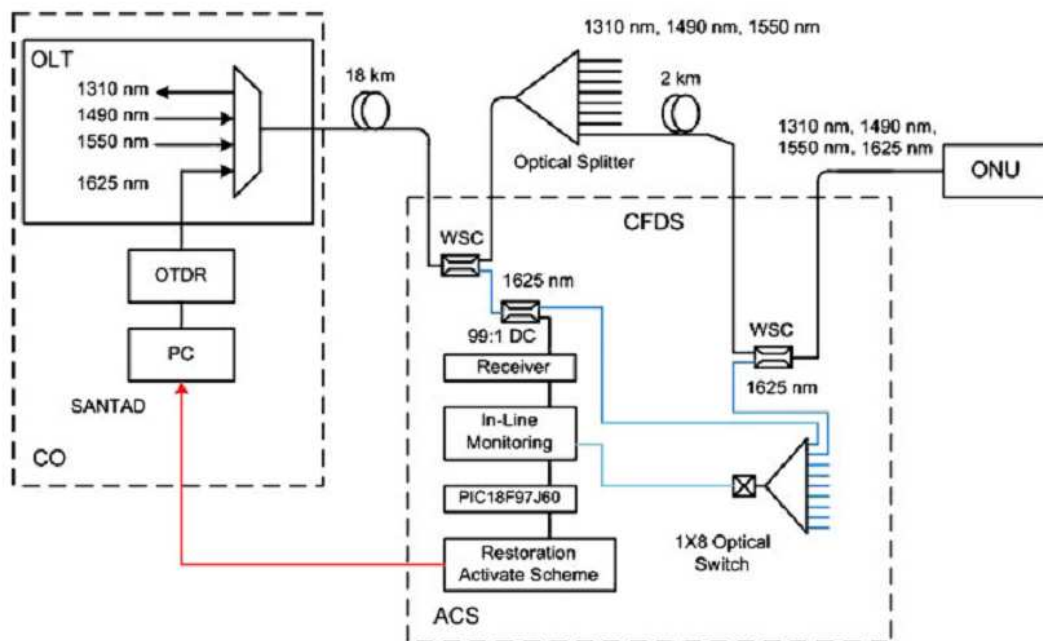
Figure 20 – Schematic diagram of the proposed surveillance and protection scheme with centralized monitoring (AB-RAHMAN B NG, 2009)

The benefits and contributions of SANTAD are:

❏ Testing a live network.

❏ Help to prevent, identify and address problems.

❏ Set up a mechanism of interactive connection between CO and customers/end users.

❏ Reduce/save time and cost.

❏ Overcome the monitoring issues in FTTH-PON by using conventional OTDR upwardly or downwardly.

❏ Increase survivability, efficiency, and flexibility of FTTH-PON with tree topology or P2MP configuration.

In 2010, Rad (RAD, 2010) experimentally demonstrated the monitoring of a PON using periodic coding technology and analysing the performance of fiber fault monitoring of a PON, by a centralized, passive optical coding (OC) system. In this work, new mathematical models were developed for monitoring system elements and signal processing operations. They considered the wavelength vs time (two–dimensional) coding in addition to the one dimensional coding. Thus, the work illustrated that the geographical distribution of the clients affects the interference in the proposed system, by considering geographical distributions describing realistic PON systems (Figure 21).
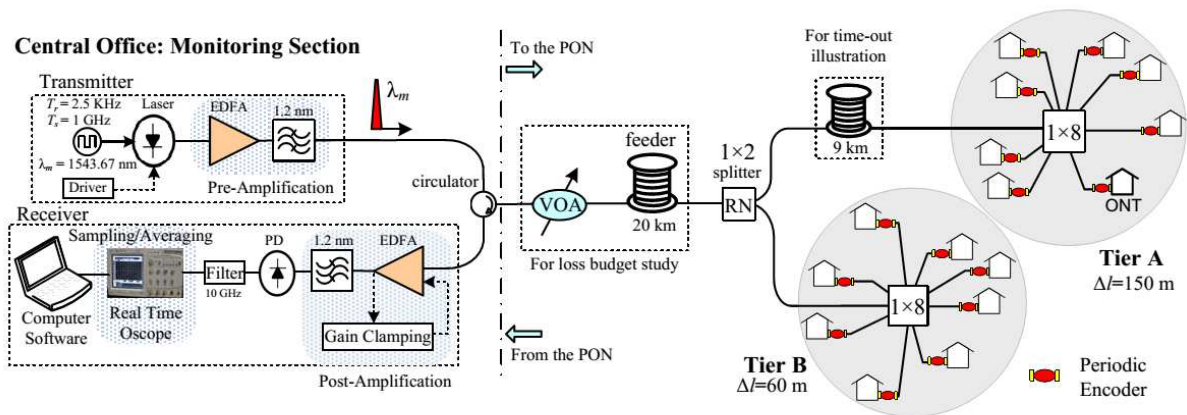
Figure 21 – Experimental setup for PON monitoring using periodic coding technology(RAD, 2010).

Their main results are the experimentally demonstrated fiber link quality monitoring of a PON using periodic codes for up to 16 customers. The proposed system actives a robust monitoring for networks with a tiered geographic distribution by exploiting information about the distance separating clusters. The experimental setup allows a capacity scale up for 64 customer PON. This work also studied the final loss budget limitation of optical coding monitoring system as a function of the post–detection circuit specifications. In addition, their numerical studies show that OC monitoring technology is able to support the current PON standards.

Ab-Rahman (AB-RAHMAN, 2011) shows that the OTDR within the network is able to detect the component that causes losses in the network. However, elements acting as a power splitter are not able to be detected by the OTDR. Therefore, the Access Control

System (ACS) is developed to bypass those elements and allows the use of OTDR entirely. With the combination of SANTAD and CAPU they ensure that the monitoring can be handled efficiently and failures can be restored immediately, just after being detected by the sensor. This method is proven to be a faster, more efficient and reliable method than the first. Additionally, it can be upgraded to monitor the line status by accumulating all the results onto only one display computer screen. The new configuration of FTTH is named as modified FTTH. Nevertheless, this mechanism is not of interest for implementation, since the installation cost is too high (three times higher). This author also proposes another device which assembles all the features offered by the modified FTTH onto one single device named as Multi access Detection Unit (MADU). In the end, they compare the installation cost between the conventional modified FTTH and MADS based solution for different network size/number of users.

The same authors (AB-RAHMAN et al., 2012) have presented a simulation of optical splitter to be applied in FTTH-PON named Multi Ratio Optical Splitter (MROS), using a Virtual Lab Waveguide design. This tool is founded on the Beam Propagation Method (BPM) as a wave propagator (KOSHIBA; TSUJI; HIKARI, 2000). This meets the principles presented in our work since we use similar physical concepts (Figure 22).
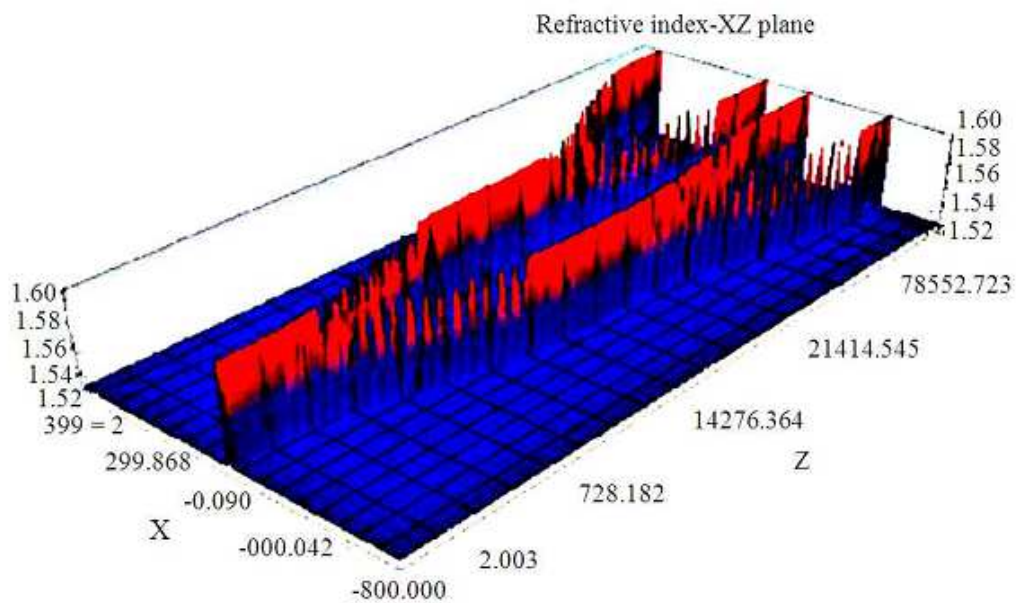
Figure 22 – 3-D graph of effective index ratio of waveguide against propagation distance(AB-RAHMAN et al., 2012)

The BPM software simulation tool considers the total output power from all splitter arms expected to be equal to the input power. However, in practice, there are various types of losses that affect the performance of the design. These losses are caused by scattering and absorption at the fiber cladding. According to the authors results, the total losses for MROS with an input power calculated is relatively small and acceptable.

These understandings are very close of our work in the Splitter Equation in section 4.2.2.

Patryk J. Urban, Gemma Vall-llosera and Eduardo Medeiros (URBAN et al., 2013) present a method to monitor power-splitter- and wavelength-splitter-based PON, through combined techniques of OTDR and optical transceiver monitoring (OTM). The method is non-invasive to data traffic flow and requires no additional functionality (hardware or software) at the ONT side. The authors presented a system named Fiber Plant Manager (FPM), which provides a comprehensive centralized monitoring activity. This solution requires an External Wavelength Adaptation Module (EWAM) which externally tunes the OTDR wavelength to route the test signal to a given group of drop links. The proposed solution is capable of supporting many different PON architectures. As one notes, the OTDR and EWAM are always shared at the CO. Sending the OTDR signal via the same feeder fiber as the data channels implies an extra filter at the CO and a corresponding loss. It is interesting to observe that the authors used as concept proof to verify the magnitude of the detectable event a single 1:8 splitter and several fiber spans (Figure 23).
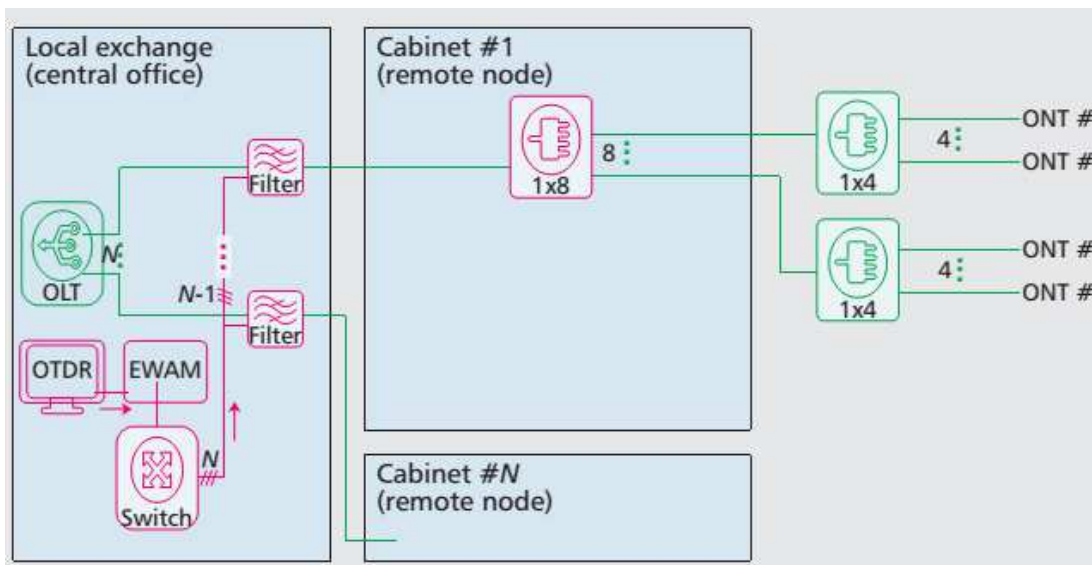
Figure 23 – FPM for cascaded PS-based PON architecture with common feeder fiber (URBAN et al., 2013)

3.4 Concluding Remarks

The goal of this chapter has been to describe published works that correlate with our work proposal, within their relevant topics. These topics were used for comparative proposes and as inspiration for the current investigation.

CHAPTER **4**

Experimental Methodology

4.1 Introduction

In this chapter we describe the experimental arrangement performed in the laboratory, based upon the architecture of a real PON FTTH network using a passive splitter typically used in metropolitan networks. Several tests were performed and the curves obtained through experiment were compared to the splitter computer simulation. Through comparison we performed a proof for the concept of the splitter equation introduced in this research work.

4.2 Experimental Setup

With the purpose of creating an experimental arrangement, similar to real networks, this setup places an OTDR in a location as if it were inside a CO (Central Office), distributing signals to multiple ONUs (Optical Network Units) at different locations of residential customers (in the downstream direction), bypassing the 1x8 optical splitter.

A commercially available OTDR model (MW9076D1– Anritsu), with a 1550 nm laser source, commonly used in failure detection control and in-service troubleshooting (without affecting the triple play transmission services) was chosen. The tested network presented in Figure 24 was set-up to serve as a platform to study the mechanisms and characteristics of optical signals in (good/ideal) working condition.

This configuration has been chosen due to the fact that it represents a common architecture (real world) where a primary 8-port splitter is installed, leaving these secondary fibers going to the secondary network until the last mile, where one can obtain the - Network Access Point (NAP).

As presented in Table 3 it is possible to correlate all optical cable characteristics (dB/Km) used for each branch with its correspondent return loss and physical/optical length.
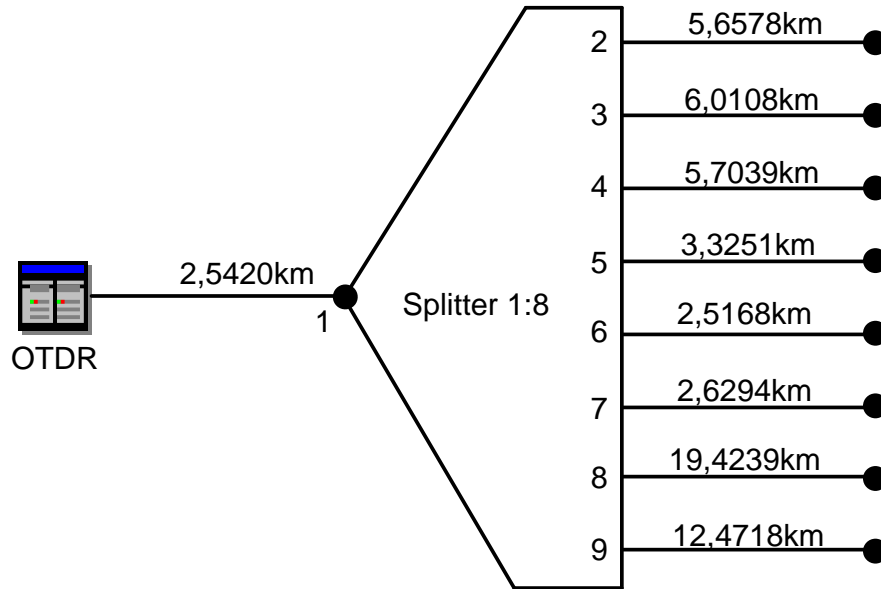
Figure 24 – Experimental Network Tested (Splitter configuration and branches)

Table 3 – Optical Cable Bobbin details connected by the branches

Branch	Insertion Loss	Optical Return Loss	Length	Loss/Km
	(dB)	(dB)	(Km)	(dB/Km)
0	-	-	2.5420	0.2
1	10.375	71.14	5.6578	0.190
2	12.173	59.61	6.0108	0.224
3	11.438	60.14	5.7039	0.200
4	10.088	73.25	3.3251	0.233
5	10.804	72.18	2.5168	0.193
6	9.684	78.01	2.6294	0.219
7	11.219	71.94	19.4239	0.203
8	10.50	72.65	12.4718	0.223

4.2.1   Test Sequence

The realized test sequence has as its goal to provide subsides to the algorithms development and proof concept. It does not mean that these tests should be performed at the time of installation of the network, since such measures would be unfeasible in practice. We are proposing this sequence of tests to validate the development proposed in this research work.

The OTDR was configured with the following parameters:

❏ DR: 25Km (should have the smallest value greater than the maximum length of the network in this case 25km);

❏ Pw: 500ns (smallest pulse width which allowed viewing of the fiber end);

❏ Avg: 60 (smaller number of averages needed to observe the fiber signal with minimal noise, researcher's discretion);

❏ The OTDR generates traces for each measurement recorded into - Comma Separated Values (CSV) text file.

Sequence A is generated analysing each separate channel of the optic fibers after the splitter, unplugging the others, (see Table 4).

Table 4 – Experimental tests with each separated channel.

Sequence A	
Test Number	Description
1	Only the optical fiber in channel 1 is connected, unplugging others
2	Only the optical fiber in channel 2 is connected, unplugging others
3	Only the optical fiber in channel 3 is connected, unplugging others
4	Only the optical fiber in channel 4 is connected, unplugging others
5	Only the optical fiber in channel 5 is connected, unplugging others
6	Only the optical fiber in channel 6 is connected, unplugging others
7	Only the optical fiber in channel 7 is connected, unplugging others
8	Only the optical fiber in channel 8 is connected, unplugging others

Sequence B is generated through an analysis of a combination of 2 on 2 channels of the optic fibers after the splitter, unplugging all others and using only those which remain connected (see Table 5)

Table 5 – Tests with combination 2 on 2 channels

Sequence B	
Test Number	Description
1	Optical fibers in channel 1 and channel 2 connected, others unplugged
2	Optical fibers in channel 3 and channel 4 connected, others unplugged
3	Optical fibers in channel 5 and channel 6 connected, others unplugged
4	Optical fibers in channel 7 and channel 8 connected, others unplugged
5	Optical fibers in channel 1, 2, 3 and 4 connected, others unplugged
6	Optical fibers in channel 5, 6, 7 and 8 connected, others unplugged
7	Optical fibers in channel 1, 2, 3, 4, 5, 6, 7, 8 connected

Sequence C is generated analyzing a crescent number of connections, see table 6

Table 6 – Tests with a crescent number of connections

Sequence C	
Test Number	Description
1	Only the optical fiber in channel 1 and unplugging all others
2	Optical fibers in channel 1 and channel 2 connected, unplugging others
3	Optical fibers in channel 1, 2, 3 connected, unplugging others
4	Optical fibers in channel 1, 2, 3, 4 connected, unplugging others
5	Optical fibers in channel 1, 2, 3, 4, 5 connected, unplugging others
6	Optical fibers in channel 1, 2,3,4,5, 6 connected, unplugging others
7	Optical fibers in channel 1, 2, 3, 4, 5, 6, 7, 8 connected

4.2.2   Splitter Equation

In this section, we introduce basic knowledge concepts to explain the splitter's equation identified in this research. Analysing the physical concept of the laser beam emitted by the OTDR equipment, the energy with value ϵ should be proportional to its respective characteristic oscillation frequency, from one hypothetical oscillator. In 1901, Plank expressed this statement by presenting the proportionality constant $\hbar$ (BARROW, 2003). Next, this energy was associated to the energy of the electromagnetic wave, accounting for the energy required to create an electromagnetic field ("quantum"). Thus, this demeanour associated to a unit ("particle"), as opposed to an electromagnetic wave, is referred to as a "photon". Nowadays, the Plank's relation describes the energy of each photon, in terms of the photons frequency (BRANSDEN; JOACHAIN, 2003). This is also known as Plank's relation:

$$\epsilon = \vartheta * \hbar \tag{1}$$

Where:

ϵ = Beam energy.

ϑ = Beam frequency or the wavelength $1/\vartheta = \lambda$.

$\hbar$ = Plank's constant.

The OTDR laser is a monochromatic beam with $\lambda = 1550$nm. Consequently, the frequency ϑ is constant. Thereafter, the energy ϵ is conserved in the OTDR PON Splitter. Energy density is the amount of energy stored in a given space system or region per unit volume or mass. Anything that can transmit energy can have an intensity associated to it. Therefore, Law of Conservation is focused on intensity, allowing the superimposition of intensities presented in Figure 25.
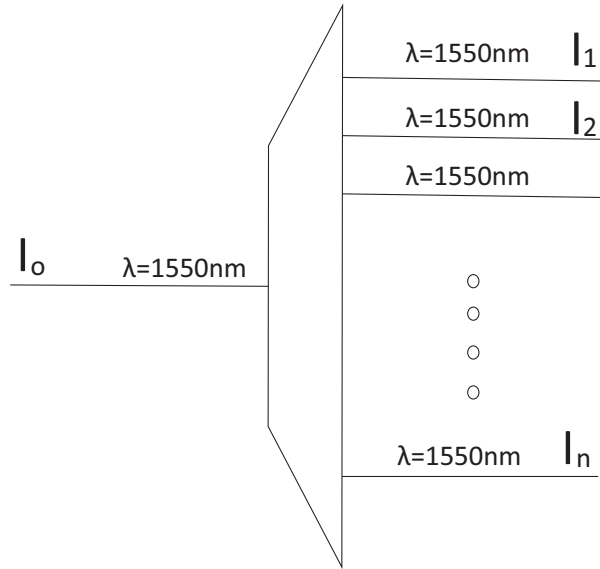
Figure 25 – Physical principle of PON splitter

Next, the verification of the following equation occurs:

$$\vec{I_0} = \sum_{i=1}^{n} I_i \tag{2}$$

Where:

I_0 = signal intensity of the incident laser light in the splitter.

I_i = signal intensity in the i-th splitter branch.

Equation 2 considers the total output power from all splitter branches expected to be equal to the input power. It is very important to clarify that there are various types of losses that affect the performance of the splitter design. For example, losses caused by scattering and absorption at the fiber cladding. In this research work, the losses associated with the PON splitter are relatively small and negligible.

Based upon the adaptation of the OPLL (Optical Phase Looked Loop) (LANGLEY et al., 1999) and Interferometry concepts (DEMTRODER; TITTEL, 1996), it is also important to consider that the OTDR photodetector acts as a mixer, since the photocurrent is proportional to the intensity of the incident optical signal. Two optical incident fields, occurring on the detector, result in a current that includes a term proportional to the product of the two fields (SATYAN, 2011).

Figure 26 presents a feedback system that enables electronic control of the output phase of the of the semiconductor's lasers output, which are the basic building blocks of most modern optical communication networks.
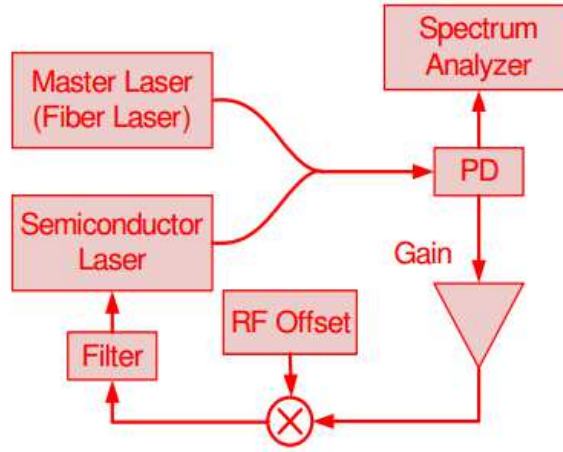
Figure 26 – A heterodyne semiconductor laser optical phase-locked loop (SATYAN, 2011).

Satyan (SATYAN, 2011) states that the semiconductor laser optical phase-locked loop beam has an output $a_s cos(\omega_s t + \phi_s(t))$, and the master laser output is given by $a_m cos(\omega_m t + \phi_m(t))$. ρ .Equation 3 is proposed by (SATYAN, 2011) to detect photocurrent, i.e. an evaluation of two beams targeting the Photodetector (PD):

$$i_{PD}(t) = \rho.(a_m^2 + a_s^2 + 2a_s a_m cos[(\omega_m - \omega_s)t + (\phi_m(t) - \phi_s(t)))])] \tag{3}$$

Here, ρ is the responsiveness of the Photodetector (PD). Taking into consideration the OTDR laser beam, the variation of the phase is null. Thus, $2a_s a_m cos[(\omega_m - \omega_s)t + (\phi_m(t) - \phi_s(t)))]$) is negligible, due to the behavior of the splitter in the passive optical network. Therefore, the only remaining part is the sum of squares. When considering OTDR measurements, the signal intensity P with respect to fiber distance z, in dB, is a well-known equation $5log_10(P(z))$ for measures of gain or attenuation given by the ratio of input and output powers of a system, or even by individual factors that contribute to such ratios. In addition, OTDR always shows two-way loss, which means that: $P_{dB}^{2way} = 5log_{10}(P(z)) = \frac{10}{2}log_{10}(P(z)) = 10log_{10}(\sqrt{P(z)})$.

Considering the superimposition of powers from different branches $P_c(z)$, the conversion of the power to linear scale is necessary since the addition of power in dB scale is not permitted:

$P_{lin}^{2way} = 10^{(\frac{1}{5}P_{c_{dB}})} = 10^{\frac{2}{10}P_{c_{dB}}} = 10^{(\frac{1}{10}P_{c_{dB}})^2} = (10^{\frac{1}{10}P_{c_{dB}}})^2$.

Grounded on these considerations, the total power over distance for all channels (or branches / drop fibers) is the sum of power over the distance of all individual branches, as shown in Equation 4:

$$S(z) = 10. \log_{10} \sqrt{\sum_{c=1}^{N}(10^{0.1.P_c(z)})^2} \tag{4}$$

Where:

P_c= OTDR measured signal per channel c of the Splitter in dB.

N = number of channels of the Splitter.

z is the fiber distance independent variable.

The authors ran validation simulations for this equation within the sequence tests, as presented in next the section. The validation process considered the isolated signals measured for each channel in a sequence A of tests. From these data, the authors simulated several combinations of channels connection sequences, shown in B (Table 5) and C (Table 6) through the application of Equation 4. Each simulation was then compared to the measured combination thereof. Using Matlab ^{TM}, the OTDR CSV files were read and respective graphics were generated with the objective of testing the equation and validating the results. All tests were successful. For other network configurations and other split ratios a new set of experiments are necessary.

Figure 27 presents one example of the realized comparisons where Channel 1 (blue) is measured by OTDR, and an Equation 1 simulates the (red) curve. Figure 28 presents the example using four channels (Ch 5, 6, 7 8) and Figure 29 presents all (eight) channels to validate the proposed Equation 4.
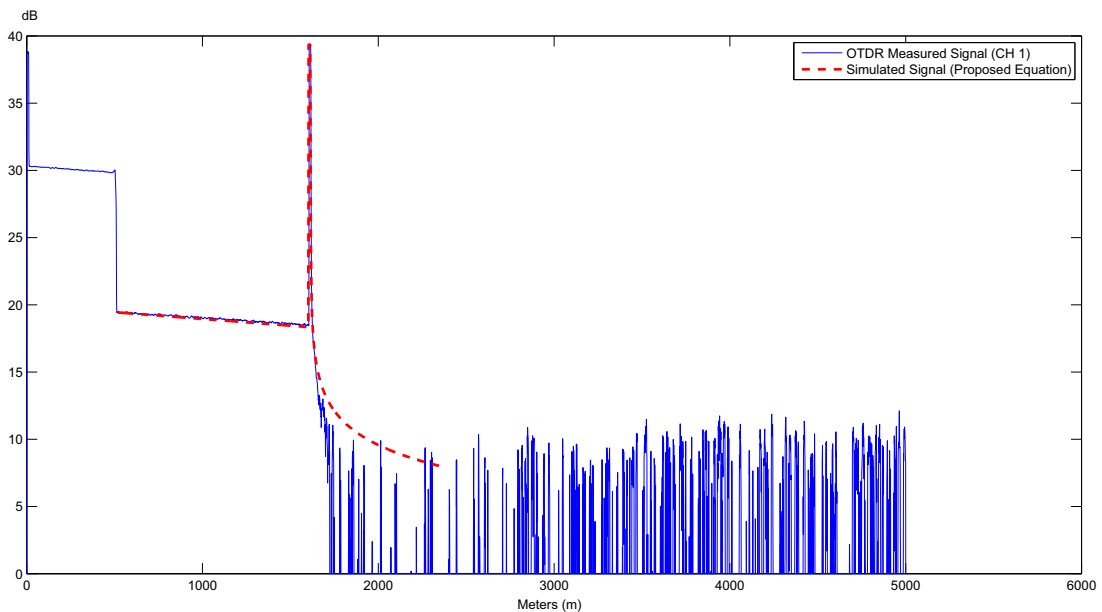
Figure 27 – Measured Signal (channel 1) x Signal Result using the Splitter Equation in one channel

In all tests, the signal is considered from Splitter until the last channel (dead zone). To guarantee precision we take the Pearson's correlation (RODGERS; NICEWANDER, 1988). For all figures tested, the value is near 1. This means (mathematically) that both variables are very similar.

The region of interest is between the splitter and the Dead Zone. Before the Splitter, Equation 4 cannot be used and neither in the Dead Zone. As one can see in Figure 27,
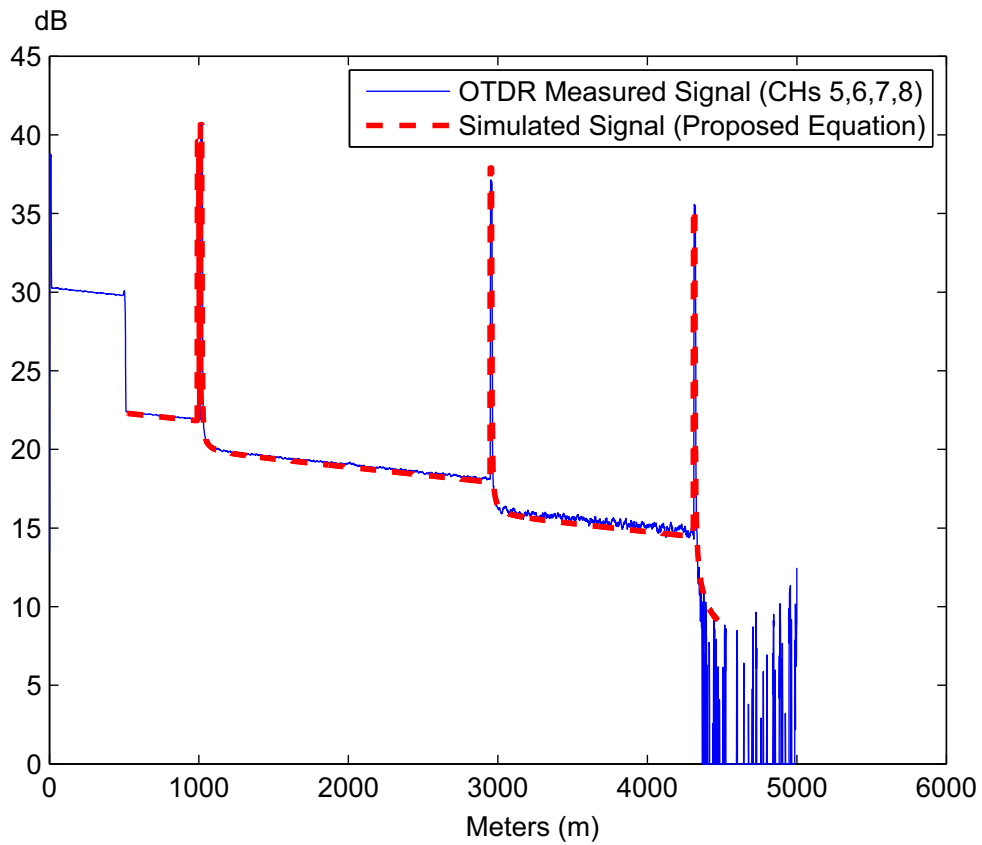
Figure 28 – Measured Signal (channels 5, 6, 7, 8) x Signal Result using the Equation in four channels

Figure 28 and Figure 29, the measured and simulated signals are highly coherent.
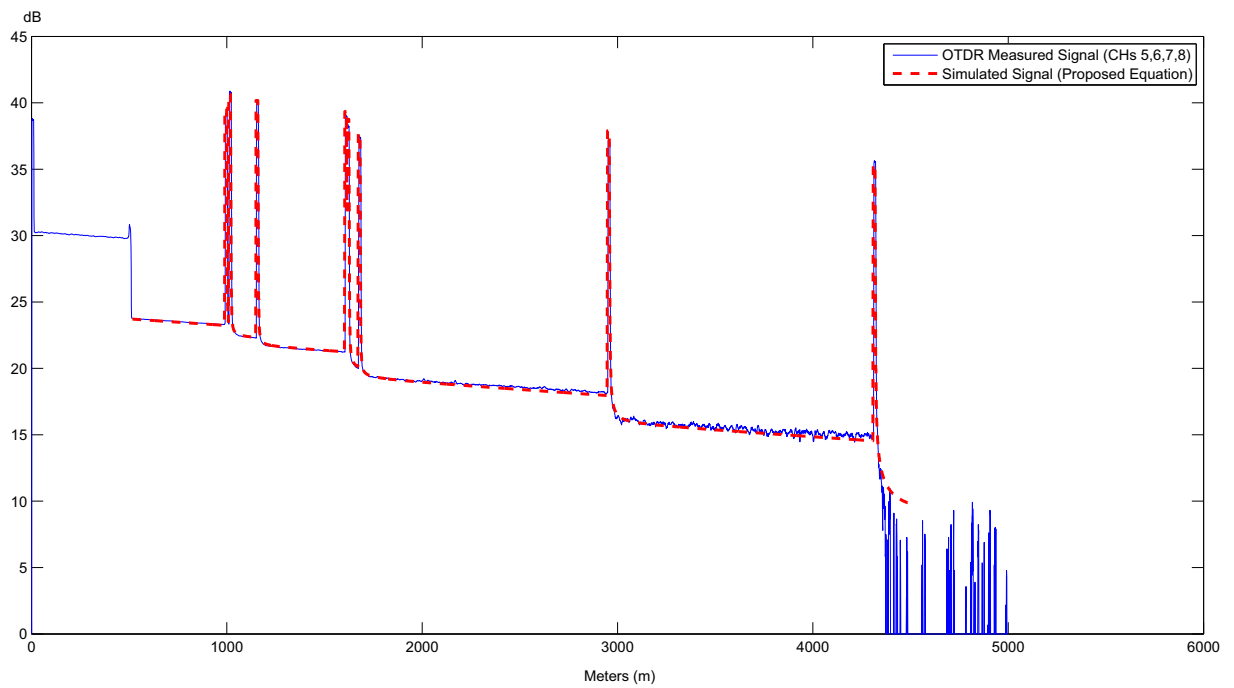
Figure 29 – Measured Signal all channels x Signal Result using the Equation in all channels.

4.3   OTDR Pulse Simulation

For simulation purposes, we divided the OTDR waveform of a pulse response reflection into the following parts, represented in Figure 30 and described in Table 7.
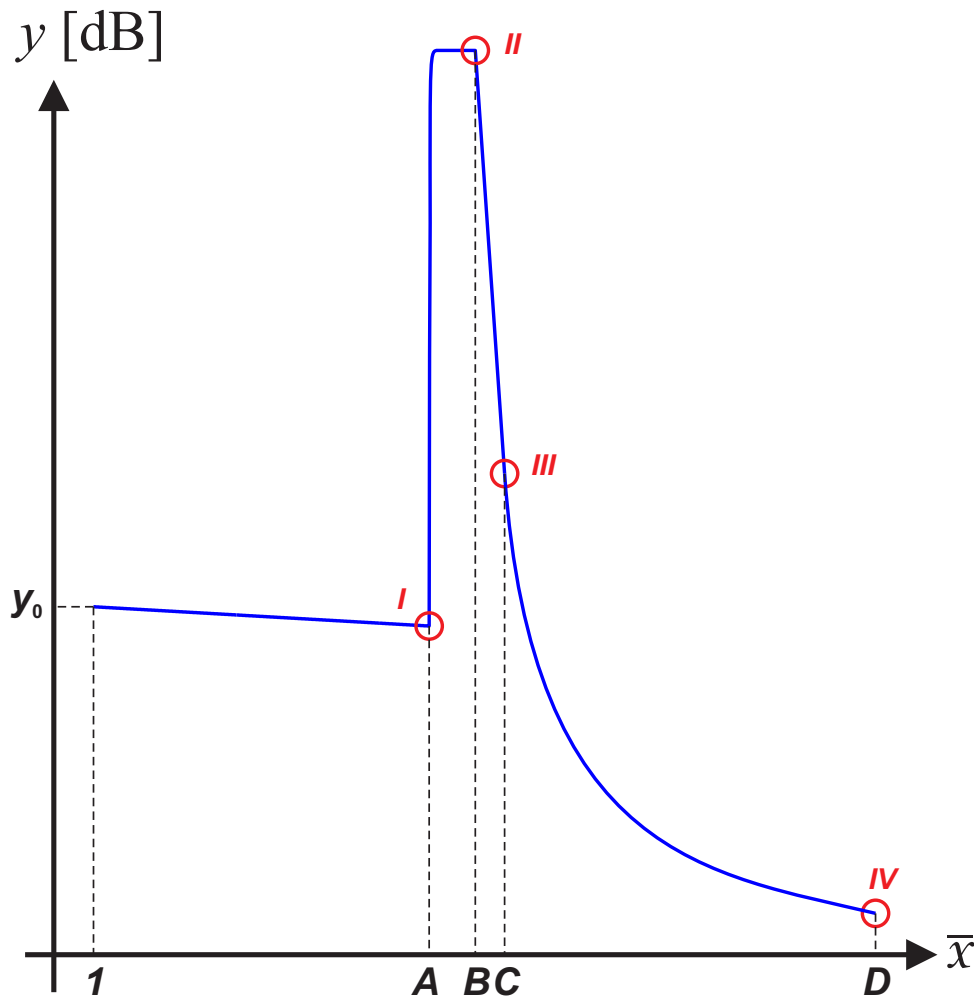
Figure 30 – OTDR signal simulation.

Table 7 – Simulated Signal in Function of sample index

Sample id (x	y(x)= ...	Number of Samples
1...A	y_0+m.x	# Samples before peak
A+1	(y(A)+ vf). $\sqrt{2}/2$	11 *
A+2...B	y(A)+vf	
B+1...C	y(B)-3.86(x-B)	4 **
C+1...D	y(C)-2.41 ln(x-C)	# Samples until end of signal

(*) Common Reflectance for these particular set of measurements, depending on the distance d between each sample. In this work the OTDR configuration uses $d = 0.5$ meters .

(**) Dead zone observation of pre-analysis of the signal.

In order to simulate the signal of a single channel, we need to implement a sort of iterator, which will write amplitudes over an array of the same size as the number of samples in the measured signal. Based on the network design project and OTDR settings,it is understood that the location of the splitter is known. Therefore, it is fair to assume that the proposed algorithm can consider just the samples after the splitter, just for simulation purposes. Suppose this measured signal has a length (starting right after the splitter) that could define a close interval 1...D (illustrated by Figure 30) that addresses the array. So, the measured signal is then represented by the simulated amplitude array y(x):

❏ Within the interval 1...A, y(x) is defined by a linear equation that reflects the Rayleigh backscattering effect. In the proposed linear equation, m is the fiber slope or fiber attenuation (typically expressed in dB/km). In this work, we use m = atan (-1/1150) based on the manufacturer's data-sheet for the experimented fiber and the ITU-T G.652 standard (ITU G.652, 2009). Considering the need to point the iterator to the next interval, i. e., to change the simulation behaviour, the trigger for this is the last sample registered before the end of the fiber. This information is also retrievable from the network design project and OTDR settings.

❏ In the interval [A+1 ... B], y(x) is defined by a constant added to the amplitude of the signal saved on the array in the last address from the previous interval. This constant represents the Fresnel's reflective event. Fresnel's reflection results from the discontinuity on indices of refraction observed when a fiber abruptly ends. For example, a Fresnel reflection may be caused by the end of a cleaved fiber, an undermined connector, a mated connector or a mechanical splice. Therefore, vf is the increase in amplitude due to reflection, expressed in dB. In this work, we use vf = 21 based on the manufacturer's datasheet for the experimented fiber. Note that the very first sample of the interval A+1 uses a scale factor of 0.707 in order to smooth the transition for the Fresnel reflective event and respects the fact that real world discontinuities are not abrupt. If the distance between samples are large enough, one can dismiss this scale factor. The trigger for changing the simulation behaviour is simply after counting up to 11 samples. This proved to be enough considering the equipment and fibers from experimentation and the OTDR's resolution of 0.5 meters between samples.

After the Fresnel reflective, the OTDR measured signal has two distinct behaviours [12], [14]. First, there is a linear decline of amplitudes. After, the signal presents an exponential declination:

❏ That first behavioural concept is simulated within the interval B + 1...C. The simulation y(x) is here defined by a linear equation, starting up to the amplitude of the

signal saved on the array in the last address from the previous interval. The authors obtained the angular coefficient of this line (constant of -3.86) has been obtained by approximation from applying linear regression to several experimental measures. The trigger for changing the simulation behaviour is simply after counting up to 4 samples. This proved to be enough considering the equipment and fibers from experimentation and the OTDR's resolution of 0.5 meters between samples.

❏ For interval C+1...D, the second behavioural concept is implemented. The signal is considered an exponential diminishing tail (ANDERSON LARRY JOHNSON, 2004) and (DERICKSON, 1998). We obtained the logarithmic coefficient (constant of -2.41) which was obtained by approximation from applying logarithmic regression modelling to several experimental measures. This behaviour is extended until the end of the array.

The resulting array constitutes the simulated signal. Note that the dead zone corresponds to the interval A+1...D. One channel at a time is simulated, according to some parameters, and Equation 4 is then applied for adding up the simulated signals. The summation of all simulated channels is the last simulated signal to be considered as a mathematical representation of the real measured signal.

4.4 Concluding Remarks

In this chapter, extremely important considerations for ongoing work were introduced. They are the splitter equation and the steps for the simulation of OTDR pulses. These considerations are used as the objective function in the proposed algorithm in the next chapter. It is important to note that these considerations are based on the physical processes of optical reflectometry.

Proposed solution: System Architecture

5.1 Introduction

During the first steps of our study, we developed a Genetic Algorithm (GA) that uses a chromosome architecture that allows for the separation of the superimposed signal after the passive optical splitter. From the limitations encountered, the procedure was enhanced by using a Differential Evolutionary algorithm (DE), resulting in a much better solution. In this chapter we present these two cases and compare the achieved results. We also present the analysis of time and correlation of values obtained computationally, which were compared to experimentally measured values.

5.2 Initial implementation - Genetic Algorithm

The Genetic Algorithm (GA) was introduced by John Holland, his colleagues and students at the University of Michigan (HOLLAND, 1975). The GA is inspired on the principles of genetics and evolution and mimics the reproductive behaviour observed in biological populations. The GA employs the principle of " Survival of the fittest " in its search process to select and generate individuals (design solutions) that are adapted to their environment (design objectives/constraints). Therefore, over a number of generations (iterations), desirable traits (design characteristics) will evolve and remain in the genome composition of the population (set of design solutions generated at each iteration), over traits with weaker undesirable characteristics. The GA is well suited to and has been extensively applied to solve complex design optimization problems as it can handle both discrete and continuous variables as well as nonlinear objectives and constraint functions without requiring gradient information (HOLLAND, 1987). In the literature, the capabilities of GA-based global optimization techniques are well known for obtaining superior separation solutions to the nonlinear blind separation problem from any random initial values. Compared to conventional gradient-based approaches, the GA-based approach for blind source separation is characterized by high accuracy, robustness, and conver-

gence rate (TAN; WANG, 2001). Inspired on Blind Source separation methods (YANG; LI; ZHUANG, 2003), we developed all implementations using Genetic Algorithms to allow an Optical signal separation after the splitter in PON Networks.

5.2.1 Genetic Algorithm - Block Diagram

To provide a good understanding of the implementation, Figure 31 presents a Block Diagram describing the algorithm through a sequence of procedures.
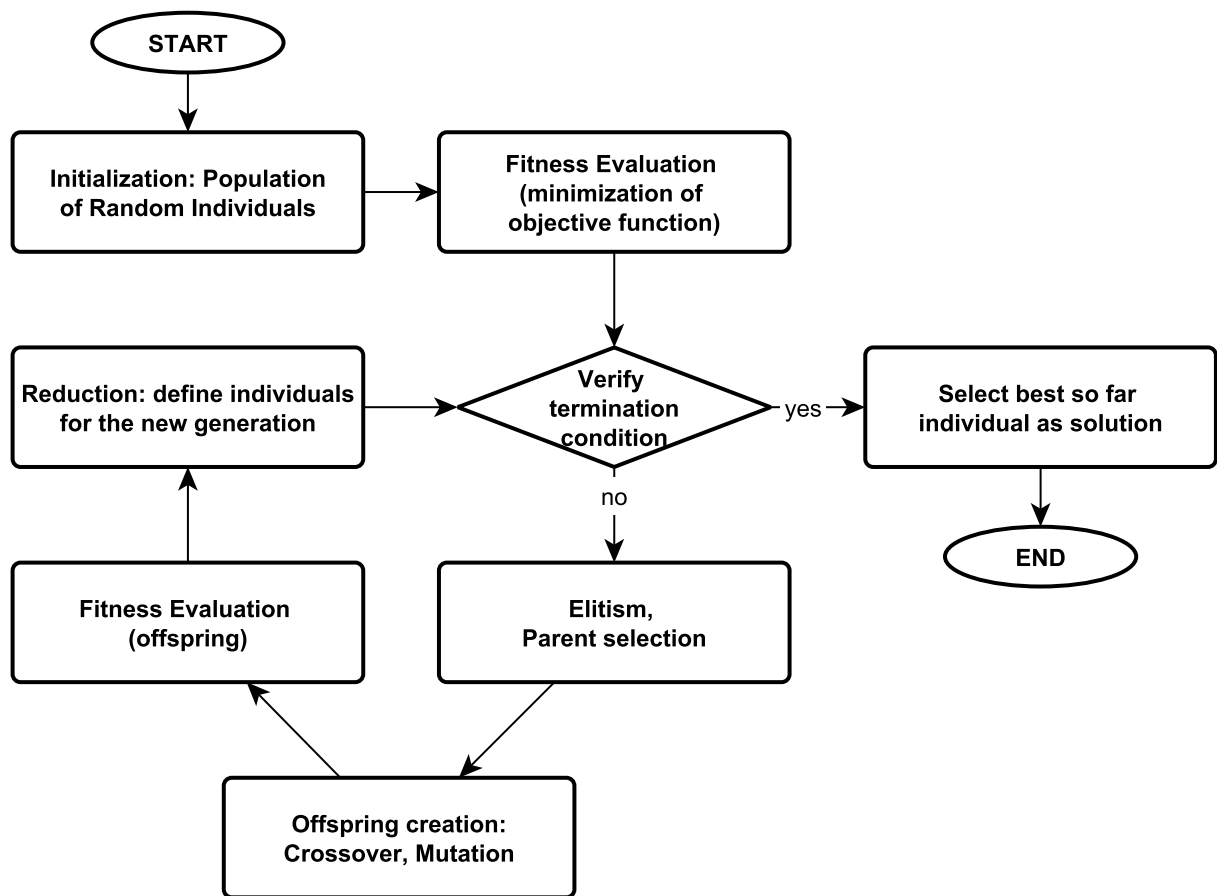
Figure 31 – Genetic Algorithm Block Diagram

5.2.2 Chromosome Architecture

In this research work, we adopt the chromosome architecture presented in Figure 32. Note that there is one element for each channel of the PON Splitter.

Channel 1	Channel 2	...	Channel n
Y_{0C_1}	Y_{0C_2}		Y_{0C_n}

Figure 32 – Chromosome representation

Where: $y0_{cn}$ is the initial value of the Power in dB in channel n after the splitter.

5.2.3 Fitness function

The GA heuristic search for the proper set of $y0_{cn}$ is presented in Equation 5.

$$\min_{y0_{cn}}(\vec{M} - \vec{S})or||\vec{M} - \vec{S}|| \tag{5}$$

Where: $\vec{M}$ is the measured OTDR signal and $\vec{S}$ is the superimposition of each one of the n simulated channels.

The approximation of both individuals, $\vec{M}$ and the superimposition simulated signal of each channel $\vec{S}$ are evaluated by applying Pearson's Correlation (KENDALL; STUART, 1973) looking to obtain values near 1. In order to guarantee the strength of the linear association between the variables. In other words, to achieve the precision of the simulated signal and the measured signal (NIKOLIĆ et al., 2012).

The generational process is repeated until a termination condition has been reached. In this research work, many different terminating forms were tested until acceptable results were reached. In the first set of experiments, we used:

❏ A solution is found that satisfies minimum criteria of correlation(nearest 1);

❏ Fixed number of generations reached above 100;

❏ Allocated budget (computation time/money) reached (lowest time as possible);

❏ The highest ranking solution's fitness is reached;

❏ such that successive iterations no longer produce improved results;

❏ Visual inspection of graphics to observe the approximation of two signals;

❏ Combinations of the above.

For all tests, we have defined a crossover rate of 85% and mutation rate of 25%. Both elitism and tournament were used; more details are given in Appendix B.

The GA performance is a factor of concern when carryng out more in depth studies, as the highlighted problem concerning signal separation imposes a very long process period

upon the GA algorithm in order for it to obtain a good correlation above the value of *0.98*. If the correlation is lower than this value of *0.98* the difference of the simulated signal and the measured signal is not enough for it to be considered a good solution. In the next section, we explain the possibility of paralleling some loops for speeding up the iterations and providing better and faster results.

Besides the problem of the long time taken by the genetic algorithm, it also appears that on many occasions, it does not converge at a good solution, reaching low correlations and not managing to converge at better solutions. After extensively analysing this problem, we arrived at the conclusion that it would be interesting to carry out significant disruption in the population to try and prevent convergence into local solutions, a common problem in GA as cited by (GUIMARAES, 2009) and presented in Figure 33.
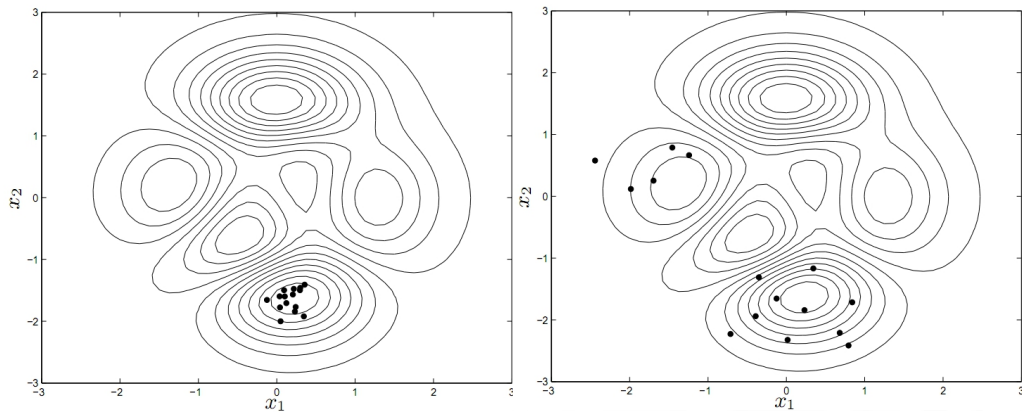
Figure 33 – Local solution candidates (Left) x Global solution Candidates (Right)

On the left of Figure 33, one can see the candidate of solutions converging at some local minimum not able to satisfy the correlation condition in order to allow for good final solution and dispensing the excessive time taken by the algorithm. On the right, we can see when the solution candidates attain more diversity allowing the fitness function to evaluate better candidates (global solution in the search space) and converging at better results with lower computational efforts. Thus, we define the implementation of Differential Evolution described in the following.

5.3   Parallelization of loops

To evaluate the possibility for increasing the GA and DE performance, we adopted the Matlab®function *parfor* [1]

The basic concept of a *parfor-loop* in MATLAB™ software is the same as the standard *for-loop*: The software executes a series of statements (the loop body) over a range of values. Part of the *parfor* body is executed in one processor core (where the parfor is

---

[1]   Matlab Parallel Toolbox found at http://www.mathworks.com/help/distcomp/parfor.html

issued) and part is executed in parallel on other processors. The necessary data on which *parfor* operates is sent from the main processor, where most of the computation happens, and the results are sent back to the other processors and pieced together.

Because several MATLAB^{TM} processes can be computing concurrently on the same loop, a *parfor-loop* can provide significantly better performance than its analogous for-loop. In our case we use for the tests a *DELL XPSL502X* computer with an internal processor of *2-GHz Intel Core i7-2630QM*. This processor has 4 physical cores allowing for the performing 4 processes in parallel.

Each execution of a *parfor-loop* body is an iteration. MATLAB^{TM} processes evaluate iterations in no particular order and independently of each other. As each iteration is independent, there is no guarantee that the iterations are synchronized in any particular way, nor is there any need for this.

A *parfor-loop* is useful in situations where you need many loop iterations of a simple calculation. The *parfor* divides the loop iterations into groups so that each worker executes some portion of the total number of iterations. The *parfor-loops* are also useful when you have loop iterations that take a long time to execute. This is because the processors (workers) can execute iterations simultaneously.

However, it is impossible to use a *parfor-loop* when an iteration in the loop depends on the results of other iterations. Each iteration must be independent to all others. Since there is a communications cost involved in a *parfor-loop*, there might be no advantage to using one when you have only a small number of simple calculations.

5.4 Differential Evolutionary Algorithm

The Differential Evolution algorithm is an evolutionary algorithm proposed in the second half of the 1990s, for solving optimization problems with continuous variables (CHAKRABORTY, 2008). Over the last decade, this algorithm has proven to be a successful technique in many applications, such as neural network training, identification of parameters, and design of devices and systems in electrical engineering and electronics. The success of this method is based on the mechanism of the differential mutation operator that is sought. This operator generates new solutions, starting from vectors constructed with differential pairs of solution candidates drawn from their own population. The differential distribution of vectors in the space of variables for optimization generates search directions with different sizes, which depend on the position of the points used in the construction of the mutant vectors. These directional domain and step sizes fit the characteristics of the problem, with the adaptation properties of self as the population progresses in the direction of the best solution.

A differential mutation employs the difference between pairs of individuals in the population to generate the current perturbation vectors called vector differentials.

However, as the algorithm progresses in the search process, the spatial distribution of the population changes according to the landscape of the objective function or cost function changing that, in turn, alters the orientations and sizes of the differential vectors that can be created from the population.

For this reason, it is observed that the distribution of the differential vectors and, therefore, the distribution of directions and step sizes of perturbations fit the landscape function. This characteristic of self adaptation mutation differential evolution algorithm gives important qualities from the point of view of optimization, such as strength, versatility and efficiency found in several problems.

The main characteristic of this method is the capacity to search very large spaces of candidate solutions. This is a problem case encountered in this research work, when we start to use a common **Genetic Algorithm**, as described in the previous section.

Differential Evolution (DE) algorithms also can be used for multidimensional real valued functions, but it does not use the gradient of the problem being optimized, which means DE does not require for the optimization problem to be differentiable is required by classic optimization methods, such as gradient descent and quasi-newton methods. DE can, therefore, also be used on optimization problems that are not even continuous, noisy, change over time, etc. (ROCCA; OLIVERI; MASSA, 2011).

However, metaheuristics as (DE) do not guarantee that an optimal solution is ever found. In fact, DE optimizes the problem by maintaining a population of candidate solutions (CHAKRABORTY, 2008).

It also creates new candidate solutions by combining already existing solutions according to their simple formulae, considering whichever candidate solution has the best

score or fitness on the optimization problem at hand. A vector of real numbers called "Chromosomes" represents each candidate solution. In this way, the optimization problem is treated as a black box that merely provides a measure of quality given a candidate solution and the gradient is, therefore, not needed (PRICE; STORN; LAMPINEN, 2005) , (ROCCA; OLIVERI; MASSA, 2011). DE is generally considered as a reliable, accurate and robust optimization technique (GUIMARAES, 2009).

The differential evolution algorithm has many qualities desirable in general purpose optimization algorithms :

❏ Ability to adapt the structure function, learning linear correlations between the variables of the problem from the spatial distribution of the population;

❏ Invariance the rotation and translation of the coordinate system;

❏ Control of few parameters to be adjusted and also the scale parameter does not need to be adjusted, since the step sizes are a self-adapted mutation;

❏ Implementation simplicity.

The basic operation principle of the Differential Evolution algorithm is to disturb the current population of solutions generating mutant vectors. These perturbations are proportional to the difference between pairs of solutions chosen randomly from the population. Therefore, to better understand the behaviour of the algorithm it is necessary to verify the distribution of possible vector's differentials at different moments of the optimization process.

The operations of the differential evolution algorithm are presented in the form of pseudo code in Algorithm 1 and also in Figure 34:

Algoritmo 1 Basic differential evolution algorithm (adapted from (GUIMARAES, 2009))

Initialize the population $X_t = \{x_{t,i}, i = 1, ..., N\}$

    While stop criteria do

        Random Selection

        $r_1, r_2, r_3 \in \{1, ..., N\}$

        Random Selection $\delta \in \{1, ..., N\}$

        For *j = 1 to n do*

            IF $v_{[0,1]} \leq C \vee j = \delta Do$

            $\mu_{t,i,j} = x_{t,r1,j} + \eta(x_{t,r2,j} - x_{t,r3,j})$

            Else $\mu_{t,i,j} = x_{t,i,j}$

        End For

    End While

    For each $x_{t,i}$, *i = 1 to N Do*

        IF $f(\mu_{t,i}) \leq f(x_{t+1,i})$ *Do* $x_{t+1,i} \leftarrow \mu_{t,i}$

        Else $x_{t+1,i} \longleftarrow x_{t,i}$

    End For

    $t \leftarrow t + 1$

End

The search engine incorporated into the differential evolution algorithm uses differential created vectors, starting from vectors pairs of its own population. Two individuals are randomly selected from the current population, creating one differential vector and with nothing more than the difference between these two individuals. This differential vector, in turn, added to a third individual, is also randomly selected to produce a new mutant solution. The new mutant solution and, therefore, the result of a disturbance in any individual in the population is a randomly constructed differential vector disturbance. Equation 6 illustrates this procedure:

$$\mu_{t,i} = x_{t,r1} + \eta(x_{t,r2} - x_{t,r3}) \tag{6}$$

with $r_1, r_2, r_3 \in \{1, ..., N\}$. The vector $\mu_{t,i}$, i is the i-th mutant solution and η and a scale factor applied to the differential vector parameter of the differential evolution algorithm. The vector $x_{t,r1}$ applied to the differential mutation called a *base vector*.

Using this procedure, we obtain a mutant population $V_t = \{v_{t,i}; i = 1, ..., N\}$. The next steps in the algorithm are very simple. Individuals in the current population X_t are recombined with individuals of the mutant population, producing offspring or a population of test solutions Ut.

In this research work we use the classical version of the Differential Evolution algorithm employing the discrete recombination with probability $C \in [0, 1]$:
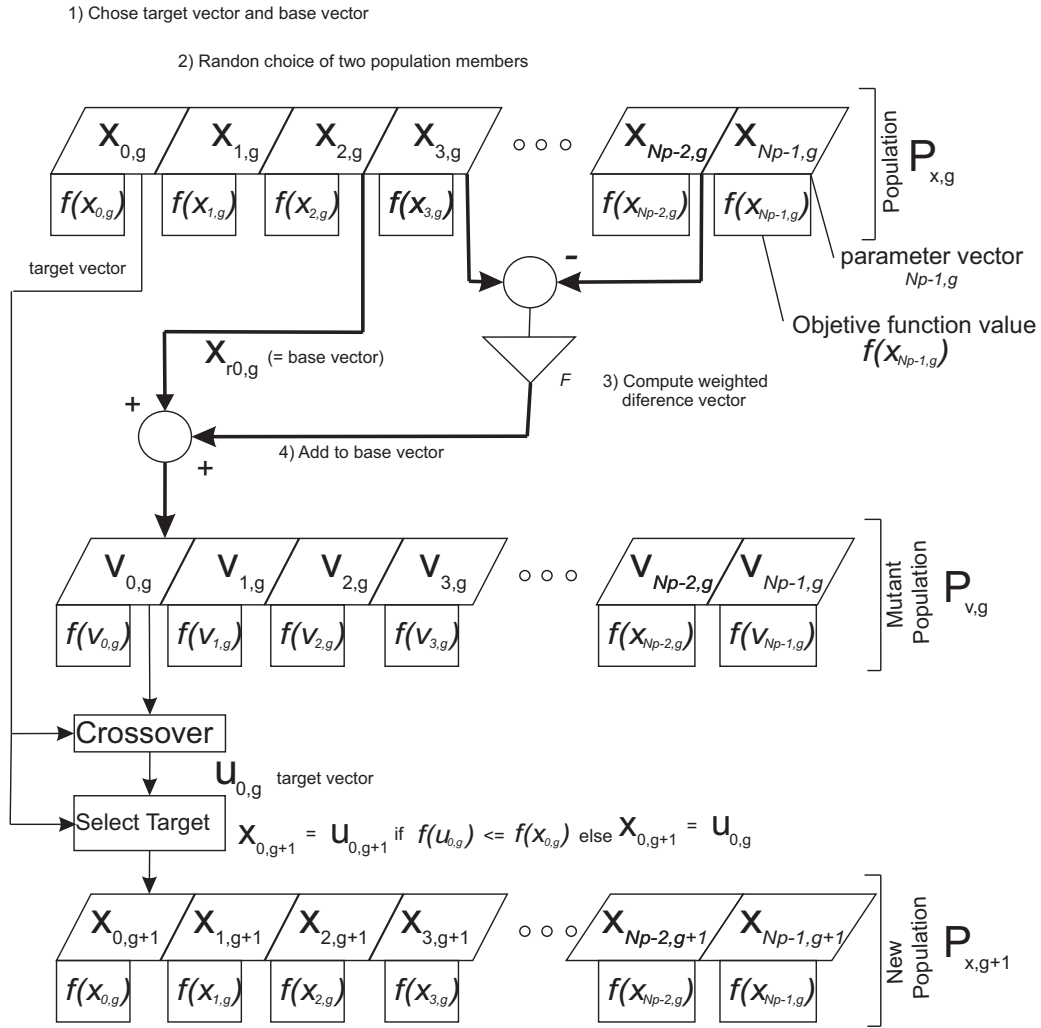
Figure 34 – Differential Evolution (DE) representation (CHAKRABORTY, 2008)

The index $\delta \in \{1, ..., N\}$ is an index drawn for the random test vector i. As at sometime equality $j = \delta_i$ will be verified, this condition ensures that at least one of the parameters of the test solution will be inherited from the mutant individual.

The parameter C controls the fraction of values in $u_{t,i}$ that are copied from the mutant vector $v_{t,i}$ as the closer to 1 the value of C becomes the greater the chance that the test solution contains many values inherited from the mutant vector. In the limit, when $C = 1$ and test vector equal to the vector mutant

Figure 35 illustrates the generation of a mutant vector and test of the possible solutions, obtained after the recombination, indicated with a dark square. Note that at least $j = \delta_i$ coordinate vector is the inherited mutant thus ensuring $u_{t,i} \neq x_{t,i}$. One observes that a result of the test solution and each solution recombination $x_{t,i}$, generates a common solution from a mutant disturbance in any single individual in the population. The direction and the size of this perturbation are defined by the difference between the solutions $x_{t,r2}$ and $x_{t,r3}$. Therefore, it depends on the relative positions of these individuals in the search domain.
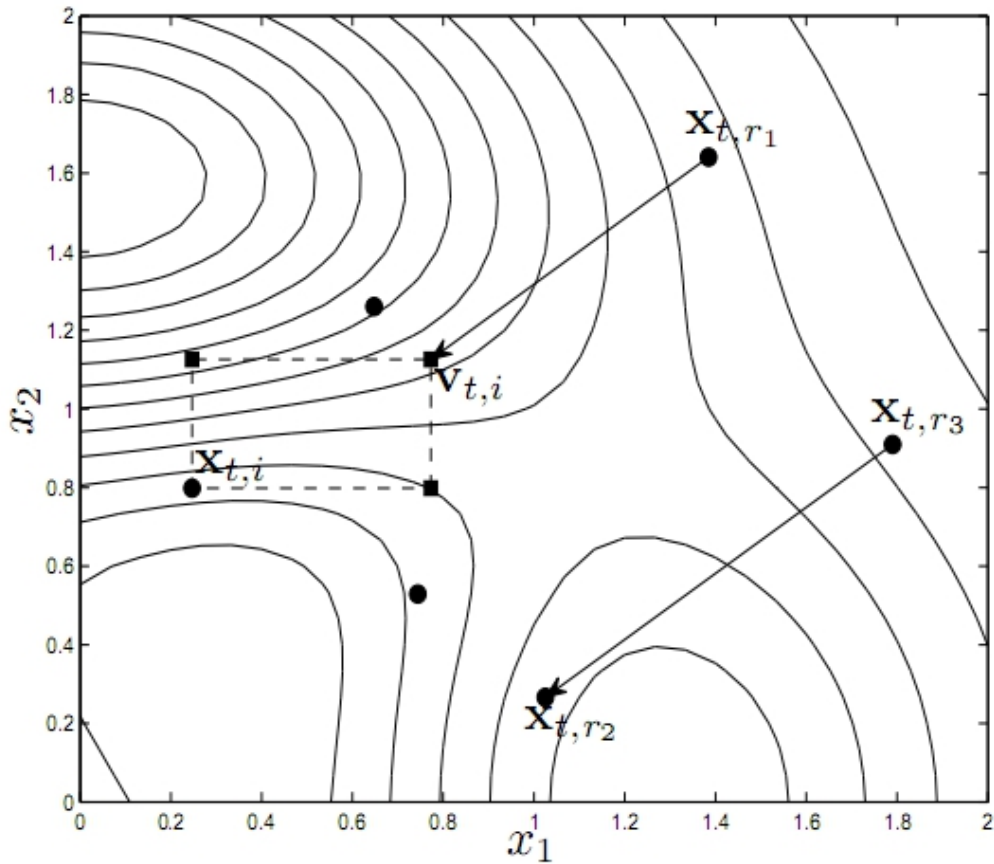
Figure 35 – Generating Mutant Solution Procedure (GUIMARAES, 2009)

Finally, the value of the objective function, or cost-function, is estimated at $u_{t,i}$. Each test solution $u_{t,i}$ is compared to its counterpart in the population chain, where $x_{t,i}$. If the test solution is better than the current solution $x_{t,i}$, the current solution is eliminated and is replaced with by $u_{t,i}$. Otherwise, the test solution is discarded and the current solution survives, remaining in the population of the next generation, represented by X_{t+1}. The process is repeated until some stop criterion defined by the user is satisfied, in our case this is the number of generations and the highest correlation between the measured signal and the simulated signal.

Each individual $x_{t,i}$ of the population at generation t is a possible solution of the problem and, in the present case, it is structured in the form of the chromosome described in Figure 32. The DE heuristic search for the proper set of $y0_{cn}$ is presented in Equation 5. The DE routines are presented in Appendix C.

Note that, when this heuristic converges, the parameters of each separated channel are obtained. It is also important to observe that this method is adequate for guaranteeing the sufficient solution which proposes to separate the superimposed OTDR signal after the splitter of the FTTH PON network.

5.5 Differential Evolutionary Algorithm Variations

The implemented Differential Evolutionary algorithm in this study was adopted in its basic version, using a random selection with uniform probability of the base vector using only one differential vector to provide a mutation and a discreet recombination between a current solution and its correspondent mutant vector. However, according to (GUIMARAES, 2009) many variations of this schema are possible. In this work we adopt the use of more than one differential vector in the mutation, looking to increase the algorithm diversity capacity. The best individual is used as the base vector, and we use three differential vectors in differential mutation therefore, we can reference the corresponding differential evolution algorithm as DE/best/3/bin. The tests were repeated 2000 times and the results are very similar to those of the basic version. The use of more than one differential vector increases the global search algorithm capacity but affects the local search capacity. In our experiment arrangement, we didn't observe any tangible benefits for improving the time nor the correlation between the simulated signal and the measured signal. Nevertheless, this strategy decreased the differential vector alignment capacity with the contour function and yet, it becomes increasingly difficult to ensure mutually distinct indices. The following results were tested using the basic version of the DE algorithm.

5.6 GA x DE Results Comparison

To allow the evaluation of all GA and DE characteristics, we performed a set of tests and present the results in Tables: 9 and 8. Also presented herein a graphical comparison found in Figure 36.

Table 8 – DE parameters

Sample	Algorithm	Individuals	Generations	Correlation	Time	Method
1	DE	200	600	0.98268	702.76	For
2	DE	100	600	0.97586	364.03	For
3	DE	100	400	0.9563	225,918	For
4	DE	100	400	0.97988	139.06	ParFor 4
5	DE	200	400	0.97476	254.27	ParFor 4
6	DE	200	600	0.98278	381.5	ParFor 4
7	DE	200	600	0.95621	6.561.784	ParFor 2
8	DE	100	500	0.96321	170.35,05	ParFor 4
9	DE	100	600	0.98104	208.85	Parfor 4
10	DE	100	500	0.93996	271.18	For
11	DE	200	400	0.97921	453.24	For
12	DE	1000	300	0.94641	1125.88	Parfor 3
13	DE	500	1000	0.9567	1457.00	Parfor 4

Table 9 – GA parameters

Sample	Algorithm	Individuals	Generations	Correlation	Time
1	AG	100	400	0.89349	900.62
2	AG	200	400	0.9305	1683.17
3	AG	200	600	0.92248	2553.58
4	AG	100	500	0.95275	1120.63
5	AG	100	600	0.9014	1310.87
6	AG	1000	300	0.94717	13850.14
7	AG	500	1000	0.9535	10836.42
8	AG	1000	1000	0.95791	21404.25
9	AG	1000	2000	0.9584	44.074.474
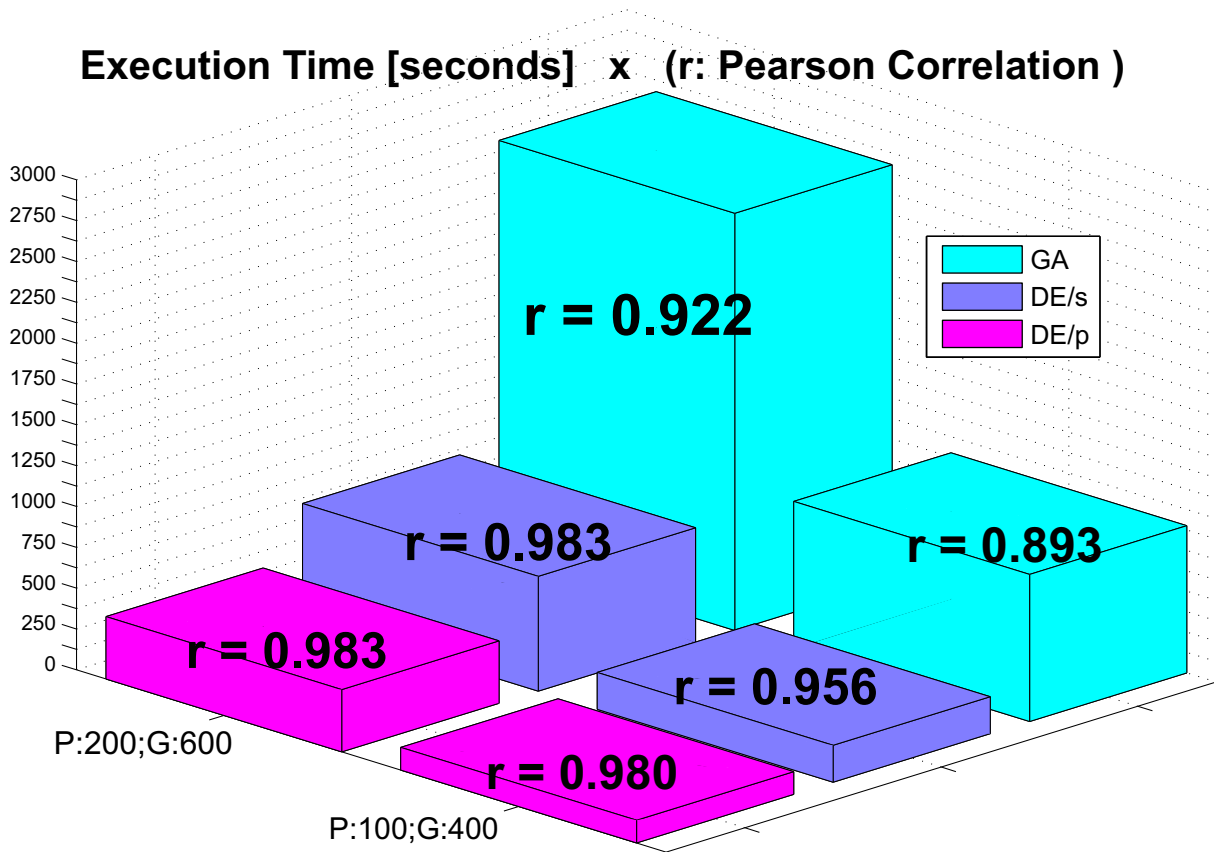
Figure 36 – GA x DE Comparative

One observes that better results are provided by the lower execution time and higher correlation that is reached by the ED Algorithm.

In the next step, we repeat the DE tests exhaustively to evaluate the ED performance and results. Therefore, we repeat *1000* times the DE plotting of the time spent and the correlation reached on the graphic. The DE parameters considered are *100* individuals in the population and *400* generations. All of these tests was performed with *parforloop* using *04* processors in parallel. Figure 37 presents a histogram displaying relative frequencies between the time in seconds in relation to the correlation. Note, that the correlations above *0.95* need more time to be reached.

In descriptive statistics, boxplot is a convenient way of graphically depicting groups of numerical data through their quartiles [2]. Figure 38 presents a boxplot of the correlation variation in *1000* repetitions of the ED algorithm, note that the degree of dispersion (spread) are between *0.94 to 0.98*. It is important to highlight the interest in obtaining correlations above *0.98* minimum.

---

[2] The boxplot is a quick way of examining one or more sets of data graphically. Boxplots may seem more primitive than a histogram or kernel density estimate but they do have some advantages
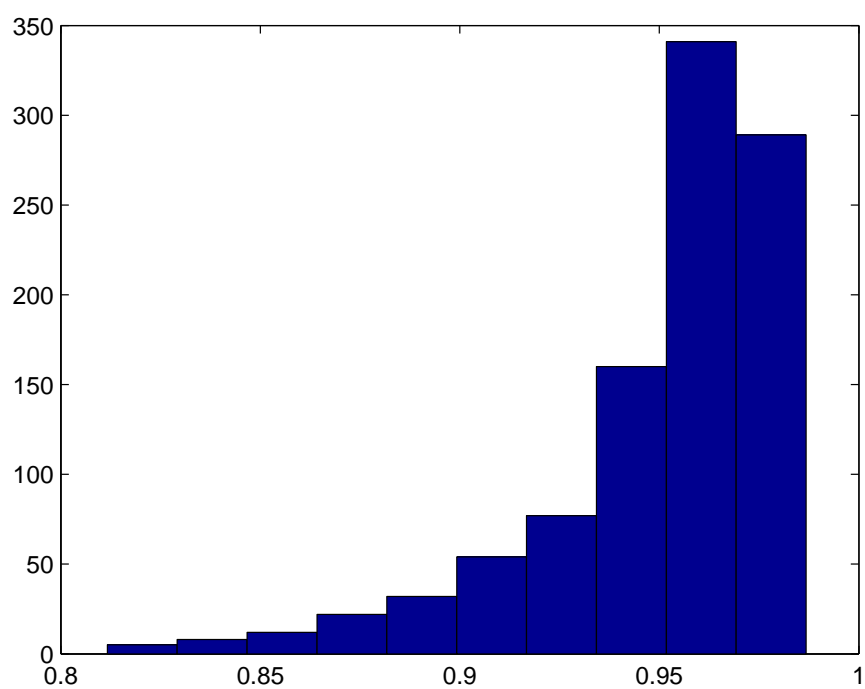
Figure 37 – Time (seconds) x Correlation Histogram
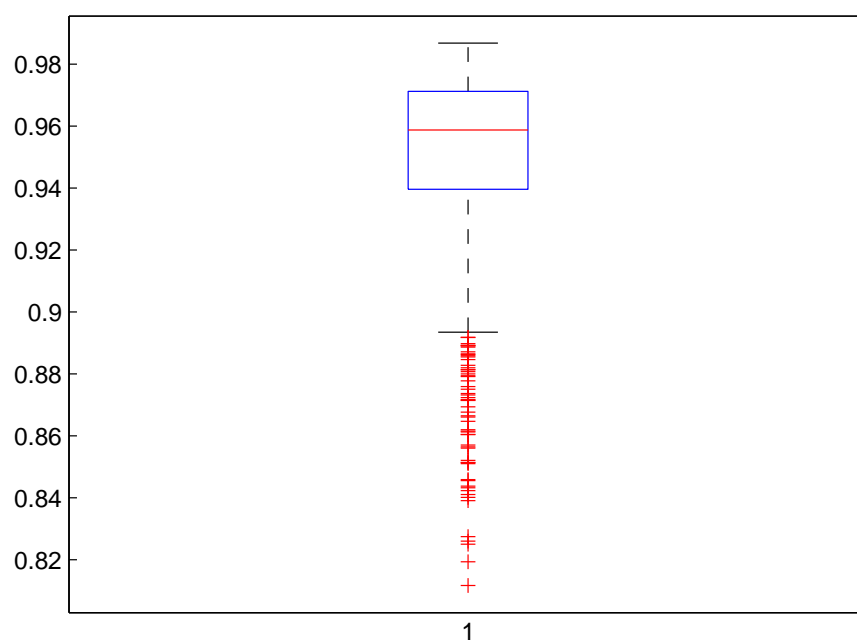
Figure 38 – Boxplot of Correlation - *1000* tests

5.7 Results

The results presented in Figure 39 illustrate the difference between the measured signal (blue) and simulated signal (red) by the ED Algorithm, when the correlation is below *0.98*. In the example it is possible to identify the difference: some peaks of the simulated signal do not fit exactly onto the peaks of the measured signal.
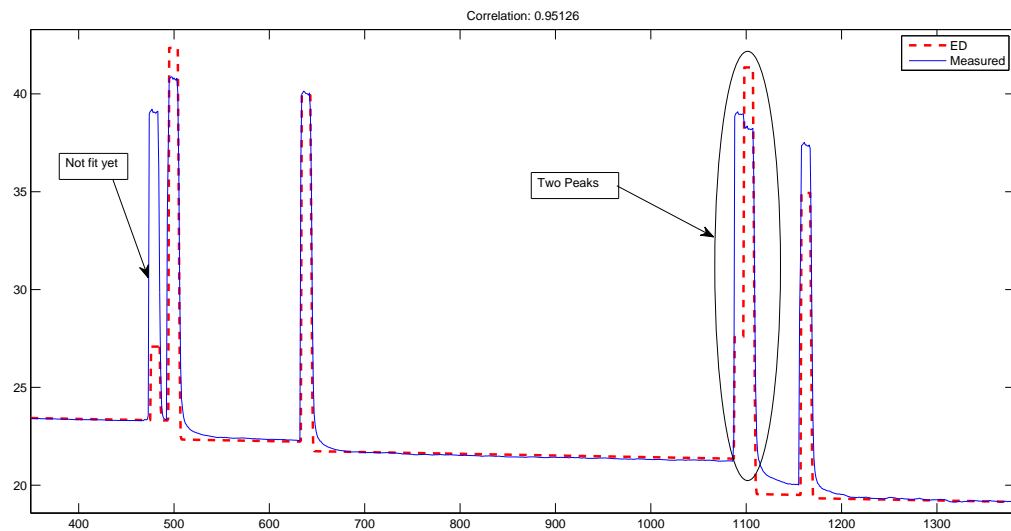
Figure 39 – Results with correlation of 0.95126

It is interesting to note that in the same figure that there exist two peaks very close to each other. Also, the algorithm solution converges at a simulation where the correlation with the measured signal is 0.95. This is not sufficient for separating these peaks. On the left hand side, it is possible to identify another peak that does not fit as well.

However, when the DE application reaches values above 0.98, the simulated signal is very close to the measured signal, as presented in Figure 40
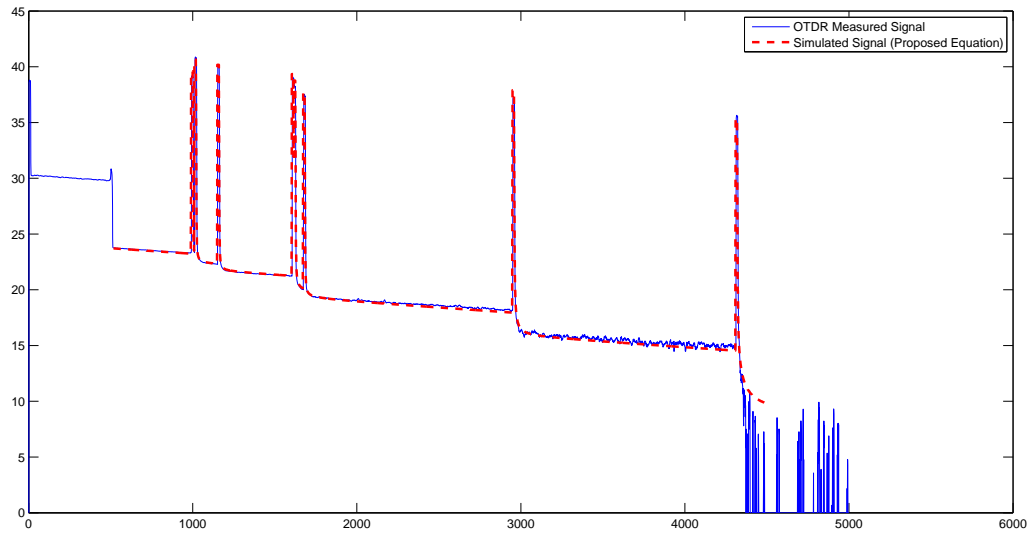
Figure 40 – Plots of the separated channel (blue), simulated signal (green), measured signal (red)

Figure 41 presents, in a 3D view, from left to right, all OTDR separated channel signals in blue. The after splitter superimposed simulated channels are in green and the measured signal in red.
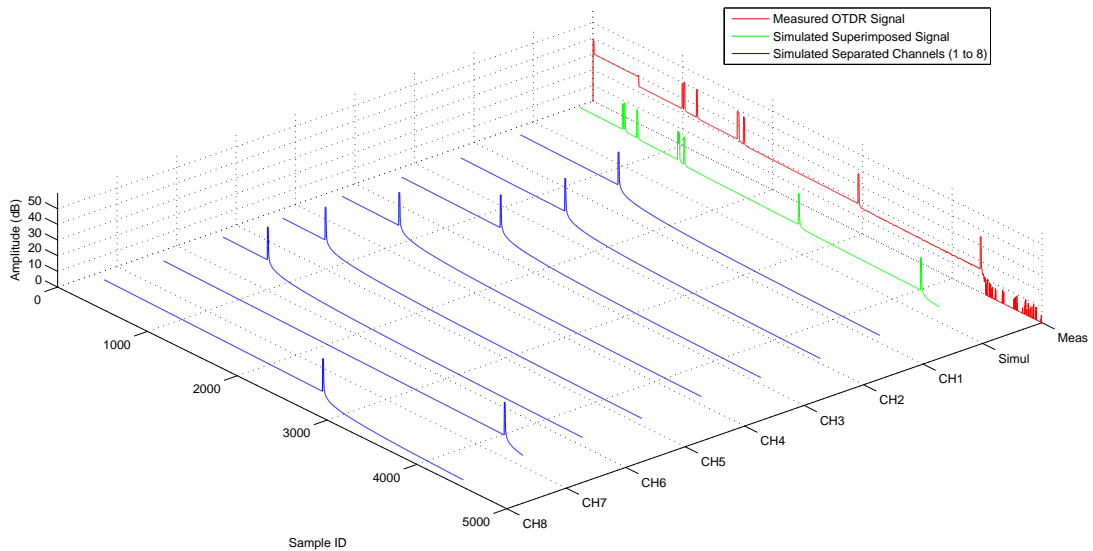
Figure 41 – Plots of the separated channel (blue), simulated signal (green), measured signal (red)

The separated signal is now saved onto an array to allow its us on the computer graphics (CAD) environment coupled with its correspondent FTTH PON design.

5.8   Concluding Remarks

In this chapter we presented a comparison of two computational intelligence algo-
rithms: the GA and DE. The results show the advantages of DE in the requisites of the
performance and quality of the outcome. The separated signal is now saved on an array
to be used in the next chapter, coupling it to the computer graphics tool (CAD), allowing
it to be incorporated into a surveillance tool.

Results and Implementation Details

6.1 Introduction

This chapter presents an implementation of the proposed techniques using a constraint database model. Results are discussed in accordance with a computer graphics environment specially develop to aid a FTTH PON network design. The proposed tool is projected to support the coupling of the network design with the OTDR system and can be used for surveillance purposes.

6.1.1 An overall view

Figure 42 shows the complete block diagram representing the methodology used to constitute the implementation process. First, we use an OTDR device connected to the CO, measuring the physical FTTH-PON network.

The acquired signal is now subjected to the DE algorithm that simulates the channels, after the splitter. This engine derives the lengths of each branch of the network to the (CAD) project FTTH PON and the number of the splitter channels. With this input data, the algorithm performs the separation of the superimposed signal and stores it in a special array. Each signal in this array is now coupled with its respective branch design on a geographic map.
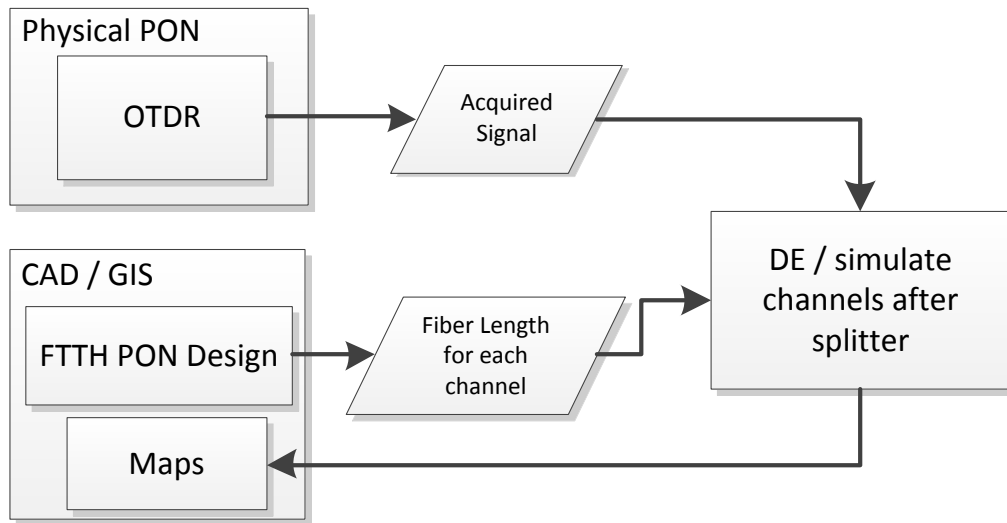
Figure 42 – OTDR Complete signal separation process

6.1.2 Signal Coupling with Computer Graphics tool

Considering the results from the experimental algorithm, the separated signal measured from the OTDR, which is obtained from the FTTH PON network is saved in the above mentioned array. Next, a coupling procedure is performed through the CAD environment, bringing to the map the corresponding optical signal (physical representation), expressed in geographic coordinates. Figure 43 presents the constraints management for this coupling process.
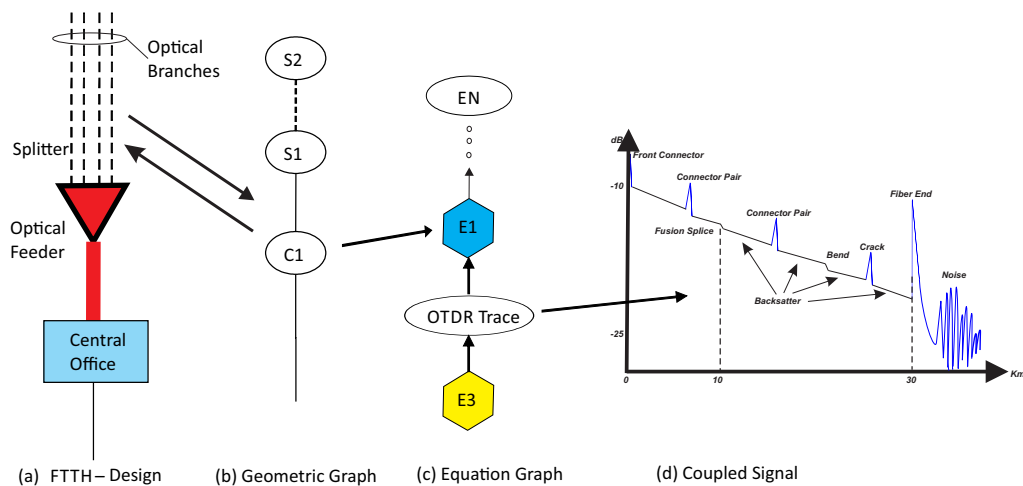
Figure 43 – Signal Coupling Constraints Management

Note that: when the user manipulates the FTTH Design (AutoCAD) entities, the Geometric Graph information is propagated over the equation graph and the information of the separated signal is accessed and presented to the user. The coupling occurs through the correspondence of the linear length of the Network cable representation (geometry)

and the signal on the axis x, where the distance is represented in the optical power scale (dB).

6.1.2.1   Database Fundamentals–Symbol tables,Transactions(AutoCAD–API)

The AutoCAD Drawing Database (DWG) is represented in Figure 44 and provides the capabilities below:

❏ In-Memory representation of the Dwg File;

❏ Objects are stored hierarchically in the database - Db Structure;

❏ All objects have identities – Objectid, like Primary Key in a relational database;

❏ Objects are always accessed in a transaction;

❏ The transaction defines the boundary of database operations;

❏ Objects have to be opened first in a transaction before they can be used;

❏ Objects can refer to other objects – such as a line having a reference to a layer.
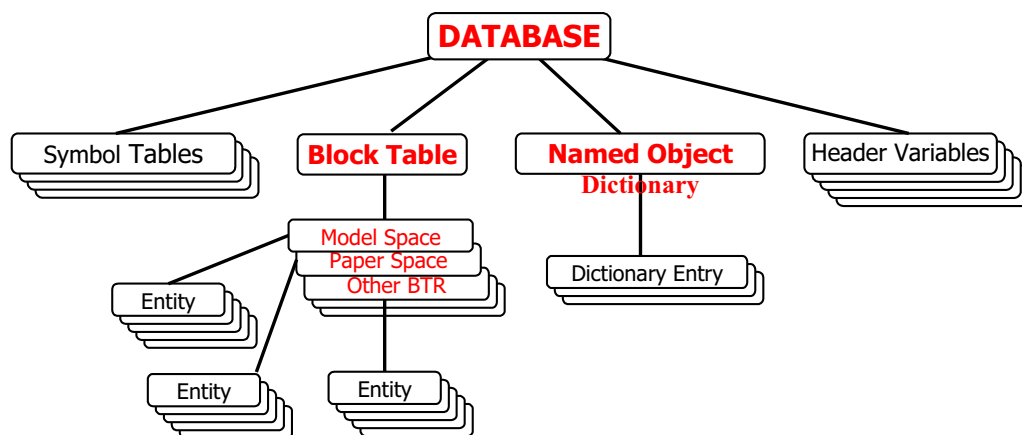
Figure 44 – AutoCAD API (LIMA; JUNIOR, 2010)

Database Components – GUI:

❏ Symbol Tables;

❏ Examples Layer Table, Line type Table, Text style Table etc;

❏ Containers to store Symbol Table Records;

❏ Example LayerTableRecord, LinetypeTableRecord etc.

All **Symbol Tables** represent a container control component:

❏ Add – to add a record;

❏ Item – to lookup an entry with a search string;

❏ Has – To know if an entry exists;

❏ Is enumerable;

❏ Each symbol table can hold only records of a specific type;

❏ For example, a LayerTable can hold only LayerTableRecords;

❏ Use SnoopDb to see where the Layers resides;

User Interface Design AutoCAD Defined:

❏ Menus – Application level menu, Context menuDialogs;

❏ AutoCAD's Enhanced Secondary Windows (Palettes);

❏ Color, Linetype, Lineweight, OpenFile dialogs;

❏ Tabbed Dialog Extensions (to Options Dialog);

❏ Status Bar;

❏ Tray;

❏ Drag-Drop;

Additionally. Explore **Autodesk.AutoCAD.Windows** namespace:

❏ Windows Defined;

❏ Windows Forms (Winform);

Host of other controls defined in **CLR**:

❏ Add Context Menu;

❏ Application Level – Application.AddDefaultContextMenuExtension;

❏ Object Level – Application. AddObjectContextMenuExtension ;

❏ Showing Modal and ModelessDialogs;

❏ Application.ShowModalDialog;

❏ Application.ShowModelessDialog;

Maintains size and position automatically.

Handling Events

Event:

❏ message sent by an object to notify if something has happened;

❏ message is received in a function call by one or more listeners;

❏ event sender only requires function pointer to dispatch a message;

❏ any interested party can implement the function and receive the event;

❏ function must have a specific signature that the sender requires;

❏ Use .NET delegates to 'wire' sender and receiver.

Delegates:

❏ Like a class (can be instantiated) but with a signature;

❏ Holds references to functions having same signature;

❏ Such as 'Type-Safe' function pointer;

❏ Can encapsulate any method that matches the specific signature.

6.1.3   FTTH PON Network CAD Design

For design purposes, CAD symbols were created to establish a specific database for FTTH PON projects. All elements in a real network can be represented by a specific symbol. In this work, we present only the elements used to simulate the experimentations realized in laboratory. However, it can be improved to create a complete set of FTTH PON design elements.

Figure 45 locates over a metropolitan map the location of the Central Office where the OTDR system is located and all other transmission systems. When the CO is inserted, the user is requested to provide the installation characteristics concerning the Primary Cable (defined by geographic parameters).
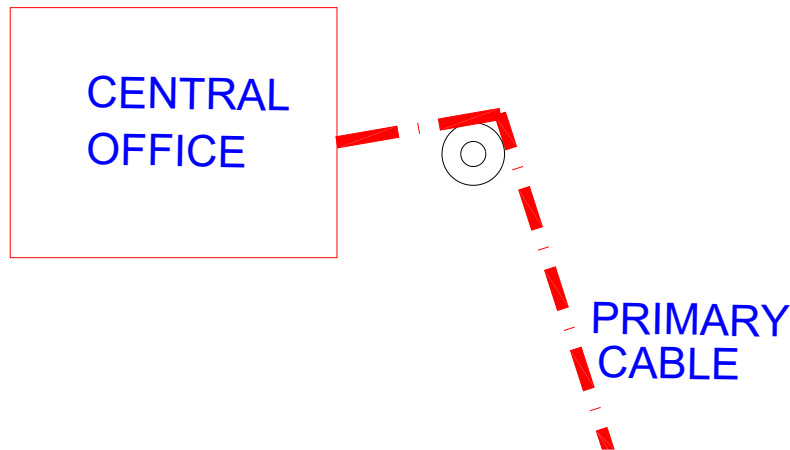
Figure 45 – Central Office Connection.

Figure 46 represents a Passive Optical Splitter and once it is inserted into a Computer Graphics environment the geometric and the equation constraints graph are created with its own parameters also established (e.g: splitter ratio).
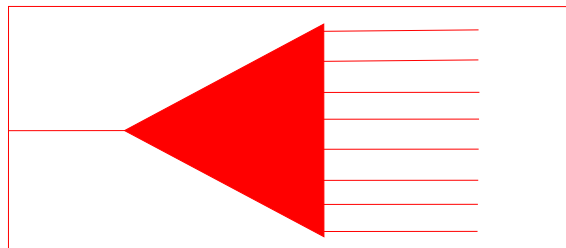
Figure 46 – Splitter Design symbology.

Figure 47, represents the line types adopted by the application to represent the Primary Cable, and Secondary Cables. Note that during the design procedure, the application generates the constraints graph connection with the other network elements (e.g: CO, Splitter, Subscriber).

PRIMARY CABLE

SECONDARY CABLE
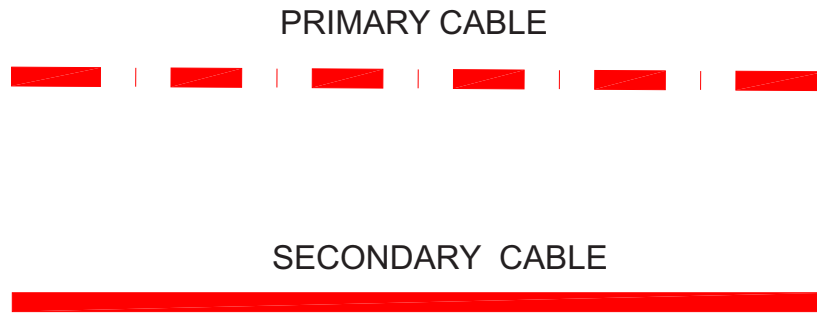
Figure 47 – Cable representation.

Figure 48, represents the subscriber position in the geographic location. The subscriber is identified by its own address or by a sequential unique database key, related to its commercial identification and geographic position (e.g: Latitude and Longitude).

SECONDARY
CABLE

20824
423 - 1

Figure 48 – Subscriber connection.

A FTTH PON sample design, that corresponds to the proposed arrangement made in the laboratory and used in this thesis, is presented in Figure 49
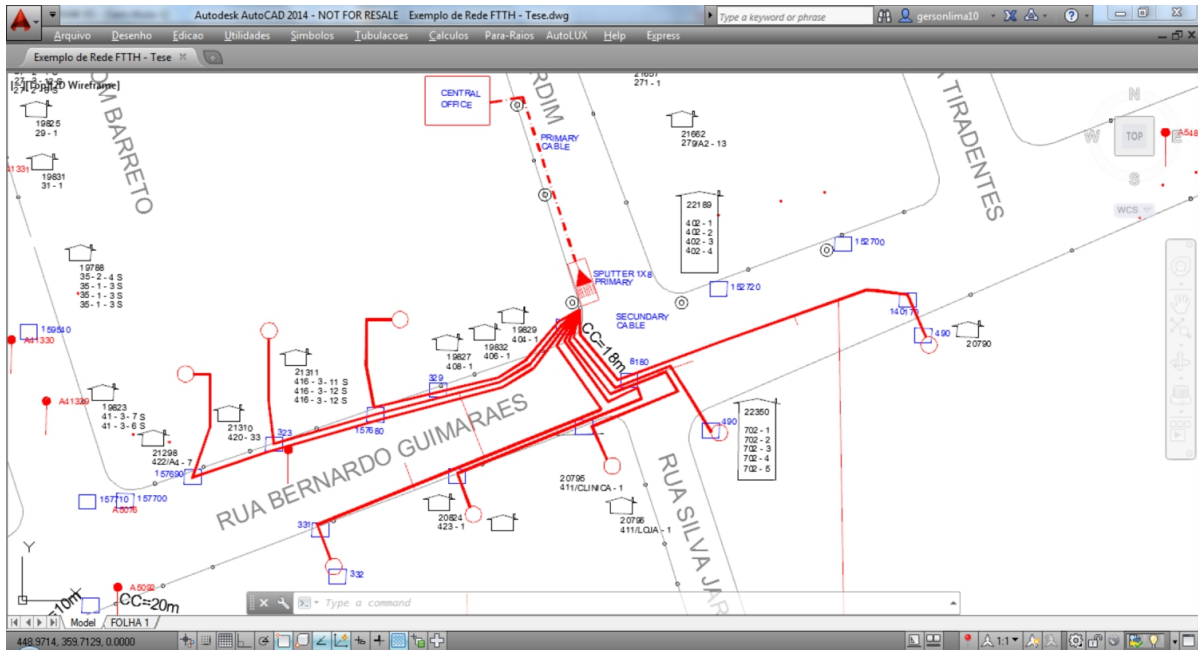
Figure 49 – PON Network

6.1.4   Graphical User Interface (GUI)

The GUI is based on AutoCAD MAP® (SDK)(AUTODESK, 2013). The capabilities of AutoCAD MAP interface provide a power tool to follow computer graphics standards and open source concepts to implement an easy-to-adopt tool, associated with an open source data base model, for many different acknowledged areas of scientific research. AutoCAD-based interface is a good tool for extending design information to users in a huge and traditional CAD community (OMURA; BENTON, 2013).

Objectives for Interacting with AutoCAD® – GUI environment and Constraint Manager Interface are:

❑ Deliver a product that requires CAD software functionality, but is not targeted at traditional CAD users;

❑ Build products that can read and create DWG™ files that are fully compatible with AutoCAD DWG files;

❑ Create host programs that run an application in a child window or through a web page;

❑ Deliver products with scaled feature sets at scaled price points and provide an AutoCAD-based platform that cannot be customized or extended by end-users;

❑ Replace an aging CAD software system and take advantage of new AutoCAD software technologies.

Features benefits for use with products built with AutoCAD® OEM software is the development platform used in order to read DWG™ and DXF™ file formats for every version of AutoCAD software through AutoCAD®. In addition, it can write DWG files for AutoCAD® software R2014 or its later versions. DXF files can be written back to older version of the AutoCAD® software. The capability to create host programs that run AutoCAD OEM design software in a child window, Microsoft® Windows® .NET from or through a web page. This development platform provides full control of the AutoCAD® functionality level exposed to the end user. It also provides encryption and binding security mechanisms that prevent copying or reverse engineering of code software programs.

A graphic interface was developed as shown in Figure 50, using AutoCAD MAP 2014®. Its purpose is to provide and to integrate solutions between the optical signal and the physical network installation design. Physical cable dimensions and geographic coordinates of network equipment are represented in real scale. All symbols were created in a library to represent the network equipment considering many brands on the Telecom market. Its connection rules are similar to real requirements in the field.

Figure 50, presents the FTTH design tool and the OTDR signal viewer. Note that it is possible to have in the same space: the map (physical network) and the signal OTDR signal of each network branch generated by our proposed algorithm.
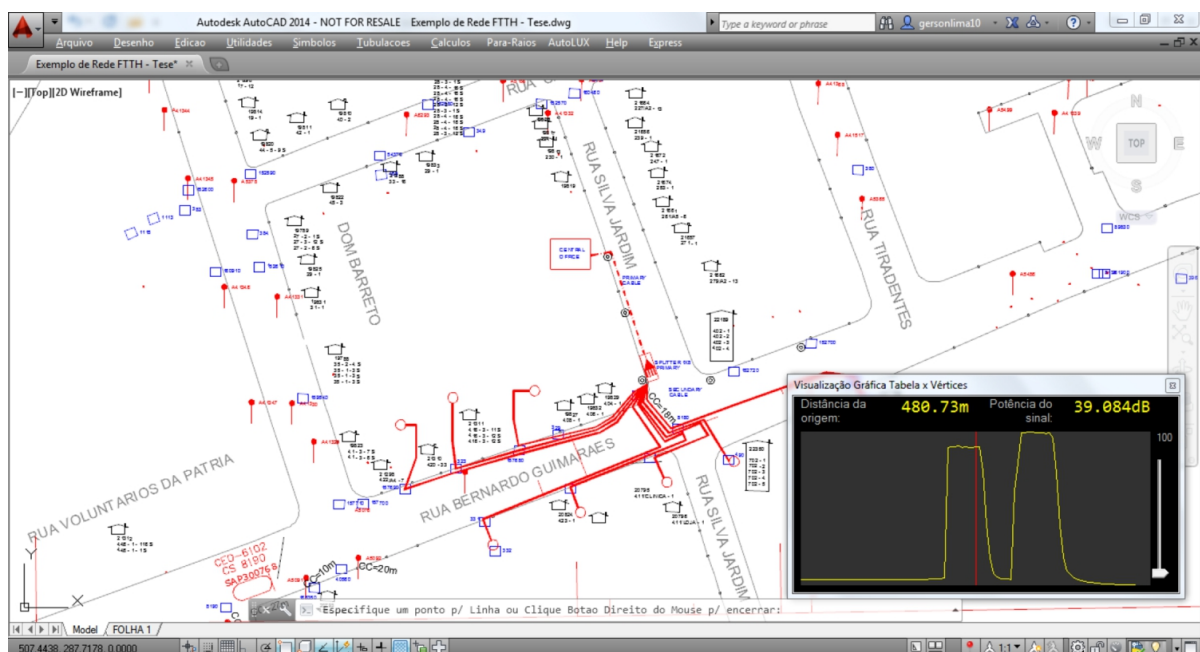
Figure 50 – PON Network

With this tool, it is possible through the "cursor" to follow the secondary network cable alignment observing in real time, in a specific window, the coupled optical signal. When varying a distance it is possible to observe the OTDR signal (dB), combining a power tool for network analysis along with surveillance purposes.

6.1.5   Concluding Remarks

The satisfaction of coupled engineering and geometric constraints trough the Equation based approach and geometric constructive coupling approach is made by the integration of both procedures and results in a graph topology database. This chapter has described the implementation process of the constraint database model proposed in this work. The implementation is produced for the main components: The GUI – Graphical User Interface and the constraint manager. The GUI is based on AutoCAD – API (Application Program Interface) and Object Oriented Classes methods. The Constraint Manager uses Graph based methods to maintain the geometric information used for AutoCAD API to update the design geometry. This chapter presented the process detailed work needed to maintain the interaction of these components and the Equation Graph, using dynamic updating as the implementation tool.

CHAPTER **7**

Conclusion and Future Work

7.1 Introduction

This thesis uses a concept of the interactive constraint-base to support the FTTH PON network design, based on the mathematical and engineering model for Optical Time Domain Relectomety. Also, it proposes an equation for Passive Optical Splitter signal simulation and the implementation of an Artificial Intelligence Algorithm using DE to allow the separation of the splitter superimposed signal.

This chapter draws upon a result comparison made from other similar works, where conclusions and discussions for long-term research are presented.

7.2 Results Comparison

To emphasize the features of this development, we perform a comparison between our work here referred to herein as CABLEVISION and other similar systems: SANTAD (RAD; FATHALLAH; RUSCH, 2010) and FPM (URBAN et al., 2013). Table 10 presents the results.

Table 10 – Solution Comparison

Feature	*CABLEVISON*	SANTAD	FPM
Centralized monitoring from CO	X	X	X
Locate network over a CAD / GIS system	X	-	-
Separate Superimposition of signal	X	-	-
Fault alarm detection	-	X	X
Signal simulation features	X	-	-
Graphical user interface (GUI) Capabilities	-	X	-

We have not yet implemented the routines for Fault detections nor implemented a special Graphical interface to be used by the operators in the central office. However, the

capability demonstrated for separating the superimposed signal and coupling it to the network's graphical design contributes towards further implementations.

7.3   Conclusion

A novel strategy to simulate the OTDR Measurement signal after the PON Splitters is presented in this research work. We propose a superimposition equation that, joined with a Differential Evolutionary algorithm, allows for the determination of the power parcel diverted after the splitters for each channel. It also allows for the separation of the OTDR signal for each channel. Furthermore, the separated signal of each channel was coupled with a real scaled CAD/GIS network design resulting in a tool for creating FTTH PON projects and which contributes towards surveillance proceedings. In practice, the proposal is to realize these measurements during the network installation phase. It is important to note that the constraint system is not able to add any occurrences of new reflective events at this moment. However, this work provides capabilities for accessing a map with the complete network design to allow the user to evaluate the coupled optical signal. The achieved time x correlation by Differential Evolutionary Algorithm is a very important parameter for future investigations, that should go on to motivate the future implementation of other algorithm techniques.

7.4   Future work

The following is suggested as a future work proposal:

❏ Expand the present implementation for more complex FTTH PON Networks;

❏ Implement similar procedures to evaluate the proposed Splitter Equation with Other Splitter ratios;

❏ Increase the symbol implementation for a more complete set of FTTH PON components, amalgamating a complete design tool inside AutoCAD;

❏ Implement routines and database control to allow alarms and surveillance tools;

❏ Implement new algorithm techniques to evaluate the relationship time x correlation ;

Bibliography

AB-RAHMAN B NG, K. J. M. Remotely control, centralized monitoring and failure analyzing in pon. **IJCSNS International Journal of Computer Science and Network Security, VOL.9 No.2, February 2009**, Vol.9 Nro.2, 2009.

AB-RAHMAN, M. S. Cost installation analysis of ftth test bed network set up-previous, present and future. **Journal of Applied Sciences Research**, v. 7, n. 11, p. 1627–1632, 2011.

AB-RAHMAN, M. S. et al. New optical splitter design for application in fibre-to-the home passive optical network using virtual lab platform. **Journal of Computer Science**, v. 8, n. 6, p. 864, 2012.

ACHARYYA, R. **A New Approach for Blind Source Separation of Convolutive Sources**. [S.l.: s.n.], 2008.

AKWANIZAM, A. Analysis and measurement fiber optic fault by using optical time domain reflectrometer (otdr). UTeM, 2009.

ALCATEL. **Alcatel Networks, Fiber-to-the-User: The Ultimate Endgame**. [S.l.], 2009. Disponível em: <http://www.celemetrix.com.au/document/item/1071>.

ANDERSON, L. J. D.; BELL, F. Chapter 10: Analyzing passive networks containing splitters and couplers. In: **Troubleshooting Optical Fiber Networks Understanding and Using Optical Time-Domain Reflectometers**. [S.l.]: California, US: Academic Press, Elsevier, pp. 279-290, 2004., 2004.

ANDERSON LARRY JOHNSON, F. G. B. D. R. **Troubleshooting Optical-Fiber Networks**. [S.l.]: Elsevier - ISBN: 0-12-0586614, 2004.

AUTODESK. **AutoCAD Customization Guide**. [S.l.], 2013. Disponível em: <http://docs.autodesk.com/ACDMAC/2013/ENU/PDFs/acdmac_2013_customization_guide-.pdf>.

BAKAR M.Z. JAMALUDIN, F. A. M. Y. M. M. A.; ABDULLAH, M. A new technique of real-time monitoring of fiber optic cable networks transmission. **Opt. and Lasers in Engineering**, vol. 45, p. pp. 126–130, 2007.

BARROW, J. D. Constants and variations: From alpha to omega. In: **The Cosmology of Extra Dimensions and Varying Fundamental Constants**. [S.l.]: Springer, 2003. p. 207–222.

BESPROZVANNICH, A. V.; NABOKA, B. G. Fiber optic tube diagnostic by using reflectograms. In: **Laser and Fiber-Optical Networks Modeling, 2000. Proceedings of LFNM 2000. 2nd International Workshop on**. [S.l.: s.n.], 2000. p. 77–79.

BRANSDEN, B. H.; JOACHAIN, C. C. J. **Physics of atoms and molecules**. [S.l.]: Pearson Education India, 2003.

CHABOT, S. **Fiber Optic Testing Challenges in Point-to-Multipoint PON Testing**. [S.l.], 2009. Disponível em: <http://www.celemetrix.com.au/document/item-/1041>.

CHAKRABORTY, U. K. **Studies in Computational Intelligence, Springer**. [S.l.]: Springer, 2008.

CLAYS, K.; PERSOONS, A. Hyper-rayleigh scattering in solution. **Physical review letters**, APS, v. 66, n. 23, p. 2980, 1991.

D.DIMITRIADIS, A. P.; MARAGOS, P. A comparison of the squared energy and teager-kaiser operators for short-term energy estimation in additive noise. **IEEE Transactions on Signal Processing,**, vol.57, p. 2569–2581, 2009.

DEMTRODER, W.; TITTEL, F. K. Laser spectroscopy: basic concepts and instrumentation. **Optical Engineering**, International Society for Optics and Photonics, v. 35, n. 11, p. 3361–3362, 1996.

DERICKSON, D. **Fiber optic test and measurement**. [S.l.]: Michigan University; ISBN9780135343302., 1998.

FATHALLAH, H.; RUSCH, L. A. Code-division multiplexing for in-service out-of-band monitoring of live ftth-pons. **J. Opt. Netw.**, OSA, v. 6, n. 7, p. 819–829, Jul 2007. Disponível em: <http://jon.osa.org/abstract.cfm?URI=JON-6-7-819>.

FEICHTINGER, H. G.; STROHMER, T. **Advances in Gabor analysis**. [S.l.]: Birkhauser Boston, 2002.

FENGLEI, L.; ZAROWSKI; J., C. Detection and location of connection splice events in fiber optics given noisy otdr data. part ii. r1msde method. **Instrumentation and Measurement, IEEE Transactions on**, IEEE, v. 53, n. 2, p. 546–556, 2004.

FERRARI, N. et al. Otdr characteristics for pon measurements. In: **Proceedings of the 57th - International Wire & Cable Symposium, November 9-12, 2008, Rhode Island, USA**. [S.l.: s.n.], 2008.

GIRARD, A. **FTTx PON Technology and Testing**. 1. ed. [S.l.]: EXFO ELECTRO-OPTICAL ENGINEERING INC., 2005. 191 p. (1, 01).

GOLDBERG, D. E. **Genetic Algorithms in Search, Optimization and Machine Learning**. [S.l.]: Addison-Wesley Longman, 1989.

GROBE, K.; ELBERS, J.-P. Pon in adolescence: from tdma to wdm-pon. **Communications Magazine, IEEE**, IEEE, v. 46, n. 1, p. 26–34, 2008.

GUIMARAES, F. G. Algoritimos de evolucao diferencial para otimizacao e aprendizado de maquina. **Anais do IX Congresso Brasileiro de Redes Neurais / Inteligencia Computacional**, V1, p. 1–17, 2009.

HANN, S.; YOO, J. sang; PARK, C.-S. Monitoring technique for a hybrid ps/wdm-pon by using a tunable otdr and fbgs. **Measurement Science and Technology**, Volume 17, Number 5, p. 1070–1074, 2006. Disponível em: <http://iopscience.iop.org/0957-0233/17/5/S22;jsessionid=0CC8FE567A4D4BB3DA0509A30BBFCCCF.c1>.

HARAN GLEN KRAMER; RUO DING, M. O. T. P. F. E. D. C. O. An introduction to pon technologies. **IEEE Communications Magazine**, v. 0163-6804/07, p. 18–25, 2007. Disponível em: <http://www.sis.pitt.edu/~dtipper/2011/PON_Tutorial.pdf>.

HAYES, J. **Connector Identifier**. [S.l.], 2009. Disponível em: <http://en.wikipedia-.org/wiki/Optical_fiber_connector>.

HILL, K. O.; MELTZ, G. Fiber bragg grating technology fundamentals and overview. **JOURNAL OF LIGHTWAVE TECHNOLOGY**, v. 13, 1997.

HOLLAND. **Genetic algorithms and classifier systems: foundations and future directions**. [S.l.], 1987.

HOLLAND, J. **Adaptation in natural and artificial systems: An introductory analysis with applications to biology, control, and artificial intelligence.** [S.l.]: U Michigan Press, 1975.

IEC 61758-1. **Fibre optic interconnecting devices and passive components - Interface standard for closure**. Disponível em: <http://webstore.iec.ch/webstore-/webstore.nsf/artnum/039256!opendocument>.

IIDA, D. et al. Design of identification fibers with individually assigned brillouin frequency shifts for monitoring passive optical networks. **J. Lightwave Technol.**, OSA, v. 25, n. 5, p. 1290–1297, May 2007. Disponível em: <http://jlt.osa.org/abstract-.cfm?URI=JLT-25-5-1290>.

ITU. **Broadband optical access systems based on Passive Optical Networks (PON)**. 2005. Disponível em: <http://www.itu.int/rec/T-REC-G.983.1-200501-I>.

ITU G.652. **Characteristics of a single-mode optical fibre and cable**. 2009. Web. Disponível em: <http://www.itu.int/rec/T-REC-G.652-200911-I/en>.

ITU G.983.1. **Broadband optical access systems based on Passive Optical Networks (PON)**. 2005. Disponível em: <http://www.itu.int/rec/T-REC-G.983.1-/en>.

ITU G.984.1. **Gigabit-capable Passive Optical Networks (GPON)**. 2008. Disponível em: <http://www.itu.int/rec/T-REC-G.984.1/en>.

JUDD, D. B. Fresnel reflection of diffusely incident light. **Contributions to color science**, NBS: for sale by the Supt. of Docs., US Govt. Print. Off., v. 545, p. 301, 1979.

KAISER, J. Some useful properties of teager's energy operators. In: IEEE. **Acoustics, Speech, and Signal Processing, 1993. ICASSP-93., 1993 IEEE International Conference on**. [S.l.], 1993. v. 3, p. 149–152.

KAISER, J. F. On a simple algorithm to calculate the energy of a signal. **Acoustics, Speech, and Signal Processing,1990. ICASSP-90, International Conference.**, v. 1, p. 381–384, 1990.

KEISER, G. **Optical Communications Essentials**. [S.l.]: McGraw-Hill Networking Professional, 2003.

KENDALL, M.; STUART, A. **The Advanced Theory of Statistics, vol. 2, Inference and Relationship , Griffin**. [S.l.], 1973.

KIM, Y. et al. Analyzing otdr measurement data using the kalman filter. **Instrumentation and Measurement, IEEE Transactions on**, IEEE, v. 57, n. 5, p. 947–951, 2008.

KOSHIBA, M.; TSUJI, Y.; HIKARI, M. Time-domain beam propagation method and its application to photonic crystal circuits. **Journal of Lightwave Technology**, IEEE, v. 18, n. 1, p. 102, 2000.

LAMOUNIER, E. **An Incremental Constraint-Based Approach to Support Engineering Design**. Tese (Doutorado) — School of Computer Studies, University of Leeds, 1996.

LANGLEY, L. et al. Packaged semiconductor laser optical phase-locked loop (opll) for photonic generation, processing and transmission of microwave signals. **Microwave Theory and Techniques, IEEE Transactions on**, IEEE, v. 47, n. 7, p. 1257–1264, 1999.

LIMA, G.; LAMOUNIER, E.; CARDOSO, A. Ilumination design using thematization and quantization of luminances in 3d environments. In: **Proceeding of Brazilian Simposium of Energy Systems - SBSE**. [S.l.: s.n.], 2010.

LIMA, G. et al. Lightning protection design using information visualization and virtual reality. In: **IEEE - PowerTech 2011 - International Conference Trondheim**. [S.l.: s.n.], 2011.

LIMA, G. F. M. A teo-based algorithm to detect events over otdr measurements in ftth pon networks. **Revista IEEE America Latina, v. 11,**, V.11, p. p. 886–891, 2013, 2013.

LIMA, G. F. M.; JUNIOR, E. A. C. L. **Constraint-based Techniques to Support Electronic TV Network Design:**. [S.l.]: Lambert Academic Publisher, 2010. 108 p. (1, 1).

LIMA, G. F. M.; LAMOUNIER, E.; BARCELOS, S. A teo-based algorithm to detect events over otdr measurements in ftth pon networks. **Latin America Transactions, IEEE (Revista IEEE America Latina)**, IEEE, v. 11, n. 3, p. 886–891, 2013.

LIMA, G. F. M. de. **Constraint-Based model to support engineering TV design**. Dissertação (Mestrado) — Universidade Federal de Uberlandia, 2008.

LIMA, G. F. M. de; LAMOUNIER, E. A.; BARCELOS, A. C. S. A teo-based algorithm to detect events over otdr measurements in ftth pon networks. In: **4TH IEEE LATIN-AMERICAN CONFERENCE ON COMMUNICATIONS 2012 ,7-9 NOVEMBER, CUENCA - ECUADOR.** [S.l.: s.n.], 2012.

LIU, F.; ZAROWSKI, C. J. Events in fiber optics given noisy otdr data. i. gsr/mdl method. **Instrumentation and Measurement, IEEE Transactions on**, IEEE, v. 50, n. 1, p. 47–58, 2001.

NIKOLIĆ, D. et al. Scaled correlation analysis: a better way to compute a cross-correlogram. **European Journal of Neuroscience**, Wiley Online Library, v. 35, n. 5, p. 742–762, 2012.

OMURA, G.; BENTON, B. C. **Mastering AutoCAD 2014 and AutoCAD LT 2014: Autodesk Official Press**. [S.l.]: Sybex, 2013.

PARK, S.-B. et al. Optical fault monitoring method using broadband light source in wdm-pon. **Electronics Letters**, v. 42, n. 4, p. 239 – 241, 2006. ISSN 0013-5194.

PEARCE, D. **Speech Processing, Transmission and Quality Aspects (STQ); Distributed speech recognition; Front-end feature extraction algorithm; Compression algorithms DRS front end**. [S.l.], 2003. Disponível em: <http://-/webapp.etsi.org/workProgram/Report_Schedule.asp?WKI_ID=18820>.

PRICE, K.; STORN, R.; LAMPINEN, J. Differential evolution: A practical approach to global optimization (natural computing series) springer; 2005. **ISBN: 3540209506**, 2005.

RAD, M.; FATHALLAH, H.; RUSCH, L. Fiber fault pon monitoring using optical coding: Effects of customer geographic distribution. **Communications, IEEE Transactions on**, v. 58, n. 4, p. 1172 –1181, 2010. ISSN 0090-6778.

RAD, M. M. **Passive Optical Network (PON) Monitoring Using Optical Coding Technology**. Tese (Doutorado) — Université Laval, 2010.

RISSANEN, J. A universal prior for integers and estimation by minimum description length. **The Annals of statistics**, JSTOR, p. 416–431, 1983.

ROCCA, P.; OLIVERI, G.; MASSA, A. Differential evolution as applied to electromagnetics. **Antennas and Propagation Magazine, IEEE**, IEEE, v. 53, n. 1, p. 38–49, 2011.

RODGERS, J. L.; NICEWANDER, W. A. Thirteen ways to look at the correlation coefficient. **The American Statistician**, Taylor & Francis, v. 42, n. 1, p. 59–66, 1988.

RUNGER, D. C. M. . G. C. **Applied Statistics and Probability for Engineers 3rd ed.** [S.l.]: John Wiley ISBN 0-471-20544-4,, 2003.

SALEH, B. E.; TEICH, M. C. **Fundamentals of photonics**. [S.l.]: Wiley-Interscience, 2013.

SANKAWA, I. et al. Fault location technique for in-service branched optical fiber networks. **Photonics Technology Letters, IEEE**, v. 2, n. 10, p. 766 –768, out. 1990. ISSN 1041-1135.

SATYAN, N. **Optoelectronic control of the phase and frequency of semiconductor lasers**. Tese (Doutorado) — California Institute of Technology, 2011.

SCHARF, L. L.; FRIEDLANDER, B. Matched subspace detectors. **Signal Processing, IEEE Transactions on**, IEEE, v. 42, n. 8, p. 2146–2157, 1994.

SERRANO, D. **Constraint Management in Conceptual Design**. Tese (Doutorado) — University of Leeds, 1987.

SILVA, A. L. d. **Using Geometric Constraints Approach to support electrical installation design**. Tese (Doutorado) — Federal University of Uberlandia, 2006.

SIMARD, M. Otdr pon testing: the challenges - the solution. **EXFO Application Note 201**, v. 201, p. 01–03, 2009.

STEPHANOPOULOS, G. A knowledge-based framework for process design and control. In: **Workshop on Artificial Intellignece in Process Engineering, Columbia University - New York - USA**. [S.l.: s.n.], 1987.

TAN, Y.; WANG, J. Nonlinear blind source separation using higher order statistics and a genetic algorithm. **Evolutionary Computation, IEEE Transactions on**, v. 5, n. 6, p. 600–612, 2001. ISSN 1089-778X.

TAVARES, J. et al. Algorithm based on teager energy operator (teo) to lines and words segmentation in manuscripts and printed texts. In: **VII Workshop Computacional Vision, 2011, Curitiba p. 219-224.** [S.l.: s.n.], 2011.

TAVARES, J. do A. et al. SLPTEO e SCORC: abordagens para segmentação de linhas, palavras e caracteres em textos impressos. In: NEVES, L. A. P.; Vieira Neto, H.; GONZAGA, A. (Ed.). **Avanços em Visão Computacional**. 1. ed. Curitiba, PR: Omnipax, 2012. cap. 13, p. 239–264. ISBN 978-85-64619-09-8.

TEAGER, H. M.; TEAGER, S. M. **Evidence for Nonlinear Production Mechanisms in the Vocal Tract**. [S.l.]: Kluwer Acad. Publ., Boston, MA, 1990., 1990.

TSUJIKAWA, K. et al. Method for predicting rayleigh scattering loss of silica-based optical fibers. **Lightwave Technology, Journal of**, v. 25, n. 8, p. 2122–2128, 2007. ISSN 0733-8724.

URBAN, P. et al. Fiber plant manager: an otdr- and otm-based pon monitoring system. **Communications Magazine, IEEE**, v. 51, n. 2, p. S9–S15, 2013. ISSN 0163-6804.

VAUGHN, M. et al. Value of reach-and-split ratio increase in ftth access networks. **Lightwave Technology, Journal of**, v. 22, n. 11, p. 2617 – 2622, 2004. ISSN 0733-8724.

WELCH, G.; BISHOP, G. **An introduction to the Kalman filter**. 1995.

YAMASAKI, D. J. **Lighting the Way to the Home Transmission System Basics: Optical Fiber and Optical Cable**. [S.l.], 2011. Disponível em: <http://www.key4biz-.it/files/000038/00003898.pdf>.

YANG, J.; LI, B.; ZHUANG, Z. Research of quantum genetic algorith and its application in blind source separation. **Journal of Electronics (China)**, Springer, v. 20, n. 1, p. 62–68, 2003.

YEH F.Y. SHIH, G. C. C.; CHI, S. Reliable tree-type passive optical networks with self-restorable apparatus. **Opt. Exp**, vol. 16, no. 8, p. pp. 4494–4498, 2008.

YEH, S. C. C.-H. Optical fiber-fault surveillance for passive optical networks in s-band operation window. **Opt. Express**, OSA, v. 13, n. 14, p. 5494–5498, Jul 2005. Disponível em: <http://www.opticsexpress.org/abstract.cfm?URI=oe-13-14-5494>.

Appendix

APPENDIX **A**

A TEO-Based Algorithm to detect events over OTDR Measurements in FTTH PON Networks

A.1   introduction

A variety of Optical Time Domain Reflectometry (OTDR) testing methods have been designed for the verification and troubleshooting of PON's, such as testing all points from the optical network terminal (ONT) to the central office (CO), testing the feeder part of the network from the CO, and, in some cases, simply not testing at all (CHABOT, 2009). OTDR methods provide reliable results and, since it is a single-ended method, it significantly reduces staff time. The cost of the OTDR instrument and the required skill level of the user are usually perceived as its drawbacks. Reflectometric signals are processed by software using different methodologies to recognize events, failures and degradations in the optical fiber. This matter has long been dominated for point-to-point fiber networks (DERICKSON, 1998). For FTTH PON architectures, however, several new challenges arise when testing through optical splitters (FERRARI et al., 2008). This is overcome by either testing from the ONT side or testing up to the splitter position only. The former is a non-economical solution as it would require an enormous amount of testing instruments and well trained field technicians (SIMARD, 2009). The latter can only see the feeder part of the network, i.e., from the CO up to the splitter position, which is usually the network portion less prone to failures. After the splitter, the OTDR measurement brings little information as Rayleigh scattering is strongly attenuated by the double-passage through the splitter, because the 64 backscattered signals from the PON branches superimpose at the OTDR receiver, making it impossible to recognize events from single PON branches, and because traditional OTDR technology has low dynamic range when used with short OTDR pulses, which is a requirement for PON measurements. Moreover, traditional OTDR technology relies on a mathematical method called Least Squares Approximation,

LSA, for event analysis. The performance of this method, which is already limited for analyzing point-to-point networks, is fully inadequate for PON networking OTDR measurement and analysis. Teager Energy Operator (TEO) methods have proven effective for a variety of audio signal processing second (SIMARD, 2009) and for the analysis of digitalized images used for text segmentation (TAVARES et al., 2012). In this work, we have used the Teager Energy Operator to develop a method, which we have named TEO-OTDR, for pos-processing OTDR signals in order to univocally recognize events in single PON branches after the splitter, when the OTDR instrument is positioned in the Central Office. As a result, instead of investing in a great number of OTDR instruments, to test from each home side, and perfecting the field technicians' expertise to deal with profound optical concepts, a single OTDR can be positioned in each CO.

A.2   The Teager Energy Operator (TEO)

In the work of Teager and Teager (TEAGER; TEAGER, 1990) on nonlinear modeling of speech, referenced in Maragos et al. (D.DIMITRIADIS; MARAGOS, 2009), an energy operator on (TAVARES et al., 2011) speech-related signals is first presented. In another work, Kaiser discussed the properties of Teager's energy-related algorithm, which was later modified as the Teager Energy Operator (TEO), or the Teager-Kaiser Operator. This, by operating on-the-fly on signals composed of a single time-varying frequency, is able to extract a measure of the energy of the mechanical process that generated this signal (KAISER, 1990). Kaiser (KAISER, 1993) has also defined the TEO in both continuous and discrete domains as very useful tools for analyzing single component signals from an energy point-of view. TEO is defined in the discrete domain by Equation 7 (KAISER, 1993). Note that this algorithm uses only three arithmetic operators applied to three adjacent samples of the signal for each time shift.

$$\psi[S_n] = S_n^2 - S_{n-1}.S_{n+1} \qquad (7)$$

Where:

ψ is the Teager operator.

S_n is the nth value of the discreet signal.

One conclusion on the work of Kaiser (D.DIMITRIADIS; MARAGOS, 2009) states that "it is as if the algorithm [of TEO] is able to extract the envelope function of the signal". This aspect gave us the indication to develop a TEO-OTDR method to overcome the current limitations of OTDR fault diagnosing in FTTH PON networks.
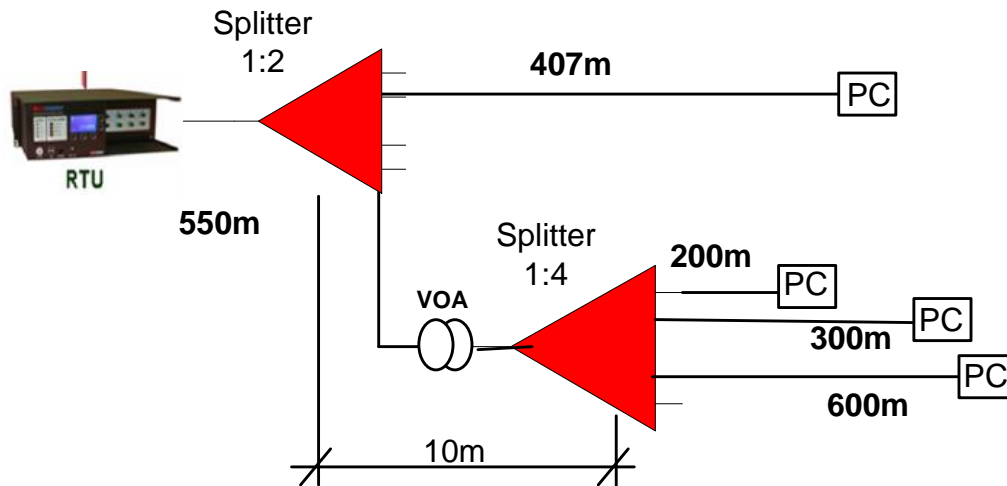
Figure 51 – Experimental arrangement

A.3   Experimental Arrangement

Figure 51 presents one of the experimental arrangements used for the simulation of scenarios where noise blurred useful event information in PON OTDR measurements, thus making it impossible for traditional OTDR solutions to extract and diagnose fault information after the PON splitter. This specific arrangement uses two cascaded splitters, 1:2 and 1:4, installed in a short distance apart. Splitting ratios up to 1:64 have been tried. In addition, a Variable Optical Attenuator (VOA) is used to impose a variable high attenuation level in one (or more) PON branches, thus allowing to simulate different reflectance events and attenuation in a single (or multi) PON branch after the splitter. Events can be originated form optical connectors, fiber splices, network end point, fiber cuts, slow fiber degradations etc.

For the OTDR measurements, we have used a RTU (remote test unit) developed by FiberWork for remote fiber testing applications, this equipment is capable of saving many OTDR measures in a relational database. The RTU was configured for 1625nm, DR=5Km and 10ns pulse width. Larger pulse widths, up to 200ns, were tested as well. The fiber ends in the PON branches are the actual set-ups used in commercial PON networks, apart from one of the fiber ends which has an open PC connector (i.e., 14dB reflectance) for calibration purpose. A 1625nm mirror device, such as Fiber Bragg Grating devices, were used to help the OTDR to identify the optical termination point in the subscriber's home. Figure 52 presents the measured OTDR curve for the PON network of figure 1. Several different curves can be obtained by adjusting the component positions, simulated event types, VOA attenuation and splitter level. An Expert eye can see some minor events hidden in the noisy portion of the OTDR curve. However, traditional OTDR software routines cannot distinguish these from noise. So, events after the splitter cannot be automatically and reliably identified. Moreover, such events cannot be quantified and
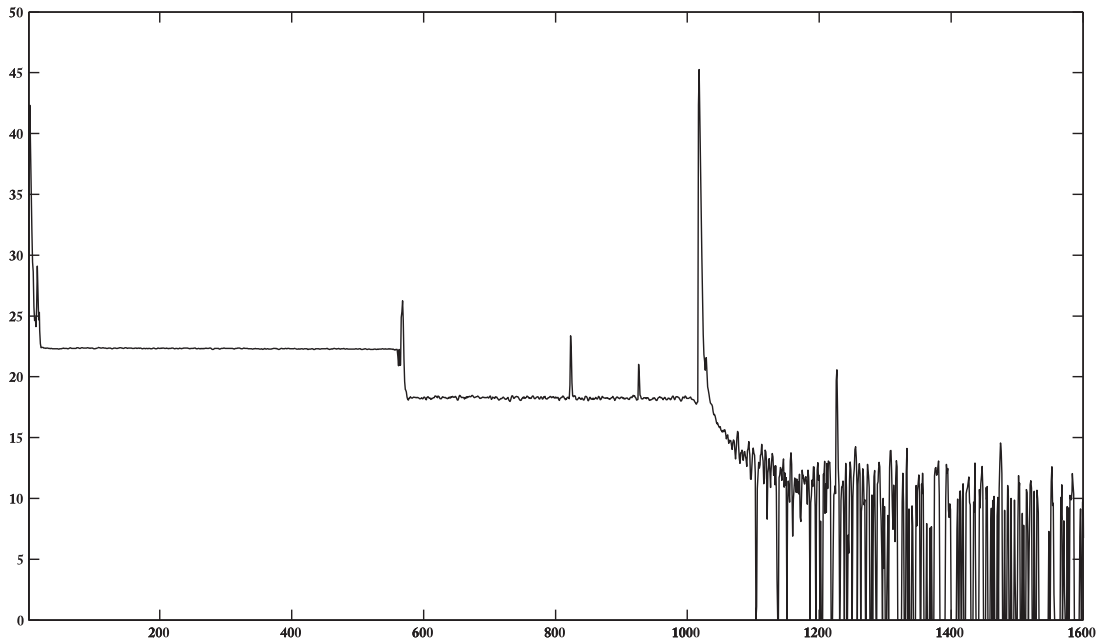
Figure 52 – Original OTDR signal

continuously monitored for tracking failures in PON networks. From left to right it's possible to first identify a reflective event caused by the connection between RTU and the optical fiber, in sequence at 550 meters occurs a small reflective event caused by the connection of the optical cable and the first splitter.

Both splitters and the Variable Optical Attenuator (VOA) events are very near and it is not possible an identification or separation of each other's. Following, it is possible to observe other reflective event near 800 meters caused by the 200 "PC" connector installed after the second splitter. In sequence the 300 meters "PC" connector Reflective event is observed. Near 1000 meters is observed the reflective event of the first splitter branch fiber (407 meters). Finally, immersed in the noise the last "PC" connector is observed (near 1200 meters).

A.4 Algorithm Description

Figure 53 presents a block diagram that describes each part of the algorithm implementation. The software application controls the RTU (OTDR is configured in this experimentation for 1625nm, DR=5Km and 10ns pulse width) to obtain the OTDR measure and save the curves in a data structure of a vector. A notch filtering operation (Equation 8) is applied to the signal (PEARCE, 2003) that aims to remove DC offset but ends attenuating the whole signal. This procedure emphasizes events blurred into the noise (see Figure 56).

$$S'_n = S_n - S_{n-1} + 0.999.S'_{n-1} \tag{8}$$

Where:

S_n is the OTDR signal.

S'_n is the resulting signal of notch filtering.

Note that only values above 0 dB are considered after notch filtering, i.e., the resulting signal of notch filtering is then cropped by its negative values. After, it is constructed the signal T (Equation 9), using the absolute values of Teager operator (TEO) of the the resulting cropped signal form notch filtering. Figure 5b presents the plotted signal .

$$T_n = \left| \psi \left[S'_n \right] \right| \tag{9}$$

Where:

ψ is the Teager operator.

S'_n is the resulting cropped signal from notch filtering.

T is the signal of interest.

The next step defines threshold based on the signal T data set. Analyzing the signal T (Figure 5b), it is possible to identify that events of interest have a significantly higher amplitude than the rest of the signal, matching the concept of extreme outliers from the statistical tool known as box plot. As Montgomery states, "A point more than 3 interquartile ranges from the box edge is called an extreme outlier" (RUNGER, 2003). Following this idea, the T signal data points are sorted and the 1st (Q1) and 3rd (Q3) quartiles are identified, in order to calculate the interquartile range (IRQ) for this "data set". After, the Threshold is set by Equation 10, the same process is used to identify the lower level of an extreme outlier.

$$\theta = Q3 + 1.5.IRQ \tag{10}$$

Where:

θ is the Threshold.

$Q3$ is the 3rd quartile

IRQ is the interquartile range

To highlight the detected events, using the signal T as a guide, a Boolean control variable is set. The proposed method identifies this variable as CTR and uses it to keep control of the last sampled point status. If this last point was identified as an "event of interest" and CTR is false, CTR is set to true; if the last point is considered a non-interest one and CTR is true, CTR is set to false. In other words, if the maximum absolute TEO value from a given OTDR sampled point is greater than the threshold and CTR is false, this point index is set as the "starting point of a possible event of interest". Reciprocally, if the maximum absolute TEO value from a given OTDR sampled point is less than the threshold and CTR is true, this point index is set as the "ending point of a possible event of interest". The flow Chart of this method is presented in Figure 3. After running through

Figure 53 – Algorithm block diagram

original and notch filter.jpg
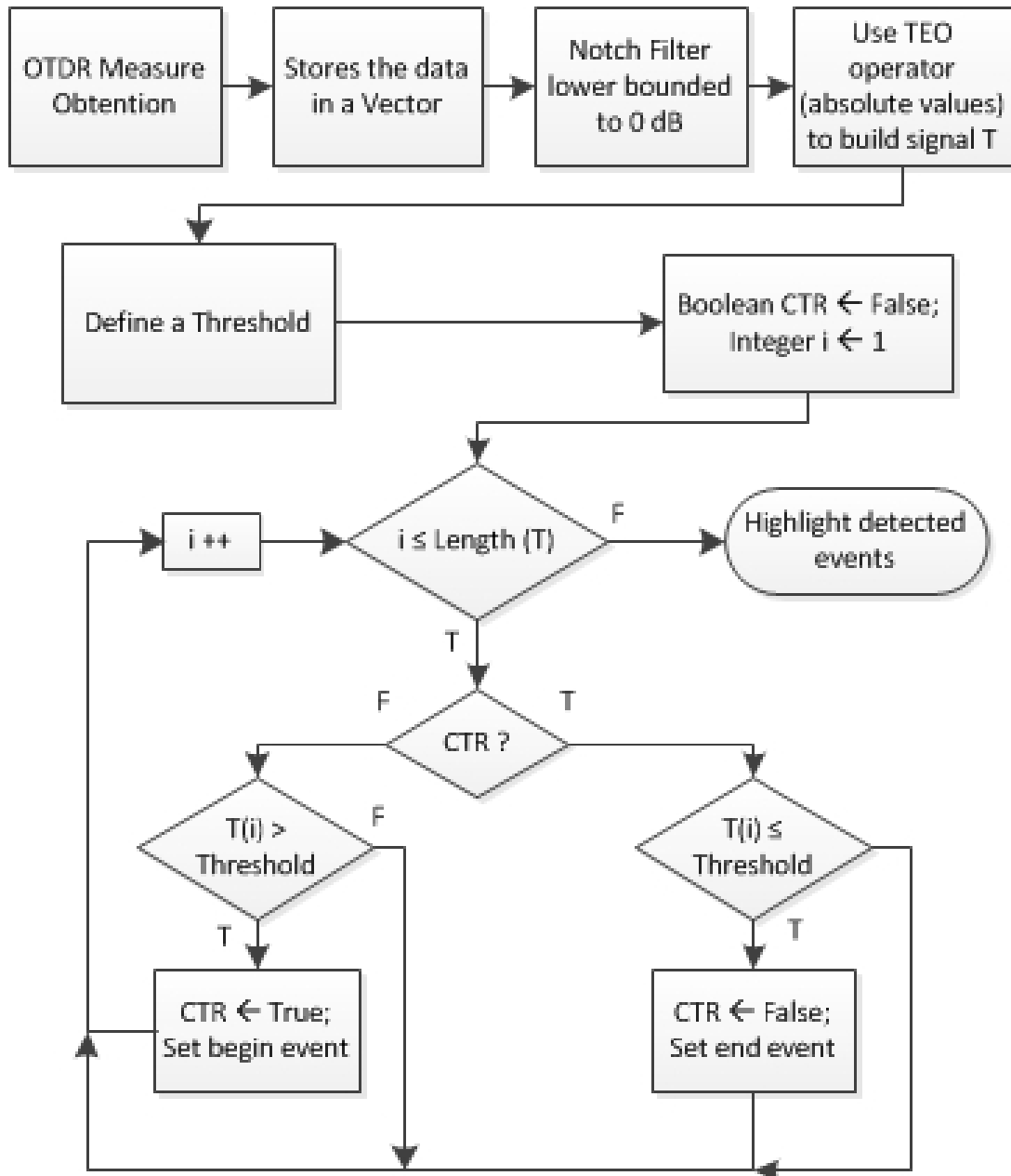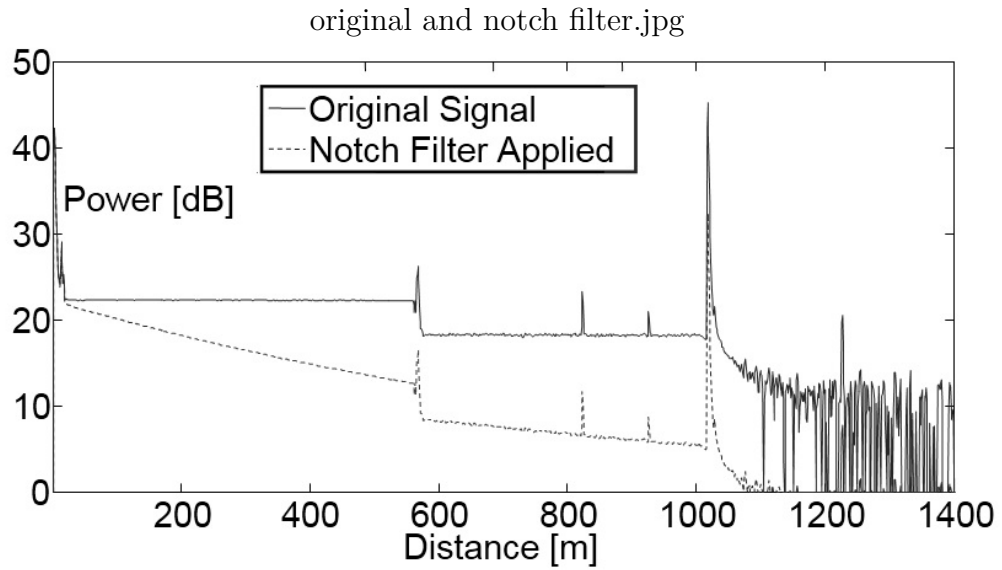

Figure 54 – OTDR original signal and notch filter
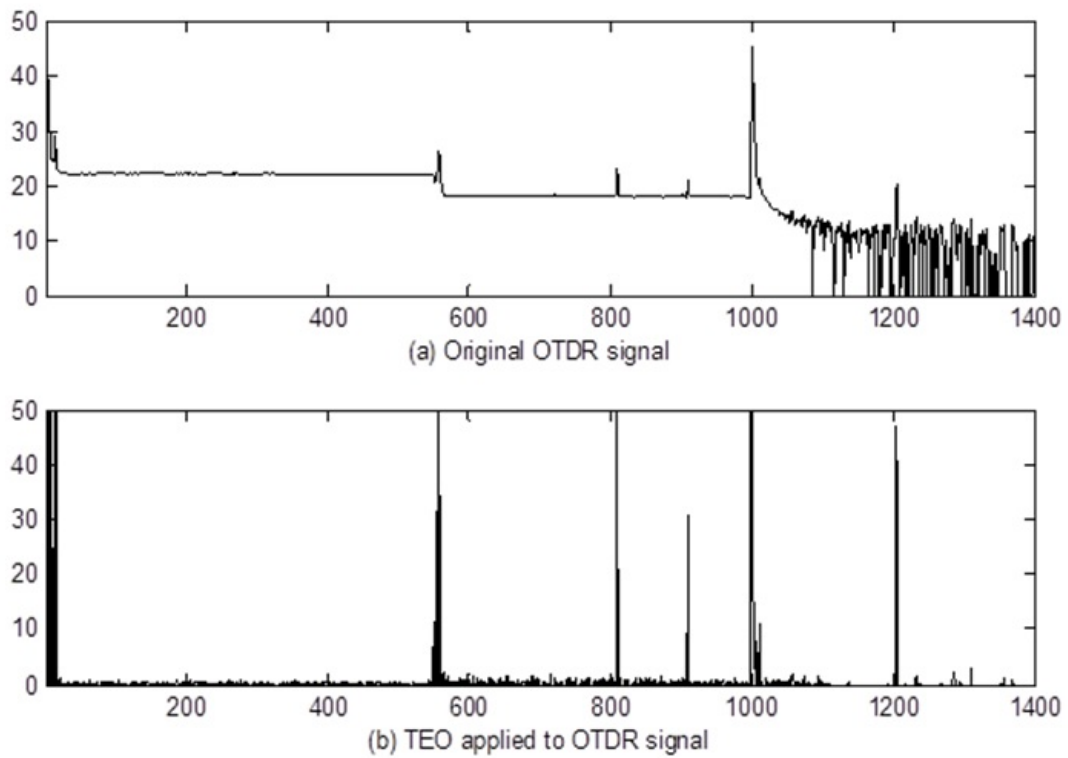
Figure 55 – (a) Original OTDR signal (b) TEO signal T

all signal T, this method returns the location of each detected event to be superposed to the OTDR signal, as can be seen in Figure 6.
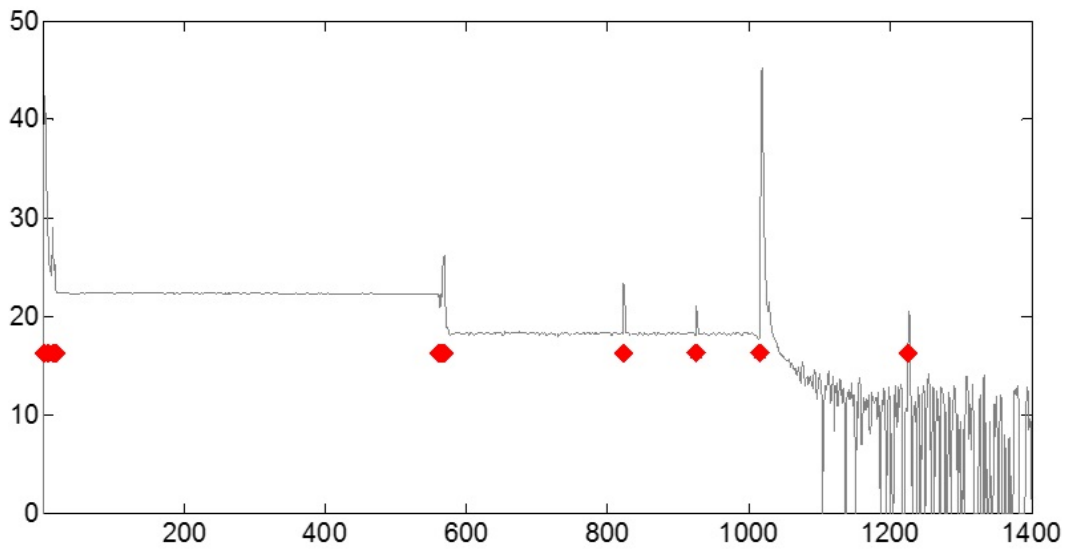
Figure 56 – Scatter plot of the TEO-OTDR results superposed to the OTDR measurement curve.

A.5 Conclusion

As FTTH is in o track to replace the twisted copper pair telephony system, fiber plants will eventually become massive infrastructures. To cope with this scenario, economically feasible maintenance methodologies must be developed. Since FTTH PON networks rely on infrastructure sharing architectures, the traditional OTDR testing methodology, which relies on Least Squares Approximation is unreliable for maintaining such new fiber plants as it cannot effectively locate and identify optical events after PON splitters. To overcome this, we have developed a TEO-OTDR method which has proven to be effective for post-processing OTDR curves and univocally recognize and locate events in the optical branches after the splitter. Moreover, this technique also improves event location (distance) accuracy over line-fit (LSA) techniques by identifying the event leading edge. This solution shall contribute to reduce FTTH maintenance costs and to improve network availability. The results obtained in this work intends to supporting the next research implementations where procedures there will be implemented for identification of OTDR events after splitter signal separation using artificial intelligence and CAD/CAE algorithms.

APPENDIX **B**

Routines to Genetic Algorithm

The MATLAB®routine are developed with the intention of OTDR Signal Separation and described in section 4.2.

```matlab
function R = testeAGotdr
clc; close all;
global sdi dx emm vf m cd
otdrr = struct('arq',{},'sinal',{});
otdrc = struct('sinal',{});
[filename,pathname] = uigetfile({'*.csv','Selecione arquivos'}, ...
    'Selecione todos os arquivos de sinais separados', ...
    'MultiSelect', 'on');
if ~isequal(filename,0)
    if ischar(filename)
        filename = cellstr(filename);
    end
    for i = 1:length(filename)
        otdrr(i).arq = filename{i};
        otdrr(i).sinal = csvread([pathname filename{i}],51,0);
    end
    [filen,pathn] = uigetfile({'*.csv','Selecione arquivo'}, ...
        'Selecione o arquivo do sinal somado');
    % plot(otdrG)
otdrref =
    if ~isequal(filename,0)
        otdrG = csvread([pathn filen],51,0);
        ncanal = 8
            minx = 520;
            maxx = 4340;
        %end
```

```matlab
sdi = otdrG(minx:maxx); lsdi = length(sdi); %sinal de
    interesse
emm = [5 45]; %espectro apos splitter(dB) min e max
dx = 9; %largura do pico de fim de linha
m = atan(-1/1150); %queda de ganho da curva
vf = 21; %tamanho (acima do sinal) do pico de fim de
    linha
cd = -0.27; %"coeficiente" de decaimento da exponencial,
    calculado por PowR
if size(sdi,1) = 1
    sdi = sdi';
end
tic
%cromoi = struct('vc',{},'x',{});
cromot = struct('cromoi',{});
% Gera populacao inicial
npop = input('Quantos individuos? ');
fit = zeros(1,npop);
for i = 1:npop
    for j = 1:ncanal
        % interval [a, b]. r = a + (b-a).*rand(100,1);
        cromot(i).cromoi(j).vc = emm(1) + (emm(2)-emm(1))
            *rand;
        a = 1; b = lsdi-dx;
        cromot(i).cromoi(j).x = round(a + (b-a)*rand);
    end
    fit(i) = fitness(cromot(i));
end
MFit = []; BFit = []; maxfit = max(fit);
% Geracoes
nger = input('Quantas geracoes? ');
pc = 0.85; %taxa de cruzamento
pm = 1 - pc; %taxa de mutacao
nelit = ceil(npop*0.05); %numero de individuos no
    elitismo
ntorn = ceil(npop*0.05); %numero de individuos no torneio
if ntorn < 3, ntorn = 3; end
for N = 1:nger
    % Separa elitismo
    [sortfit,indelit] = sort(fit,'ascend');
    nfit = fit;
    elite = cromot(indelit(1:nelit));
```

```matlab
64              indiv = 1;
65              while (indiv <= npop)
66                  miss = true;
67                  X = rand;
68                  if X < pc && indiv < npop-1
69                      % Seleciona pais
70                      p1 = []; p2 = [];
71                      for i = 1:2
72                          indpop = randperm(npop);
73                          torncromo = cromot(indpop(1:ntorn));
74                          [sortfit,indelit] = sort(fit(indpop(1:
                                ntorn)),'ascend');
75                          if isempty(p1)
76                              p1 = torncromo(indelit(1));
77                          else
78                              p2 = torncromo(indelit(1));
79                          end
80                      end
81                      % Cruzamento
82                      [novocromo(indiv),novocromo(indiv+1)] =
                            crossover(p1,p2);
83                      % Novo fitness
84                      nfit(indiv) =  fitness(novocromo(indiv));
85                      nfit(indiv+1) =  fitness(novocromo(indiv+1));
86                      indiv = indiv + 2;
87                      miss = false;
88                  end
89                  X = rand;
90                  if X < pm && indiv < npop
91                      % Mutacao
92                      novocromo(indiv) = mutation(cromot(indiv));
93                      % Novo fitness
94                      nfit(indiv) =  fitness(novocromo(indiv));
95                      indiv = indiv + 1;
96                      miss = false;
97                  end
98                  if miss
99                      novocromo(indiv) = cromot(indiv);
100                     indiv = indiv + 1;
101                 end
102             end
103             % Prepara nova geracao
```

```matlab
104              k = 0; l = 0;
105              [sortnfit,indfit] = sort(nfit,'ascend');
106              for i = 1:length(cromot)
107                  if k < nelit
108                      k = k + 1;
109                      cromot(i) = elite(i);
110                  else
111                      l = l + 1;
112                      cromot(i) = novocromo(indfit(l));
113                  end
114                  fit(i) = fitness(cromot(i));
115              end
116              % Mostra evolucao
117              MFit = cat(1,MFit,mean(fit));
118              BFit = cat(1,BFit,min(fit));
119              plot(MFit,'b'); hold on; plot(BFit,'r'); grid on;
                     hold off;
120              legend('Media','Melhor');
121              set(gca,'XLim',[1 nger]); set(gca,'YLim',[0 2*max(fit
                     )]); pause(0.01);
122          end
123          % Mostra resultado
124          [sortnfit,indfit] = sort(nfit,'ascend');
125          R = cromot(indfit(1));
126          save('R','R');
127          figure, grid on, hold on
128          mx = 0;
129          sinalX = struct('sinal',{}); sinalY = struct('sinal',{});
130          for i = 1:length(R.cromoi)
131              sinalx = 1:R.cromoi(i).x;
132              sinaly = R.cromoi(i).vc + m.*sinalx;
133              sinalx = cat(2,sinalx,sinalx(end)+1:sinalx(end)+dx+1)
                     ;
134              sinaly = cat(2,sinaly,(sinaly(end)+vf).*ones(1,dx));
135              sinaly = cat(2,sinaly,vf.*((1:length(sdi)-length(
                     sinaly)).^cd));
136              otdrc(i).sinal = sinaly;
137              if length(sinaly) > mx, mx = length(sinaly); end
138              sinalX(i).sinal = sinalx;
139              sinalY(i).sinal = sinaly;
140          end
141          otdr = zeros(1,mx);
```

```matlab
142        for i = 1:length(sinalY)
143            otdr = otdr + [(10.^(sinalY(i).sinal./10)).^2 zeros
                (1,mx-length(sinalY(i).sinal))];
144        end
145        somasinal = 10.*log10(otdr.^0.5);
146        plot(otdrG,'r'); plot((1:length(somasinal))+minx,
                somasinal,'g');
147        for i = 1:length(otdrc)
148            sinaly = otdrc(i).sinal;
149            plot((1:length(sinaly))+minx,sinaly,'b');
150        end
151        title(['Correlacao: ' num2str(corr(somasinal',otdrref))])
                ;
152     % title('Sinal somado');
153        legend('Medido','Encontrado pelo AG','Sinais individuais
                AG')
154 %        for i = 1:length(otdrr)
155 %            G = otdrr(i).sinal;
156 %            figure
157 %            plot(1:length(G),G,'b');
158 %            H = otdrc(i).sinal;
159 %            hold on, plot((1:length(H))+minx,H,'r');
160 %            T = otdrr(i).arq;
161 %            title(T);
162 %            legend('Medido','Encontrado pelo AG');
163 %        end
164        toc
165 end
166 end
167
168 function [F,somasinal] = fitness(cromot)
169 global sdi dx vf m cd
170 otdr = zeros(1,length(sdi));
171 for i = 1:length(cromot.cromoi)
172     sinalx = 1:cromot.cromoi(i).x;
173     sinaly = cromot.cromoi(i).vc + m.*sinalx;
174     sinaly = cat(2,sinaly,(sinaly(end)+vf).*ones(1,dx));
175     sinaly = cat(2,sinaly,vf.*((1:length(sdi)-length(sinaly)).^cd
                ));
176     otdr = otdr + (10.^(sinaly./10)).^2;
177 end
178 somasinal = 10.*log10(otdr.^0.5);
```

```matlab
179  F = 0.5*sum((sdi-somasinal).^2);

180

181  function [f1,f2] = crossover(p1,p2)
182  global sdi dx
183  a = 1; b = length(sdi)-dx;
184  pf = struct('cromoi',{});
185  X = rand;
186  if X < 1/4
187      %Para X
188      for t = 1:length(p1.cromoi)
189          pf(1).cromoi(t).x = round(abs(0.5*p1.cromoi(t).x + 0.5*p2
                  .cromoi(t).x));
190          if pf(1).cromoi(t).x > b || pf(1).cromoi(t).x == 0
191              pf(1).cromoi(t).x = round(a + (b-a)*rand);
192          end
193          pf(2).cromoi(t).x = pf(1).cromoi(t).x;
194          pf(1).cromoi(t).vc = p1.cromoi(t).vc;
195          pf(2).cromoi(t).vc = p2.cromoi(t).vc;
196          pf(3).cromoi(t).x = round(abs(1.5*p1.cromoi(t).x - 0.5*p2
                  .cromoi(t).x));
197          if pf(3).cromoi(t).x > b  || pf(3).cromoi(t).x == 0
198              pf(3).cromoi(t).x = round(a + (b-a)*rand);
199          end
200          pf(4).cromoi(t).x = pf(3).cromoi(t).x;
201          pf(3).cromoi(t).vc = p1.cromoi(t).vc;
202          pf(4).cromoi(t).vc = p2.cromoi(t).vc;
203          pf(5).cromoi(t).x = round(abs(-0.5*p1.cromoi(t).x + 1.5*
                  p2.cromoi(t).x));
204          if pf(5).cromoi(t).x > b  || pf(5).cromoi(t).x == 0
205              pf(5).cromoi(t).x = round(a + (b-a)*rand);
206          end
207          pf(6).cromoi(t).x = pf(5).cromoi(t).x;
208          pf(5).cromoi(t).vc = p1.cromoi(t).vc;
209          pf(6).cromoi(t).vc = p2.cromoi(t).vc;
210      end
211      pfit(1) = fitness(pf(1));
212      pfit(2) = fitness(pf(2));
213      pfit(3) = fitness(pf(3));
214      pfit(4) = fitness(pf(4));
215      pfit(5) = fitness(pf(5));
216      pfit(6) = fitness(pf(6));
217  elseif X < 2/4
```

```matlab
218        %Para VC
219        for t = 1:length(p1.cromoi)
220            pf(1).cromoi(t).vc = abs(0.5*p1.cromoi(t).vc + 0.5*p2.
                   cromoi(t).vc);
221            pf(2).cromoi(t).vc = pf(1).cromoi(t).vc;
222            pf(1).cromoi(t).x = p1.cromoi(t).x;
223            pf(2).cromoi(t).x = p2.cromoi(t).x;
224            pf(3).cromoi(t).vc = abs(1.5*p1.cromoi(t).vc - 0.5*p2.
                   cromoi(t).vc);
225            pf(4).cromoi(t).vc = pf(3).cromoi(t).vc;
226            pf(3).cromoi(t).x = p1.cromoi(t).x;
227            pf(4).cromoi(t).x = p2.cromoi(t).x;
228            pf(5).cromoi(t).vc = abs(-0.5*p1.cromoi(t).vc + 1.5*p2.
                   cromoi(t).vc);
229            pf(6).cromoi(t).vc = pf(5).cromoi(t).vc;
230            pf(5).cromoi(t).x = p1.cromoi(t).x;
231            pf(6).cromoi(t).x = p2.cromoi(t).x;
232        end
233        pfit(1) = fitness(pf(1));
234        pfit(2) = fitness(pf(2));
235        pfit(3) = fitness(pf(3));
236        pfit(4) = fitness(pf(4));
237        pfit(5) = fitness(pf(5));
238        pfit(6) = fitness(pf(6));
239    elseif X < 3/4
240        %Para X
241        for t = 1:length(p1.cromoi)
242            pf(1).cromoi(t).x = round(abs(0.5*p1.cromoi(t).x + 0.5*p2
                   .cromoi(t).x));
243            if pf(1).cromoi(t).x > b || pf(1).cromoi(t).x == 0
244                pf(1).cromoi(t).x = round(a + (b-a)*rand);
245            end
246            pf(2).cromoi(t).x = round(abs(1.5*p1.cromoi(t).x - 0.5*p2
                   .cromoi(t).x));
247            if pf(2).cromoi(t).x > b  || pf(2).cromoi(t).x == 0
248                pf(2).cromoi(t).x = round(a + (b-a)*rand);
249            end
250            pf(3).cromoi(t).x = round(abs(-0.5*p1.cromoi(t).x + 1.5*
                   p2.cromoi(t).x));
251            if pf(3).cromoi(t).x > b  || pf(3).cromoi(t).x == 0
252                pf(3).cromoi(t).x = round(a + (b-a)*rand);
253            end
```

```matlab
254        end
255        %Para VC
256        for t = 1:length(p1.cromoi)
257            pf(1).cromoi(t).vc = abs(0.5*p1.cromoi(t).vc + 0.5*p2.
                   cromoi(t).vc);
258            pf(2).cromoi(t).vc = abs(1.5*p1.cromoi(t).vc - 0.5*p2.
                   cromoi(t).vc);
259            pf(3).cromoi(t).vc = abs(-0.5*p1.cromoi(t).vc + 1.5*p2.
                   cromoi(t).vc);
260        end
261        pfit(1) = fitness(pf(1));
262        pfit(2) = fitness(pf(2));
263        pfit(3) = fitness(pf(3));
264    else
265        %Para X e VC
266        for t = 1:length(p1.cromoi)
267            pf(1).cromoi(t).x = p2.cromoi(t).x;
268            pf(1).cromoi(t).vc = p1.cromoi(t).vc;
269            pf(2).cromoi(t).x = p1.cromoi(t).x;
270            pf(2).cromoi(t).vc = p2.cromoi(t).vc;
271        end
272        pfit(1) = fitness(pf(1));
273        pfit(2) = fitness(pf(2));
274    end
275    %save('pf','pf')
276    [sortfit,indfit] = sort(pfit,'ascend');
277    f1 = pf(indfit(1));
278    f2 = pf(indfit(2));
279
280    function [mutated] = mutation(tomutate)
281    global sdi dx emm
282    nal = length(tomutate.cromoi);
283    X = randperm(nal); a = 1; b = length(sdi)-dx;
284    Y = rand;
285    if Y < 1/3
286        tomutate.cromoi(X(1)).vc = emm(1) + (emm(2)-emm(1))*rand;
287    elseif Y < 2/3
288        tomutate.cromoi(X(1)).x = round(a + (b-a)*rand);
289    else
290        tomutate.cromoi(X(1)).vc = emm(1) + (emm(2)-emm(1))*rand;
291        tomutate.cromoi(X(1)).x = round(a + (b-a)*rand);
292    end
```

```
293   mutated = tomutate;
```

APPENDIX **C**

Routines to Differential Evolutionary Algorithm

The MATLAB®routine are developed with the intention of OTDR Signal Separation and described in section 4.4.

```matlab
function best = DE2(nchan, npop, maxgen, eta, C)
  %Example >> DE(8,70,100,0.09,0.3)
  close all
  global otdrG dx teoG otdrG
  dx = 10;
  teoG = otdrG(2:end-1).^2-otdrG(1:end-2).^2.*otdrG(3:end)
      .^2;
t = 1;
%inicializa populacao
Pop = zeros(npop,nchan*2);
%measX = [473 492 632 1087 1097 1155 2431 3792];
for i = 1:nchan
    Pop(:,2*(i-1)+1) = randi(length(otdrG), [npop  1]); %measX(i)
        ;
    Pop(:,2*i) = max(otdrG).*rand(npop,1);
end
N = size(Pop,1);
n = size(Pop,2);
Offs = zeros(size(Pop));
while (t <= maxgen)
    for i = 1:N
        r1 = randi(N);
        r2 = randi(N);
        while (r2 == r1), r2 = randi(N); end
        r3 = randi(N);
```

```matlab
24          while (r3 == r1 || r3 == r2), r3 = randi(N); end
25          di = randi(n);
26          for j = 1:n
27              if rand <= C || j == di
28                  Offs(i,j) = Pop(r1,j) + eta*(Pop(r2,j)-Pop(r3,j))
                        ;
29              else
30                  Offs(i,j) = Pop(i,j);
31              end
32              if mod(j,2) == 0 %vc
33                  if Offs(i,j) > max(otdrG)
34                      Offs(i,j) = max(otdrG);
35                  elseif Offs(i,j) < 0.1
36                      Offs(i,j) = 0.1;
37                  end
38              else %x
39                  Offs(i,j) = round(Offs(i,j)); % ensure integer
                        nature of some  alleles
40                  if Offs(i,j) > length(otdrG) - dx;
41                      Offs(i,j) = length(otdrG) - dx;
42                  elseif Offs(i,j) < 1
43                      Offs(i,j) = 1;
44                  end
45              end
46          end
47      end
48      idBest = 1;
49      for i = 1:N
50          if fitn(Offs(i,:)) <= fitn(Pop(i,:))
51              Pop(i,:) = Offs(i,:);
52          % else keep Pop(i,:)
53          end
54          if fitn(Pop(i,:)) <= fitn(Pop(idBest,:))
55              idBest = i;
56          end
57      end
58      Offs = zeros(size(Pop)); % Reset Offspring;
59      best = Pop(idBest,:);
60      t = t + 1;
61      [f,simul] = fitn(best);
62      %[f,simul,teos] = fitn(best);
63      %subplot(211),
```

```matlab
64      plot(otdrG), hold on, plot(simul,'r'), hold off
65      title(['Generation: ' num2str(t-1) ' - Fitness: ' num2str(f)
           ])
66      set(gca,'XLim',[1 length(otdrG)],'YLim',[0 2*max(otdrG)])
67      %subplot(212), plot(teoG), hold on, plot(teos,'r'), hold off
68      %set(gca,'XLim',[1 length(teoG)],'YLim',[0 2*max(teoG)])
69      pause(0.01);
70  end
71  plotBest(best);
72
73  function [f,simul,teos] = fitn(Indiv)
74  global otdrG dx %teoG
75  n = length(Indiv)*0.5;
76  sdi = otdrG; %lsdi = length(sdi); %sinal de interesse
77  %dx = 11; %largura do pico de fim de linha
78  m = -0.001; % OTDR HEADER: Data Spacing(km) * <dB/km>
79  %atan(-1/1150); %queda de ganho da curva
80  vf = 21; %tamanho (acima do sinal) do pico de fim de linha
81  cd = -0.27; %"coeficiente" de decaimento da exponencial,
           calculado por PowR
82  otdr = zeros(size(sdi));
83  sinaly = zeros(size(sdi));
84
85  for i = 1:n
86      sinalx = (1:Indiv(2*(i-1)+1))';
87      sinaly(1:length(sinalx)) = Indiv(2*i) + m.*sinalx;
88      auxvec = sinaly(1:length(sinalx));
89      auxvec = cat(1,auxvec,[(sinaly(Indiv(2*(i-1)+1))+vf).*sqrt(2)
           .*0.5;(sinaly(Indiv(2*(i-1)+1))+vf).*ones(dx-1,1)]);
90      auxvec = cat(1,auxvec,-3.86.*(0:4)'+(sinaly(Indiv(2*(i-1)+1))
           +vf)); % decaimento linear
91      auxend = auxvec(end); auxvec = auxvec(1:end-1);
92      auxvec = cat(1,auxvec,-2.41.*log(1:size(sdi))'+ auxend);
93      %plot(auxvec); pause(10)
94      sinaly = auxvec(1:size(sdi));
95  %     if length(sinalx)+dx < length(otdr)
96  %         sinaly(length(sinalx)+1:length(sinalx)+dx) = [(sinaly(
       Indiv(2*(i-1)+1))+vf).*sqrt(2).*0.5
97  %                                                 (sinaly(
       Indiv(2*(i-1)+1))+vf).*ones(dx-1,1)];
98  %                                              %(sinaly(
       Indiv(2*(i-1)+1))+vf).*sqrt(2).*0.5];
```

```matlab
99  %        elseif length(sinalx)+dx == length(otdr)-1
100 %            sinaly(end) = (sinaly(Indiv(2*(i-1)+1))+vf).*sqrt(2)
        .*0.5;
101 %        else
102 %            sinaly(length(sinalx)+1:end) = [(sinaly(Indiv(2*(i-1)
        +1))+vf).*sqrt(2).*0.5
103 %                                           (sinaly(Indiv(2*(i-1)
        +1))+vf).*ones(length(otdr)-length(sinalx)-1,1)];
104 %        end
105 %        if Indiv(2*(i-1)+1)+dx < length(otdr)
106 %            sinaly(length(sinalx)+dx+1:end) = vf.*(1:length(otdr)-(
        Indiv(2*(i-1)+1)+dx))'.^cd;%(sinaly(Indiv(2*(i-1)+1))+vf).*(1:
        length(otdr)-(Indiv(2*(i-1)+1)+dx))'.^cd;
107 %        end
108
109
110     otdr = otdr + (10.^(sinaly./10)).^2;
111 end
112 simul = 10.*log10(otdr.^0.5);
113 %residuos = otdrG - simul;
114 %f = 1 - corr(sort(residuos)./std(residuos),norminv(linspace(1e
        -3,.999,length(residuos)))');
115 %teos = simul(2:end-1).^2-simul(1:end-2).^2.*simul(3:end).^2;
116 %f = sum(abs(log10(teoG)-log10(teos)));
117 %%%%%%%%%%%%%%%%%%%%%%%%%%f = sum(abs(sdi-simul));
118 f1 = sum(sqrt((sdi-simul).^2));
119 f2 = 1;%sum(sqrt((TEO(sdi)-TEO(simul)).^2));
120 f = f1*f2;
121
122
123 function plotBest(Indiv)
124 global otdrG dx %teoG
125 n = length(Indiv)*0.5;
126 sdi = otdrG; %lsdi = length(sdi); %sinal de interesse
127 %dx = 11; %largura do pico de fim de linha
128 m = -0.001; % OTDR HEADER: Data Spacing(km) * <dB/km>
129 %atan(-1/1150); %queda de ganho da curva
130 vf = 21; %tamanho (acima do sinal) do pico de fim de linha
131 sinaly = zeros(size(sdi));
132
133 for i = 1:n
134     sinalx = (1:Indiv(2*(i-1)+1))';
```

```
135    sinaly(1:length(sinalx)) = Indiv(2*i) + m.*sinalx;
136    auxvec = sinaly(1:length(sinalx));
137    auxvec = cat(1,auxvec,[(sinaly(Indiv(2*(i-1)+1))+vf).*sqrt(2)
           .*0.5;(sinaly(Indiv(2*(i-1)+1))+vf).*ones(dx-1,1)]);
138    auxvec = cat(1,auxvec,-3.86.*(0:4)'+(sinaly(Indiv(2*(i-1)+1))
           +vf)); % decaimento linear
139    auxend = auxvec(end); auxvec = auxvec(1:end-1);
140    auxvec = cat(1,auxvec,-2.41.*log(1:size(sdi))'+ auxend);
141    %plot(auxvec); pause(10)
142    sinaly = auxvec(1:size(sdi));
143    figure, plot(sinaly); title(['Channel ' num2str(i)]);
144 end
```